SPEED AND PARAMETER ESTIMATION FOR INDUCTION MACHINES

by

Miguel Vélez-Reyes

BACHELOR OF SCIENCE IN ELECTRICAL ENGINEERING
UNIVERSITY OF PUERTO RICO, MAYAGÜEZ
(1985)

Submitted to the Department of Electrical Engineering and Computer Science
in Partial Fulfillment of the Requirements for the Degrees of

ELECTRICAL ENGINEER

and

MASTER OF SCIENCE IN ELECTRICAL ENGINEERING

at the

MASSACHUSETTS INSTITUTE OF TECHNOLOGY

May, 1988

Signature of Author _____
Department of Electrical Engineering and Computer Science
May 13, 1988

Certified by _____
George C. Verghese
Thesis Supervisor

Accepted by _____
Arthur C. Smith
Chairman, Departmental Committee on Graduate Students

Speed and Parameter Estimation for Induction Machines

by

Miguel Vélez-Reyes

Submitted to the Department of Electrical Engineering and Computer Science on May 13, 1988 in partial fulfillment of the requirements for the degrees of Electrical Engineer and Master of Science in Electrical Engineering.

Abstract

This thesis investigates the estimation of the electrical parameters and rotor speed of an induction machine. In particular, an estimator is developed that determines these quantities from the stator voltages and currents of the machine. The estimator is novel in the way that estimation theory is combined with the properties of the dynamic system.

The dynamics of the induction machine are nonlinear, which makes estimation difficult. The dynamic structure of the machine system is studied using participation factors. It is shown that for small induction machines the dynamic structure of the system is described by two weakly coupled subsystems with significant difference in time-scales: the slow dynamics are associated with the mechanical variables while the fast dynamics are associated with the electrical variables. Based on this time-scale separation, two linear regression models are derived that relate the machine parameters and rotor speed to the stator voltages and currents and their derivatives. It is shown how so-called state variable filters circumvent the unavailability of the derivative terms.

Due to the time-scale separation between the rates of change associated with the machine parameters and the rotor speed, further simplification of the estimator design is attained. The resulting estimator is structured as a two-stage procedure, with a fast stage that estimates the rotor speed, and a slow stage that estimates the machine parameters. The stages are designed using the recursive least squares estimator for a linear regression model. To take into account time variations in the parameters, forgetting factors are used.

Numerical simulations are used to demonstrate operation of the estimator. The tracking capabilities and the performance of the estimator with noisy measurements are discussed. The design of a test bench to test the algorithm with real data in an off-line mode is described, and the results of initial validation tests are presented and discussed.

Thesis Supervisor: Dr. George C. Verghese
Title: Associate Professor of Electrical Engineering

Acknowledgements

It is really difficult to try to thank all the persons that in one way or another have contributed to make the experience of being at MIT as rich as it has been. I hope nobody is left out.

I would like to thank from the bottom of my heart, my thesis supervisor Professor George C. Verghese for all the help, patience, friendship and guidance during these years. His contribution to this thesis is inmeasurable.

The moral support and friendship of some people in the lab was very important. In particular, I would like to thank Seth Sanders whose initial work in state estimation for induction machines was the starting point for this research; Larry Jones for all the help and insight given during the test-bench design; Karen Walrath for her help and advice in dealing with the lab software and computer related things; and to Kazuaki Minami and Louis Roehrs for their help in building and testing the induction machine test-bench. Other people in the lab that I'm very grateful to for their friendship and jokes at three o'clock in the morning: Kris, Clem, Carlos, Bahman, Leon, Antonio (now in Sweden).

I was supported during the course of these years by a generous fellowship from the Cooperative Research Fellowship Program (CRFP) of AT&T Bell Laboratories. Also, I would like to thank CRFP for the AT&T 6300 personal computer given to me; in it I did most of the text editing and part of the number crunching. Dr. Michael Hluchyj, now with CODEX, was my mentor and first advisor in MIT matters; for him my deepest appreciation.

Also I would like to thank Professor Jeffrey H.Lang and Dr. Steve Umans for many discussions and for allowing me to use their data acquisition equipment during the off-line experimentation. The drive system was donated by Industrial Drives, and additional support for parts was provided by the MIT/Industry Power Electronics Collegium and the MIT Soderberg Chair in Power Engineering.

Also I would like to thank the people of the Department of Electrical and Computer Engineering of the University of Puerto Rico, who supported and encourage me to continue graduate studies. Specially, to Profesor Baldomero Llorens for convincing me that MIT was the place to go. You were right.

I also need to thank my family for their love, support and continuing faith in me that gave me the strength to get to this point in my life. Last, but not least, I would like to thank my wife Jannete for her love and support during all these years, for washing the dishes during the last two months, for making me coffee to keep me awake during those long nights of May, for being patient, loving, and tender with me during those difficult moments. I know you have been almost a widow during this term.

A mis abuelos, Don Fidel Vélez y Doña Santiaga Rios por todo el amor que me han brindado durante estos años y por alentarme a siempre luchar para alcanzar las más altas metas.

Contents

List of Figures

List of Tables

Chapter 1

Introduction

1.1 Problem Statement, Contributions, Outline

The advances during the past fifteen years in the areas of power semiconductor devices and signal processing electronics have made possible the use of induction machine drives in high performance industrial applications where dc drives were exclusively used. The interest in induction machine drives follows from the simple and robust structure, low maintenance, and low cost of these machines compared to dc machines.

The control of an induction machine is considerably more complex than that of dc machines and this complexity increases when more rigorous specifications are imposed. For the induction machine drive to have a performance comparable to the dc drive it is necessary to have an accurate knowledge of the parameters and the electrical and mechanical variables of the induction machine. Therefore two significant problems arise in the control of induction machines: first, the estimation or measurement of the electrical and mechanical variables; second, the estimation or measurement of the machine parameters. Recent Master's theses by Seth Sanders [45] and Vincent J. Cotter [9] on flux estimation offer fine discussions on estimation of the electrical variables, see also [10,55,56].

This research work addresses the problem of estimating the rotor speed and the

machine parameters based on measurements of the stator voltages and currents. In this thesis the design and testing of an estimation algorithm for these quantities is presented. The approach developed takes advantage of the two-time-scale structure of the dynamics of the system under consideration. Based on this property two linear regression models that relate the desired rotor speed and machine parameters with the stator voltages and currents are derived. These linear regression models are used by the estimation procedure as reference models for speed and parameter estimation. The estimation algorithm is derived by using the Recursive Linear Least Squares Estimator (RLSE) algorithm for a linear regression model. Further simplification on the design is achieved by taking advantage of the time scale separation between the variations of the machine parameters and the rotor speed. The end result is that a two-stage estimation procedure is derived. It has a fast stage that computes an estimate for the rotor speed using the most recent parameter estimate and a slow stage that update the parameter estimates periodically.

The contribution of this work lies in the way we combine the tools provided by estimation theory with the properties of the induction machine system to come out with an algorithm to estimate the speed and the machine parameters. The methodology and approach presented promise to be of great use for estimation involving induction machines as well as other electrical machines, thought further development will be needed.

Another contribution of this research work is to show how participation factors can be used to study the structure of nonlinear models and how the obtained results can be used to develop reduced order models of nonlinear systems.

This thesis is organized as follows. Chapter 1, introduces the induction machine model and reviews recent literature in speed and parameter estimation for induction machines. In Chapter 2, the regression models used for speed and parameter estimation are derived. Chapter 3, discusses the estimation algorithm and introduces some of the

issues related to the estimator design. In Chapter 4, the performance of the estimator is studied by means of simulations. The experimental test-bench and the some results obtained from testing the estimator with real data are presented in Chapter 5. A sumary and suggestions for further research work are presented in Chapter 6. Few results in the analysis of multiple-time-scales phenomena in induction machines, and its implications to develop reduced order models for the induction machine are included in Appendix A.

1.2 Modeling an Induction Machine

The modeling of an induction machine is a well understood area, and [5,30,34] provide a good description of these models. A brief review is included here to establish the notation. To simplify the modeling of the induction machine, hysteresis and magnetic diffusion are neglected, and a model with lumped parameters is presented. A good assumption for the machines under consideration is the assumption of magnetic linearity and sinusoidally distributed windings in the stator.

The voltages across the terminals of the machine are related to the phase currents and the flux linkage by the matrix equation

$$\mathbf{v} = \mathbf{R}\,\mathbf{i} + \frac{d\,\psi}{dt} \tag{1.1}$$

where t is time, $\mathbf{v} = [\mathbf{v}_s^T, \mathbf{v}_r^T]^T$ is the terminal voltage vector, $\mathbf{i} = [\mathbf{i}_s^T, \mathbf{i}_r^T]^T$ is the phase current vector, and $\psi = [\psi_s^T, \psi_r^T]^T$ is the flux linkage vector. The subscripts **s** and **r** stand for stator and rotor quantities. **R** is the diagonal matrix of phase resistances. For a squirrel cage induction motor (SCIM) the vector of input voltages take the form $\mathbf{v}_s = \left[\mathbf{v}_s^T, \mathbf{0}\right]$

From the assumption of magnetic linearity, the flux linkage and the phase currents are related by

$$\psi = \mathbf{L}(\theta_r)\,\mathbf{i} \tag{1.2}$$

where $\mathbf{L}(\theta_r)$ is the inductance matrix and θ_r is the rotor position. In the case of a two-phase, single pole pair smooth air gap induction machine, the resistance and inductance matrices are symmetric and positive definite, and take the form

$$\mathbf{R} = \begin{bmatrix} R_s\mathbf{I} & \mathbf{0} \\ \mathbf{0} & R_r\mathbf{I} \end{bmatrix}, \quad \mathbf{L}(\theta_r) = \begin{bmatrix} L_s\mathbf{I} & M\exp(\mathbf{J}\theta_r) \\ M\exp(-\mathbf{J}\theta_r) & L_r\mathbf{I} \end{bmatrix}$$

where

$$\mathbf{J} = \begin{bmatrix} 0 & -1 \\ 1 & 0 \end{bmatrix}, \quad \exp(\mathbf{J}\theta_r) = \begin{bmatrix} \cos\theta_r & -\sin\theta_r \\ \sin\theta_r & \cos\theta_r \end{bmatrix}$$

R_s and R_r are the stator and rotor resistances, and L_s, L_r and M are the stator, rotor and mutual inductance respectively. It is important to point out that three-phase machines are the most commonly used in high performance applications. These machines in general have their stator windings connected either in delta or wye, which allows the use of a power invariant transformation (d-q-0) to transform the three-phase machine into an equivalent two-phase machine. We can therefore use models of two-phase machines without loss of generality.

Using conservation of energy and the assumption of magnetic linearity, the mechanical equation of the machine is given by

$$H\,\frac{d\omega_r}{dt} = -B\,\omega_r + \tau_{em} - \tau_L \tag{1.3}$$

where

$$\begin{aligned} \tau_{em} &= \frac{1}{2}\,\mathbf{i}^T\,\frac{\partial\,\mathbf{L}(\theta_r)}{\partial\theta_r}\,\mathbf{i} \\ &= -\frac{1}{2}\,\psi^T\,\frac{\partial\,L^{-1}(\theta_r)}{\partial\theta_r}\,\psi \end{aligned}$$

and ω_r is the rotor speed, B is the friction coefficient, H is the combined inertia of the rotor plus the mechanical load, τ_{em} is the electromagnetic torque, and τ_L is the load torque.

Combining equations (1.1) to (1.3), a state space representation of the machine equations can be derived. This is given by:

$$\frac{d\,\psi}{dt} = -\mathbf{R}\mathbf{L}^{-1}(\theta_r)\,\psi + \mathbf{v} \tag{1.4}$$

$$\frac{d\,\omega_r}{dt} = -\frac{B}{H}\,\omega_r + \frac{(\tau_{em} - \tau_L)}{H} \tag{1.5}$$

The dependence of the inductance matrix on the rotor position is because of the relative displacement between the magnetically coupled circuits of the stator and the rotor of the machine. This dependence makes difficult the analysis of the induction machine. Because of the assumption of a sinusoidal distribution of the windings in the stator, this dependence can be eliminated by transforming the rotor and stator circuits to a reference frame where the transformed stator and rotor circuits are stationary with respect to each other. This transformation is due to Blondel-Park [4,42,36].

Let us consider the coordinate transformation on the flux of the form

$$\lambda = \mathbf{P}(\phi)\,\psi \tag{1.6}$$

where

$$\mathbf{P}(\phi) = \begin{bmatrix} \exp(-\mathbf{J}\phi) & \mathbf{0} \\ \mathbf{0} & \exp(-\mathbf{J}(\phi - \theta_r)) \end{bmatrix} \tag{1.7}$$

and λ is the Park-transformed flux vector. This transformation can be thought as a coordinate change as illustrated in Figure 1.1. The Park-transformed machine equations are given by:

$$\frac{d\,\lambda}{dt} = -\left(\mathbf{R}\mathbf{L}^{-1} + \delta \begin{bmatrix} \mathbf{J} & \mathbf{0} \\ \mathbf{0} & \mathbf{J} \end{bmatrix}\right)\lambda + \omega_r \begin{bmatrix} \mathbf{0} & \mathbf{0} \\ \mathbf{0} & \mathbf{J} \end{bmatrix}\lambda + \begin{bmatrix} \mathbf{I} \\ \mathbf{0} \end{bmatrix}\mathbf{v}_s \tag{1.8}$$

$$\frac{d\,\omega_r}{dt} = -\frac{B}{H}\,\omega_r + \frac{(\tau_{em} - \tau_L)}{H} \tag{1.9}$$

$$\tau_{em} = \frac{1}{2}\,\frac{M}{L_s L_r - M^2}\,\lambda^T \begin{bmatrix} \mathbf{0} & \mathbf{J} \\ -\mathbf{J} & \mathbf{0} \end{bmatrix}\lambda \tag{1.10}$$

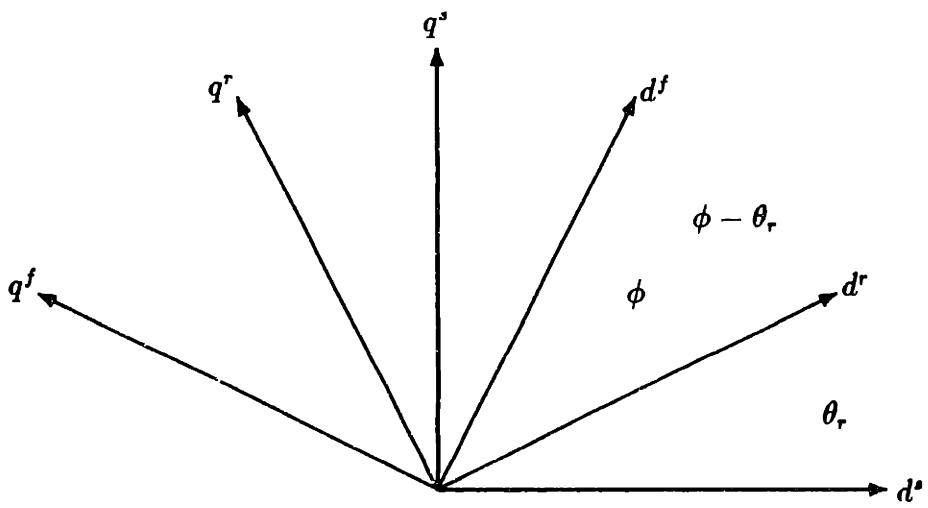

Figure 1.1: Park-Transformation of the Electrical Variables.

$$\lambda = \mathbf{L}\mathbf{i} \tag{1.11}$$

where

$$\mathbf{L} = \begin{bmatrix} L_s\mathbf{I} & M\mathbf{I} \\ M\mathbf{I} & L_r\mathbf{I} \end{bmatrix}$$

and δ is the angular speed of the reference frame. The most commonly used reference frames are the stator-fixed frame and the synchronous reference frame. These are obtained by letting $\delta = 0$ and $\phi = 0$ for the stator-fixed frame and $\delta = \omega_e$ and $\phi = \omega_e t + \gamma$ (ω_e is the voltage source frequency and γ an arbitrary phase) for the synchronous frame.

A simplified representation of the machine equations (1.8) to (1.11) can be obtained by using the isomorphism between the complex numbers $a + jb$ and matrices of the form $a\mathbf{I} + b\mathbf{J}$ [41,45]. Using this isomorphism, equations (1.8)-(1.11) referred to the stator reference frame are given by:

$$\frac{d\,\tilde{\lambda}}{dt} = -\left(\tilde{\mathbf{R}}\tilde{\mathbf{L}}^{-1} - \omega_r \begin{bmatrix} 0 & 0 \\ 0 & j \end{bmatrix}\right)\tilde{\lambda} + \begin{bmatrix} 1 \\ 0 \end{bmatrix}\tilde{v}_s \tag{1.12}$$

$$\frac{d\omega_r}{dt} = -\frac{B}{H}\,\omega_r + \frac{(\tau_{em} - \tau_L)}{H} \tag{1.13}$$

$$\tau_{em} = \frac{M}{L_s L_r - M^2}\; Im\left(\tilde{\lambda}_s\, \tilde{\lambda}_r^*\right) \tag{1.14}$$

$$\tilde{\lambda} = \tilde{\mathbf{L}}\,\tilde{\mathbf{i}} \tag{1.15}$$

where $\tilde{\mathbf{f}} = [\tilde{f}_s, \tilde{f}_r]^T$, $\tilde{f}_s = f_{sd} + jf_{sq}$, $\tilde{f}_r = f_{rd} + jf_{rq}$ and f stands for voltages, currents, or flux linkages, and d and q refers to the direct and quadrature components. The transformed resistance and inductance matrices are given by

$$\tilde{\mathbf{L}} = \begin{bmatrix} L_s & M \\ M & L_r \end{bmatrix}, \quad \tilde{\mathbf{R}} = \begin{bmatrix} R_s & 0 \\ 0 & R_r \end{bmatrix}$$

It is important to point out that under constant speed operation equation (1.12) is the model of a linear time invariant (LTI) system. Under constant speed operation it is therefore possible to compute a closed expression for the transfer function from stator voltage to stator current. This is given by:

$$H(s) = \frac{\frac{L_r}{\sigma}\left(s + \frac{1}{T_r} - j\omega_r\right)}{s^2 + \left(\frac{L_r R_s + L_s R_r}{\sigma} - j\omega_r\right)s + \frac{L_s R_s}{\sigma}\left(\frac{1}{T_r} - j\omega_r\right)} \tag{1.16}$$

where $T_r = L_r/R_r$ is the rotor time constant and $\sigma = L_r L_s - M^2$. Note that the rotor speed ω_r enters as a parameter in the coefficients of this transfer function as well as other machine parameters. *This transfer function is central to the estimation algorithm developed in this thesis.* The use of this transfer function to estimate rotor speed and machine paramaters was introduced in [45].

1.3 Literature Review: Speed Estimation

The common approach in high performance control of induction machine drive systems involves the use of a speed transducer connected to the shaft of the machine. The use of

this transducer has two major drawbacks. First, it obstructs the mechanical interface between the motor and the load, interfering with the requirements of tight coupling or close spacing in the mechanical layout or imposing the application of undesirable gear trains or belts. Second, it generally requires the use of brushes or light sources that require maintenance, which represents a weak link in the system in terms of reliability. Therefore, the use of the transducer in the induction machine drive systems spoils the mechanical simplicity and robust structure of the machine, which are two of the most important reasons to use these drives instead of their dc counterpart.

Three basic approaches can be identified in the literature that addresses the problem of speed estimation based on measurements of the stator voltages and currents. First, because the rotor speed is a state variable of the system, a nonlinear observer can be used to estimate the rotor speed as part of the state vector of the machine. Second, since the speed can be thought of as a parameter in the electrical equations of the induction machine, and if all the electrical quantities and the machine parameters are known, it might be possible to estimate the rotor speed from equation (1.8). Third, since the rotor speed ω_r and the slip ω_{sl} are related by,

$$\omega_r = \omega_e - \omega_{sl} \tag{1.17}$$

where ω_e is the frequency of the electrical signals, an indirect way to estimate the rotor speed is by estimating the slip. Note that because of (1.17) estimating the slip is equivalent to estimate the rotor speed.

1.3.1 Rotor Speed as a State Variable

Because of the nonlinearities involved in the machine model, the estimation of the state variables of the induction machine requires the use of a nonlinear observer. The most common approach to the nonlinear observer problem is using the Extended Kalman Filter (EKF). This algorithm is based on the application of the linear Kalman filter to a linearization of the system model and measurement equation around the current

estimate of the state. The reader is referred to [6] for a formal treatment of this subject. The EKF has been applied to the problem of induction machine speed and parameter estimation by Hillenbrand [24].

To introduce Hillenbrand's approach, let us review the machine model that he uses in his estimation algorithm. The machine model in the stator reference frame, with the stator flux, stator current, and the rotor speed as state variables, is given by:

$$\frac{d\tilde{\lambda}_s}{dt} = -R_s\tilde{i}_s + \tilde{v}_s \tag{1.18}$$

$$\frac{d\tilde{i}_s}{dt} = \left(\frac{R_r}{\sigma} - j\frac{L_r}{\sigma}\omega_r\right)\tilde{\lambda}_s - \left(\frac{R_sL_r + R_rL_s}{\sigma} - j\omega_r\right)\tilde{i}_s + \frac{L_r}{\sigma}\tilde{v}_s \tag{1.19}$$

$$\frac{d\omega_r}{dt} = -\frac{B}{H}\omega_r + \frac{1}{H}Im\left(\tilde{\lambda}_s\,\tilde{i}_s^*\right) - \frac{1}{H}\tau_L \tag{1.20}$$

Because the stator currents and voltages are known quantities, it is only necessary to estimate the stator flux and the rotor speed. This could be done by using a reduced order observer based on equations (1.18) and (1.20). If we have available the value of the derivative of the stator current, the measurement equation for the EKF is given by (1.19). The special feature of the reduced order model used by Hillenbrand is that for a known value of the stator current, equations (1.18) and (1.20) are linear in the state dynamics, with nonlinearities only in the measurement equations, which makes easier the application of the EKF to the solution of this problem. In his implementation, Hillenbrand uses a discrete time model derived from these equations. Since the derivative of the stator current is not directly available as a measurable quantity, in this algorithm the signals are prefiltered by "mod-function" filters and the output signals are used as the measured signals by the estimation algorithm. To incorporate the estimation of the rotor time constant, the state vector is augmented to include this variable as another state variable, see [6] for an explanation of this procedure, where the EKF is used for the simultaneous estimation of state and parameters.

Hillenbrand's simulation results are encouraging, but neither stability nor convergence are discussed. Implementation issues are not addressed, even though it is claimed

that the implementation of this algorithm could be simple using a microprocessor.

1.3.2 Rotor Speed as a Parameter in the Machine Electrical Equations

Looking at the electrical equations of the induction machine (1.8) we can see that the speed can be thought of as a parameter in these equations. Therefore, if the values of the machine parameters as well as the electrical variables are available, the rotor speed can be estimated from (1.8).

de Fornel et al.'s Speed Estimator

In [11] de Fornel et al. derive an expression for the rotor speed in terms of the rotor flux, stator current and the derivative of the stator current. The machine model used in the derivation of this algorithm is the model referred to the synchronous reference frame with the constraint that the reference axis is aligned with the stator current vector. This model, using the stator currents and the rotor flux as state variables, is given by the following set of equations:

$$\frac{d\lambda_r}{dt} = -\left(\frac{1}{T_r}\mathbf{I} - \omega_{sl}\mathbf{J}\right)\lambda_r + \frac{M}{T_r}\mathbf{i}_s \tag{1.21}$$

$$\frac{d\mathbf{i}_s}{dt} = -\left(\frac{R_s L_r^2 + R_r M^2}{\sigma L_r^2}\mathbf{I} + \omega_e \mathbf{J}\right)\mathbf{i}_s + \left(\frac{M}{T_r \sigma}\mathbf{I} - \omega_r \frac{M}{\sigma}\mathbf{J}\right)\lambda_r + \frac{L_r}{\sigma}\tilde{v}_s \tag{1.22}$$

Because of the constraint that the stator current lies along the reference axis of the machine, the second component of the matrix equation (1.22) is equal to zero, i.e. $i_{s2} = 0$.

If the values of the rotor flux, the stator current and the derivative of the stator current are known in (1.22), the rotor speed can be estimated from either of the components of the vector equation:

$$\omega_r \mathbf{J}\lambda_r = -\left(\frac{R_s L_r^2 + R_r M^2}{M L_r^2}\mathbf{I} + \frac{\sigma}{M}\omega_e \mathbf{J}\right)\mathbf{i}_s + \frac{R_r}{L_r}\lambda_r - \frac{\sigma}{M}\frac{d\mathbf{i}_s}{dt} \tag{1.23}$$

Because of the constraint set on the stator current, the second component of the matrix equation (1.23) does not have a derivative term on it. Both estimators are studied in [11]. Their results show that the estimator without the derivative term has the better performance.

A point which is not very clear in this paper is the following. Assuming that the derivative of the stator current is known, the only quantity that is not directly available is the rotor flux. The rotor flux can be estimated from (1.21). However, to compute this estimate it is necessary to know the value of the speed. The slip and the rotor speed are related by:

$$\omega_{sl} = \omega_e - \omega_r$$

where ω_{sl} stands for slip. In [11] the relationship between slip and the rotor speed is not made clear and in the derivation these look like two unrelated quantities. Simulation results are presented that show a satisfactory performance of the algorithm. However, the stability and convergence properties of the algorithm are not studied. The fact that the estimate of the rotor speed has to be used for the rotor flux estimation leaves many unclear points about the stability and robustness of this algorithm.

Tamai et al.'s Model Reference Approach

In this section we present the basic idea of the speed estimator presented in [50]. The speed estimator presented in this paper is based on the theory of Model Reference Adaptive Systems (MRAS) [33]. A block diagram that will be used to explain this approach is presented in Figure 1.2.

The basic idea behind this approach is as follows. The induction machine is the reference system whose parameters, we want to estimate. The adjustable model is an ideal vector-controlled induction motor model, in which the rotor speed enters as a parameter. The rotor speed in the adjustable model is tuned so that the difference between the output of the induction machine and the output of the adjustable model

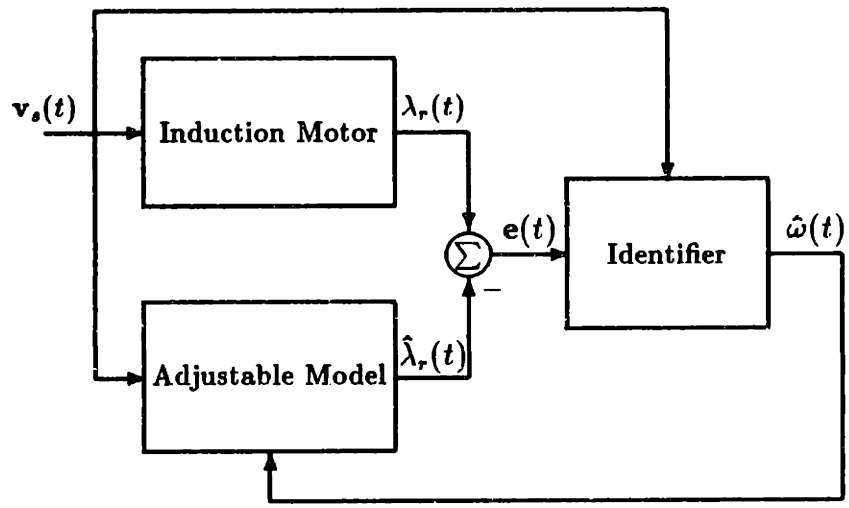

Figure 1.2: Model Reference Adaptive System for Rotor Speed Estimation.

is made equal to zero. When the error is made equal to zero, if the input signal is rich enough, the speed estimate $\hat{\omega}_r$ should be equal to the value of the rotor speed.

1.3.3 Slip Estimation

An indirect way to estimate the rotor speed is by estimating the slip. If an estimate of the slip is available it is obvious that an estimate of the rotor speed can be obtained. Also, to control induction machines sometimes is more desirable to use slip rather than rotor speed. Two basic forms of slip estimators can be identified in the literature on slip estimation, namely steady state and dynamic slip estimators.

1.3.3.1 Steady State Slip Estimators

The estimators studied in this subsection are based on the assumption that the electrical variables of the machine are in steady state.

Abbondanti and Brennen's Estimator

The first estimator studied in this section was originally presented by Abbondanti and Brennen in [2]. This estimator is based on the fact that at low values of slip the steady state electromagnetic torque is proportional to the slip, i.e.

$$\tau_{em} \approx M^2 R_r \frac{V_m^2}{\omega_e} \omega_{sl} \tag{1.24}$$

where V_m represents the peak value of the stator voltage. If the value of the steady state electromagnetic torque is known, the slip can be estimated from (1.24). Since the electromagnetic torque is not directly measurable, [2] estimates it from an estimate of the airgap power. The electromagnetic torque and the airgap power in steady state are related by

$$\tau_{em} \omega_e = P_g \tag{1.25}$$

where P_g stands for airgap power. The airgap power can be estimated from stator voltages and currents using:

$$\hat{P}_g = \mathbf{v}_s^T \mathbf{i}_s - \mathbf{i}_s^T R_s \mathbf{i}_s \tag{1.26}$$

Combining (1.24) to (1.26), Abbondanti's estimator is obtained. The equation for the estimator is given by

$$\hat{\omega}_{sl} = \frac{\mathbf{v}_s^T \mathbf{i}_s - \mathbf{i}_s^T R_s \mathbf{i}_s}{R_r M^2 V_m^2} \tag{1.27}$$

Different implementations of this estimator are shown in [2,53]. In [53], it is noted that this estimator is accurate only in steady state operation.

Naunin's Estimator

A similar estimator is presented by Naunin in [40]. This estimator is similar to Abbondanti's estimator in the sense that a linear relationship between slip and torque is used. This linear relationship is derived from experimental data rather than using (1.24). It is pointed out that this relationship is valid for a limited range of slip. The estimator is implemented as part of a digital control system and the experimental results seem to be satisfactory. However, it is observed that for low speed operation the system becomes unstable.

de Fornel et al.'s Steady State Slip Estimators

Another approach to the problem of slip estimation based on the steady state assumption is presented by de Fornel et al. in [12]. The electrical equations of the machine model in the synchronous rotating frame in steady state are given by:

$$(R_s\mathbf{I} + \omega_e L_s\mathbf{J})\,\mathbf{i}_s + \omega_e M\mathbf{J}\mathbf{i}_r = \mathbf{v}_s \tag{1.28}$$

$$\omega_{sl} M\mathbf{J}\mathbf{i}_s + (R_r\mathbf{I} + \omega_{sl} L_r\mathbf{J})\,\mathbf{i}_r = \mathbf{0} \tag{1.29}$$

Since the stator currents and voltages can be measured, equations (1.28) and (1.29) form a system of four equations and three unknowns. Solving for the rotor current in (1.28) and substituting back into (1.29) results in

$$\omega_{sl}\frac{L_r}{R_r}\left[\mathbf{J}\mathbf{v}_s + \left(\frac{\omega_e\sigma}{L_r}\mathbf{I} - R_s\mathbf{J}\right)\mathbf{i}_s\right] = \mathbf{J}\mathbf{v}_s - (R_s\mathbf{J} - \omega_e L_s\mathbf{I})\,\mathbf{i}_s \tag{1.30}$$

A slip estimator can be obtained from either of the components of the vector equation (1.30). To compensate for parameter variation, a rotor resistance estimation method is implemented as part of the estimation algorithm in [12]. Simulation results are presented in the paper that show the performance of the estimator with and without rotor resistance variation.

The second steady state slip estimator presented in this section is based on another paper by de Fornel et al. [13]. The model used tc derive this estimator is given by equations (1.21) and (1.22) with the reference axis aligned with the stator current vector. Assuming steady state conditions on the electrical variables from (1.21), an equation that relates the slip to the rotor flux is given by

$$\omega_{sl} = \frac{1}{T_r}\frac{\lambda_{r1}}{\lambda_{r2}} \tag{1.31}$$

If the value of the rotor flux is known, the slip can be estimated from (1.31). A rotor flux observer is implemented as part of the control algorithm, but the rotor flux estimate is dependent on the slip estimate. The simulation results presented show a good performance of the controlled system and show a good performance for the slip estimation. Issues related to robustness, stability and convergence of the estimation algorithm are not addressed, however.

1.3.3.2 Dynamic Slip Estimators

The poor performance of steady state estimators during electric transient conditions motivates the design of algorithms that take into account the dynamics of the electrical subsystem.

Joetten and Maeder's Estimator

In Joetten and Maeder's [27] a slip estimator is presented that tries to incorporate electrical transients into the slip estimation. The machine model used for this estimator is the model in stator fixed coordinates, see eq. (1.8) with $\phi = \delta = 0$. The electrical subsystem equations are given by:

$$\frac{d\lambda}{dt} = \left(-\mathbf{R}\mathbf{L}^{-1} + \begin{bmatrix} \mathbf{0} & \mathbf{0} \\ \mathbf{0} & \omega_r \mathbf{J} \end{bmatrix}\right)\lambda + \begin{bmatrix} \mathbf{I} \\ \mathbf{0} \end{bmatrix}\mathbf{v}_s \tag{1.32}$$

$$\lambda = \mathbf{L}\mathbf{i} \tag{1.33}$$

Two expressions for the electromagnetic torque that are used later are:

$$\tau_{em} = \lambda_r^T \mathbf{J}\, \mathbf{i}_r \tag{1.34}$$

$$\tau_{em} = \frac{M}{L_r}\, \mathbf{i}_s^T \mathbf{J}\, \lambda_r \tag{1.35}$$

If the control algorithm is such that the magnitude of the rotor flux is kept constant, the rotor flux derivative can be approximated by,

$$\frac{d\lambda_r}{dt} \approx \omega_e \mathbf{J} \lambda_r \tag{1.36}$$

Combining (1.32) through (1.34) we get that

$$\tau_{em} = \frac{\omega_{sl}}{R_r}\, \lambda_r^T \lambda_r \tag{1.37}$$

Using (1.35) and (1.37) an equation for the slip in terms of the rotor flux and the stator current is obtained. This is given by

$$\omega_{sl} = \frac{M}{T_r}\, \frac{\mathbf{i}_s^T \mathbf{J}\, \lambda_r}{\lambda_r^T \lambda_r} \tag{1.38}$$

If the stator current and the rotor flux are known, an estimate of the slip can be obtained from (1.38). However, the rotor flux is not directly available. A flux estimator is implemented in [27]. The flux estimator is derived from (1.32) and (1.36) and is given by

$$\hat{\lambda}_r = -\frac{L_r}{\omega_e M} \mathbf{J} \left(\mathbf{v}_s - R_s \mathbf{i}_s - \frac{\sigma}{L_r} \frac{d\mathbf{i}_s}{dt} \right) \tag{1.39}$$

where $\hat{\lambda}$ stands for flux estimate. Note that it is assumed that the derivative of the stator current is available. The implementation in [27] uses a differentiator as part of the estimation algorithm. In general the use of a differentiator is undesirable because of the noise, but [27] claims that it has a smoothing effect. The effect of the machine parameters on the performance of the estimator is discussed. A control algorithm where this estimator is used is presented in [49].

In a paper by Nabae et al. [39] a similar slip estimator to the one presented in [27], based on equation (1.38), is used. The difference is that a rotor flux observer is used,

instead of (1.39), to estimate the rotor flux. The rotor flux observer is based on the direct flux observer scheme [45,56,55], the equations for the observer being given by

$$\frac{d\hat{\lambda}_r}{dt} = \frac{L_r}{M}(\mathbf{v}_s - R_s\mathbf{i}_s) - \frac{\sigma}{M}\mathbf{i}_s \tag{1.40}$$

That eliminates the use of a differentiator in the rotor flux estimator. Note that the flux estimate does not depends on the estimate of the slip, unlike with the flux observer used in [12]. However, as discussed in [45,56,55] this rotor flux estimation scheme has two major drawbacks: first, its poor behavior at low speeds; and second, the estimation error (i.e. the difference between the estimated and real values of the rotor flux) does not go to zero.

1.4 Literature Review: Parameter Estimation

The modeling of an induction machine is a well studied area, and equations (1.8)-(1.10) are accepted as being a good model of the induction machine for control purposes. The question that comes to mind is how we estimate the parameters of this model, i.e. R_s, R_r, L_s, L_r, M. In general, two approaches can be followed. First, off-line identification can be performed, collecting a batch of data from the induction machine and subsequently, as a separate procedure, estimating the values of the parameters.

A well known off-line procedure involves two tests, the no-load and locked rotor tests [18]. Further improvements to the parameter values estimated from the no-load and locked rotor tests can be obtained by including other operating conditions in the estimation procedure. A paper by Bellini et al. [3] describes an estimation procedure that includes data on torque, speed, stator currents and voltages at different operating conditions. The parameter estimation procedure is formulated as a constrained nonlinear optimization problem, where the data is fitted to the steady state torque characteristic. The constraints are obtained from physical knowledge of the system. A different procedure is presented by Consoli et al. in [8], who identify the parameters

of a linearized reduced order model of the induction machine. In both cases the least squares criterion is used for identification.

The obvious disadvantage of the off-line methods is that the variation in the machine parameters during machine operation is not taken into account. The estimated value of the machine parameters can be used in machine simulations and for control design. In control design the use of these parameters presents a tradeoff between implementation and performance, i.e. it is easier to design a control algorithm for a system with known parameters than for a system where the parameters are time varying quantities, but as the parameters change the performance may degrade.

The development of high performance control algorithms, like field oriented control [5,34,35], have made possible the use of induction machine drives where formerly dc drives were exclusively used. Most of these high performance control algorithms rely on an accurate knowledge of the machine parameters at all times. Because the machine parameters change widely during machine operation, it is necessary to estimate the values of these parameters during operation. The machine model then is updated when variations in the machine parameters are detected.

Motivated by the importance of the rotor time constant or rotor resistance in field oriented control [31], most of the on-line parameter estimation methods discussed in the literature are devoted to their estimation. In most of the cases, except Hillenbrand [24], the measured variables are the rotor speed and the stator voltages and currents, so the estimation procedure is based on equation (1.8). Therefore, it is not surprising that most of the parameter estimation algorithms presented in the literature are analogous to the speed estimators discussed previously, where the speed is considered as a parameter of equation (1.8) too. We will therefore, not repeat the analysis done for the speed estimation algorithms, but simply give the classification of the literature in this area.

In principle the extended Kalman filter (EKF) is applicable to the speed and parameter estimation problems. In [14,24,59] the EKF is used to estimate part of the

state vector of the induction machine and the state vector is augmented to include the rotor time constant. The static estimators for rotor resistance or rotor time constant are presented in [25,32,38,57], i.e. an expression for these parameters is derived from equations (1.28)-(1.29) and used to estimate them, based on measurements of the rotor speed and the stator voltages and currents. Different parameter tuning algorithms following the MRAS approach are contained in [20,19,29,48], where the parameter tuning is done by monitoring the parameter variations indirectly, using a quantity that is defined as a function of the machine variables to monitor the change of the machine parameters. If the machine parameters and the model parameters are equal, the value of this function for the machine and the model should be the same. If the parameter changes, the value of the function for the model and the machine differ. This difference is feed to a tuning procedure that change the model parameter values until the output of the model and the machine are equal.

A few observations can be made about these algorithms. First, some of these methods are parameter dependent themselves, i.e. depend on the inductances, which change with operating conditions too. Second, the robustness and stability properties of these adaptive control algorithms are not discussed and sometimes implementation issues are not addressed.

Chapter 2

Linear Regression Models for Speed and Parameter Estimation

2.1 Introduction

Most of the approaches followed for speed estimation involve the use of the equations of the electrical subsystem (1.8) of the machine. In some of these schemes, it is assumed that an accurate knowledge of the machine parameters is available. As a result of this assumption these schemes are parameter dependent themselves. Since the machine parameters change during operation, the performance of the estimator will be affected by these variations. Therefore, to be able to estimate the rotor speed accurately, the estimator itself should involve a mechanism to compensate for parameter variations.

In this chapter we will present two linear regression models that relate the speed and the machine parameters to the stator voltages and currents. Therefore, the speed and parameter estimation problem for the induction machine will be reformulated as the problem of estimating the parameters of a linear regression model.

2.2 Two-Time-Scale Phenomena in Induction Machines

Induction machines involve dynamic phenomena with widely spread time constants. This is due to the difference between the time constants associated with the electrical and mechanical subsystems. Based on this phenomenon, we are able to decompose the dynamic structure of the machine into its fast and slow subsystems. Reduced order models of the machine can be developed using the time scale decomposition. The resulting models can be used for estimation purposes.

A natural way to decompose the machine model is into its mechanical and electrical subsystems [54]. The nonlinearities involved in the induction machine model make it difficult to understand how the electrical and mechanical subsystems interact. One way to study this structure is by looking at the linearized model of the induction machine operating at constant speed. This model turns out to be time invariant, which makes possible the use of the participation factors introduced in [43] to study the local dynamic structure of the linearized machine model. The analysis and the derived reduced order models are presented in Appendix A and in [51]. In this section we only present some of the results for small induction machines.

The eigenvalues of the linearized model for a 3 hp machine are shown in Table 2.1 and the corresponding participation factors in Table 2.2. Based on the participation factors we are able to discern clear dynamic patterns, i.e. associations between state variables and modes of the linearized model. There are three groups: the *stator eigenvalues* $\mu_{1,2}$, the *rotor eigenvalues* $\mu_{3,4}$ and a *rotor speed eigenvalue* μ_5. Note that the *fast* eigenvalues (i.e. the ones with the larger real part) are associated with the electrical subsystem and the *slow* eigenvalue is associated with the mechanical variable. Therefore, we are able to decompose the machine model of the 3 hp induction motor into its fast and slow subsystems, where the fast subsystem involves the electrical variables while the slow subsystem involves the mechanical ones. It is shown in Appendix A that

Name	Value
$\mu_{1,2}$	-86.62±315.71
$\mu_{3,4}$	-228.44±71.04
μ_5	-4.38

Table 2.1: Eigenvalues of the 3 hp Induction Machine.

State Variable	Participation Factors		
	$\mu_{1,2}$	$\mu_{3,4}$	μ_5
λ_{S1}	**0.5722**	-0.0722	0
λ_{S2}	**0.5732**	-0.0732	0.0001
λ_{R1}	-0.0730	**0.5834**	-0.0207
λ_{R2}	-0.0715	**0.5712**	0.0005
ω_r	-0.0009	-0.0092	**1.0200**

Table 2.2: Participation Factors for the 3 hp Machine.

this decomposition will hold for small machines only; for large machines a different slow/fast decomposition holds.

The implication of this two-time-scale property is that if we look at the evolution of the electrical and mechanical variables in an interval of time much smaller than the mechanical time constant, we will see that the machine fluxes and currents may change significantly, while the rotor speed will remain *almost constant.* Therefore, the electrical equations of the machine model (1.8) essentially constitute a linear time invariant system (LTI) during that interval of time.

It is important to point out that the rotor speed as well as the machine parameters enter as parameters of (1.8). We shall see later that a parameter estimation algorithm based on the electrical equations, with a convergence rate faster than the mechanical time constant, will be able to estimate rotor speed and machine parameters based on measurements of the stator voltages and currents.

In the estimation methods reviewed in Chapter 1 we saw how the electrical equations were used to derive expressions for the rotor speed or machine parameters in terms of the electrical quantities. To solve the problem of the unavailability of the derivative terms and of the rotor quantities, the electrical quantities were assumed to be in steady state and rotor flux estimators were implemented. Therefore the assumption of separation of time scales between the electrical and mechanical subsystems as well as the use of the electrical equations for speed and parameter estimation has been widely used by the different methods presented in the literature. In the next sections we use the time scale separation property to come out with a linear regression model that relates the rotor speed and machine parameters to the stator voltages and currents. Furthermore we show how, by using so-called state variable filters, the problem with the derivative terms is avoided.

2.3 Derivation of the Linear Regression Models

Over a short interval of time the evolution of the electrical variables of the machine can be approximated by an LTI model. The transfer function between stator currents and stator voltages for this LTI model was computed and given in (1.16).

In this section we will derive two linear regression models based on (1.16). The estimation algorithm will estimate the parameters of these linear regression models. From these estimates, estimates of the machine parameters as well as the rotor speed can be obtained.

2.3.1 Linear Regression Model for Speed and Parameter Estimation

Let us, for notational simplicity, rename the transfer function coefficients in the following way:

$$\begin{aligned} a_1 &= \frac{R_s L_r + R_r L_s}{\sigma} - j\omega_r \\ a_0 &= \frac{L_r R_s}{\sigma}\left(\frac{1}{T_r} - j\omega_r\right) \\ b_1 &= \frac{L_r}{\sigma} \\ b_0 &= \frac{L_r}{\sigma}\left(\frac{1}{T_r} - j\omega_r\right) \end{aligned} \tag{2.1}$$

Using this notation the transfer function (1.16) is given by:

$$H(s) = \frac{b_1 s + b_0}{s^2 + a_1 s + a_0} \tag{2.2}$$

Taking the inverse Laplace transform, a second order differential equation relating stator voltages and currents can be obtained from (2.2). This equation is given by:

$$\frac{d^2 i_s}{dt^2} + a_1 \frac{d i_s}{dt} + a_0 i_s = b_1 \frac{d v_s}{dt} + b_0 v_s$$

(We have, for notational simplicity, droped the tildes used in the development of (1.12). Solving for the second derivative of the stator current we get:

$$\frac{d^2 i_s}{dt^2} = \begin{bmatrix} -\frac{d i_s}{dt} & -i_s & \frac{d v_s}{dt} & v_s \end{bmatrix} \begin{bmatrix} a_1 \\ a_0 \\ b_1 \\ b_0 \end{bmatrix} \tag{2.3}$$

Let us assume for the moment that the derivatives are available as measurable quantities. Later on we will see how, by applying a filter to the stator voltages and currents, we handle the problem of the derivative terms while keeping the linear relationship between the measurable quantities and the parameters to be estimated.

Since we would like to implement this algorithm digitally, let us define the measurement equation at time $k\Delta$, where Δ is the sampling interval. This is given by:

$$y_f(k) = \mathbf{C_f}(k)\,\theta_f \tag{2.4}$$

where

$$\begin{aligned} y_f(k) &= \frac{d^2 i_s}{dt^2} \text{ at time } k\Delta \\ \mathbf{C}_f(k) &= \left[-\frac{d\,i_s}{dt} \;\; -i_s \;\; \frac{d\,v_s}{dt} \;\; v_s\right] \text{ at time } k\Delta \\ \theta_f &= [a_1 \;\; a_0 \;\; b_1 \;\; ; b_0]^T \text{ is the vector of unknown parameters} \end{aligned}$$

where the subscript f refers to full regressor, since this model relates *speed and parameters* to the stator voltages and currents. Note that this is in a linear regression form, i.e. the unknown parameters and the measurements are linearly related. On-line parameter estimation methods for this type of model are widely discussed in the literature on system identification, see for example [37,58]. By estimating the parameters of the regressor model (2.4) we can identify the parameters described in (2.1). With algebraic combinations of these quantities, we can obtain many of the machine paramaters, including rotor speed ω_r, the rotor time constant T_r, L_r/σ, R_s, etc.

2.3.2 Linear Regression Model for Speed-Only Estimation

A variation of equation (2.3) can be obtained if the machine parameters are known. In this case the known quantities become the "measurements" and the speed becomes the only parameter to be estimated. Following this procedure, a linear regressor model where the speed is the only unknown parameter is obtained,

$$y_\omega(k) = C_\omega(k)\,\omega_r \tag{2.5}$$

where

$$\begin{aligned} y_\omega(k) &= \frac{di_s}{dt} + \frac{R_s L_r + R_r L_s}{\sigma}\frac{di}{dt} + \frac{R_r R_s}{\sigma} i_s - \frac{L_r}{\sigma}\frac{dv_s}{dt} - \frac{R_r}{\sigma} v_s \\ C_\omega(k) &= j\left(\frac{di_s}{dt} + \frac{L_r R_s}{\sigma} i_s - \frac{L_r}{\sigma} v_s\right) \end{aligned}$$

where all the quantities are measured at time $k\Delta$. The subscript ω is used here to point out the difference between this model and (2.4).

2.4 Avoiding Derivatives

The derivatives of the stator voltages and currents are not available as measurable quantities, so it is not possible to directly use the linear regression models derived previously for the estimation of speed and machine parameters. The question that arises is what kind of signal processing can be done to the measurable quantities (i.e. stator voltages and currents) so that the linear regression models are still useful for speed and parameter estimation. In this section we will present one possible method. A general treatment of this problem is presented in [16].

2.4.1 Linear Transformation of the Data

The linear structure of the regression model makes easy the use of a linear operator to solve the problem with the derivative terms. If a linear operator $T(\cdot)$ is applied to both sides of (2.4) we get:

$$T(y(k)) = T(\mathbf{C}(k))\ \theta$$

Let us pick a $T(\cdot)$ that commutes with the derivative operator inside (2.4). We are then able to interchange the derivative and $T(\cdot)$ operations, i.e.

$$T\left(\frac{d^i\, x(t)}{dt^i}\right) = \frac{d^i}{dt^i} T(x(t))$$

Let us introduce the notation

$$\begin{aligned} T_i(\cdot) &= \frac{d^i}{dt^i}\, T(\cdot) \\ x^{(i)}(t) &= \frac{d^i\, x(t)}{dt^i} \end{aligned}$$

to denote the i-th derivative of the transformed quantity and of the function $x(t)$ respectively.

Using this notation, the transformed linear regression model for speed and parameter estimation (2.4) is given by:

$$\bar{y}(k) = \bar{\mathbf{C}}(k)\,\theta \tag{2.6}$$

where

$$\begin{aligned} \bar{y}(k) &= T_2(i_s) \text{ at time } k\Delta \\ \bar{\mathbf{C}}(k) &= [-T_1(i_s) \;\; -T_0(i_s) \;\; T_1(v_s) \;\; T_0(v_s)] \text{ at time } k\Delta \\ \theta &= \text{ same as in (2.4)} \end{aligned}$$

The operator $T(\cdot)$ will be chosen so that all the quantities in (2.6) are obtainable without differentiation from measurable quantities. Note that by using the transformed stator voltages and currents, and their transformed derivatives instead of the true quantities, we are able to keep the linear relationship between parameters and measurements, which makes easier the estimation process. Therefore, instead of using the true derivatives of the stator voltages and currents, the estimation algorithm will use the derivatives of the transformed stator voltages and currents for estimation purposes. The use of this signal processing method for speed and parameter estimation is illustrated in Figure 2.1.

Up to this point we have said nothing specific about the selection of $T(\cdot)$. It is clear that the choice of $T(\cdot)$ will affect the properties of the estimation scheme, e.g. the kind of information produced, the speed of convergence to the solution, the possible bias of the solution, the influence of noise.

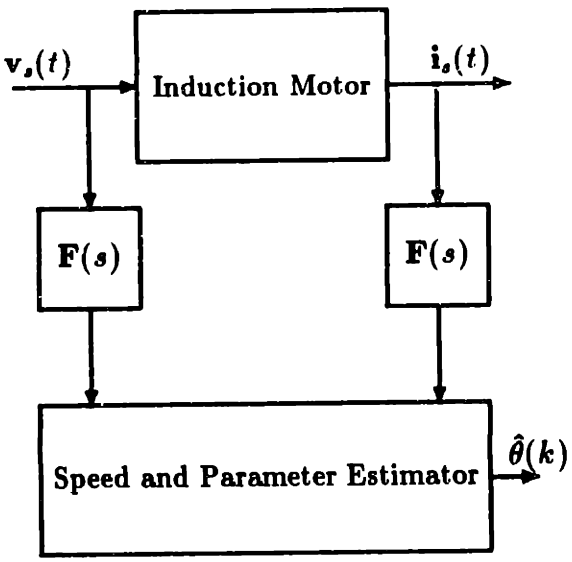

Figure 2.1: Speed and Parameter Estimation with Transformed Stator Voltages and Currents.

2.4.2 State Variable Filter

One possible $T(\cdot)$ is a stable LTI filter with impulse response $f(t)$. Applying this transformation to the equation (2.3) we get,

$$f * i_s^{(2)}(t) = \begin{bmatrix} -f * i_s^{(1)} & -f * i_s & f * v_s^{(1)} & f * v_s \end{bmatrix} \begin{bmatrix} a_1 \\ a_0 \\ b_1 \\ b_0 \end{bmatrix} \tag{2.7}$$

where $*$ denotes convolution. To get something of the form (2.6) we will need the following relationships (assume that $x(t)$ is bounded),

$$\begin{aligned} (f * x)(t) &= \int_0^\infty f(t-\tau)\, x(\tau)\, d\tau \\ \left(f * x^{(1)}\right)(t) &= x(0)\, f(0) + \int_0^\infty f^{(1)}(t-\tau)\, x(\tau)\, d\tau \\ \left(f * x^{(2)}\right)(t) &= x(0)\, f(0) + x^{(1)}(0)\, f^{(1)}(0) + \int_0^\infty f^{(2)}(t-\tau)\, x(\tau)\, d\tau \end{aligned}$$

If we pick $f(t)$ such that $f(0) = f^{(1)}(0) = 0$ we get that

$$f * x^{(1)} = f^{(1)} * x \tag{2.8}$$

$$f * x^{(2)} = f^{(2)} * x \tag{2.9}$$

These relationships can be used in (2.7) to process the stator voltages and currents and obtain the measurements for the estimation procedure.

One possible filter is the so called State Variable Filter (SVF). This is a stable LTI low-pass filter with transfer function $F(s)$ of the form

$$F(s) = \frac{1}{s^m + f_{m-1}s^{m-1} + \ldots + f_1 s + f_0} \tag{2.10}$$

This filter is realized in the standard controllable form, where *m-1* is the maximum order of the desired derivative.

In Figure 2.2 a block diagram of a third-order SVF is shown. Note that if we take as outputs the output of each integrator, the transformed signal and its derivatives are obtained. The normalized Bode plots of the transfer functions from the input to each of the outputs are shown in Figure 2.3. Ideally, if the measurements were noise free we could differentiate the stator voltages and currents to obtain the desired quantities for the estimator. However, due to noise effects this is not possible. By looking at the SVF Bode plots in Figure 2.3 it is clear that at frequencies below cutoff the filter basically differentiates the input signal. At higher frequencies the SVF provides the roll-off necessary for noise rejection.

Techniques for the design of filters of the form (2.10), e.g. Butterworth, Chebyschev, Bessel, are widely discussed in the literature. Certainly, the critical parameter in this design will be filter bandwidth. The selection of the bandwidth will represent a tradeoff between the noise rejection properties of the SVF and the richness of the signals input to the estimation algorithm. A rule of thumb is that the bandwidth should be greater than the system bandwidth. An upper bound will be given by the noise.

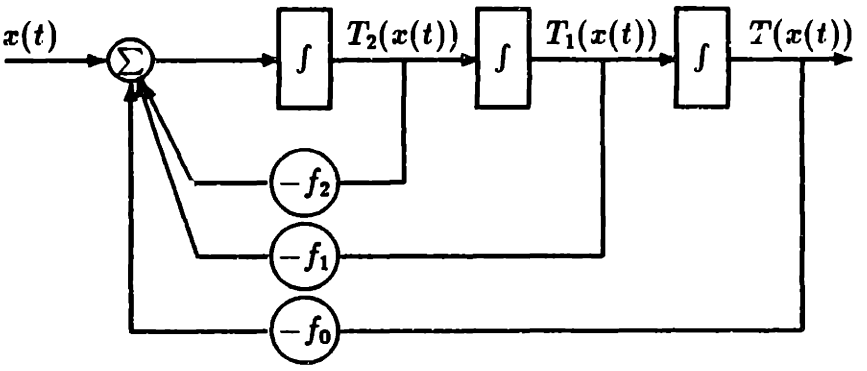

Figure 2.2: Third Order State Variable Filter.

Some examples involving the use of state variable filters in estimation algorithms for electromechanical system are presented in [21,22,26]. An example involving another kind of signal processing is presented in [17,24], where modulating functions (or mod-functions) [16] were used.

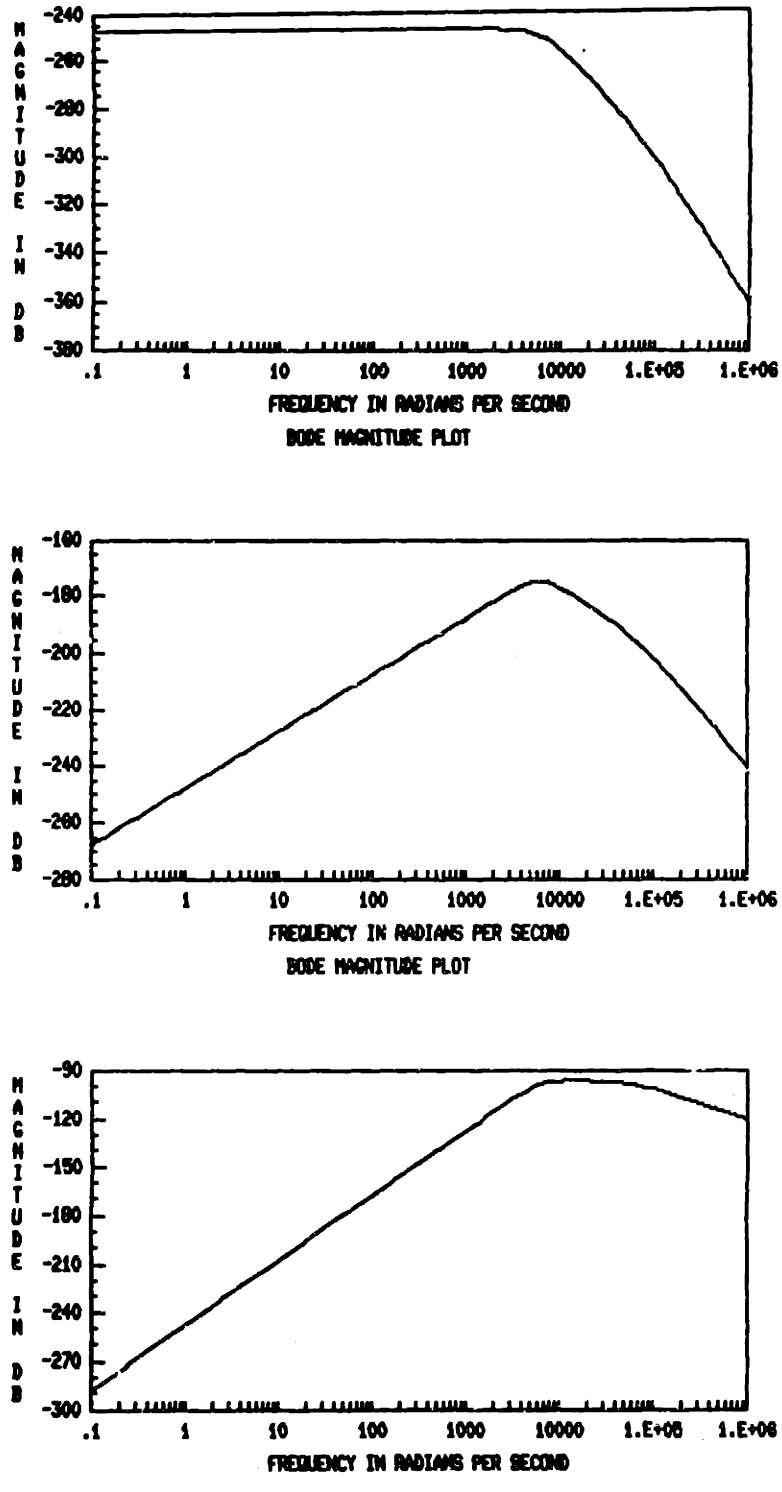

Figure 2.3: Bode Plots of a Third Order State Variable Filter.

Chapter 3

Recursive Least Squares Estimation of Speed and Machine Parameters

3.1 Introduction

In Chapter 2 two linear regression models that relate rotor speed and machine parameters to stator voltages and currents were presented. In this chapter we will develop an algorithm to estimate the machine parameters as well as the rotor speed using these two models. The derivation involves the use of the Recursive Linear Least Squares Estimation (RLSE) algorithm to estimate the parameters of the linear regression models (2.4) and (2.5).

This chapter is structured as follows. First, a brief introduction to output error methods to estimate the parameters of a linear regression model is given. Second, an introduction to the RLSE algorithm to estimate time varying parameters using a forgetting factor is given. Third, the algorithm design procedure is presented.

3.2 Output Error Methods for the Estimation of the Parameters of a Linear Regression Model

In Chapter 2 the induction machine speed and parameter estimation problem was reformulated as the parameter estimation problem for a linear regression model:

$$y(k) = \mathbf{C}(k)\,\theta \tag{3.1}$$

where $y(k) \epsilon \mathcal{C}$ and θ, $\mathbf{C}^T(k) \epsilon \mathcal{C}^4$. Here $\mathcal{C}^n$ denotes the n-dimensional complex space.

One way to estimate the parameters of this model is by comparing the measured output $y(k)$ with its best estimate based on the available information up to time $(k-1)\Delta$, namely $\hat{y}(k/k-1)$. The basic idea of the estimation algorithm is to tune the parameters of the model so that the model will *fit* as closely as possible, in some sense, the measured behavior of the system.

Let us define the *output error* $e(k)$ to be the difference between the model output and the system output. That is,

$$e(k) = y(k) - \hat{y}(k/k-1)$$

The estimation algorithm will look at $e(k)$ and adjust the model parameters accordingly. This is illustrated in Figure 3.1.

The form of the estimator we are interested in is linear. That is,

$$\hat{\theta}(k) = \hat{\theta}(k-1) + \mathbf{K}(k)e(k) \tag{3.2}$$

where $\hat{\theta}(k)$ is the parameter estimate at time k, $\mathbf{K}(k)$ is the updating gain and $e(k)$ is the output error. Estimators of the form (3.2) appear in many contexts in estimation theory. The parameter updating is done according to the product $\mathbf{K}(k)e(k)$. The design problem turns out to be: *how to choose the updating gain such that the algorithm meets the desired performance specifications.*

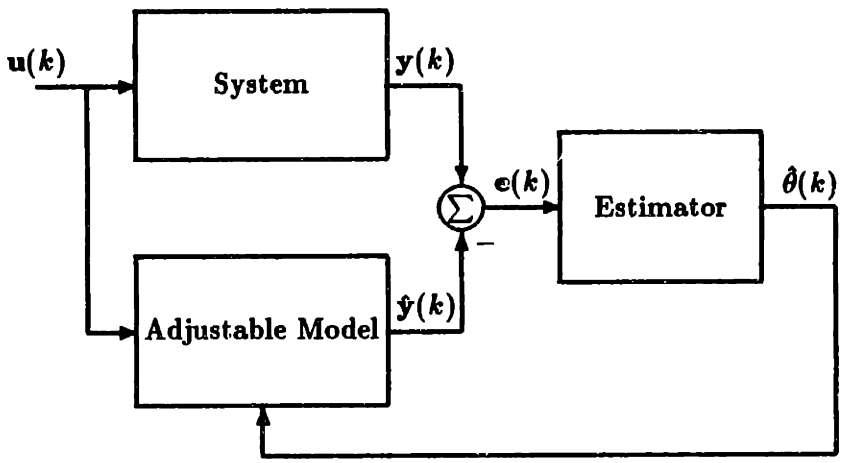

Figure 3.1: Output Error Methods for Parameter Estimation.

The prime objective of this research work is the design and testing of an estimation algorithm that will *track* variations in rotor speed as well as in the machine parameters. Taking a look at equation (3.2), we can see that in order for the estimation algorithm to be able to track parameter variations, it should stay *alert*. This is done by keeping the updating gain $\mathbf{K}(k)$ from going to zero. Another requirement will be that the algorithm has good performance under the presence of noise in the measurements.

There are many ways to achieve these objectives. The reader is referred to [23,37,58] for further information. In this chapter we introduce the algorithm used in this thesis to perform this task.

3.3 Recursive Linear Least Squares Parameter Estimation for a Linear Regression Model

A common criterion used to measure how well the model fits the measured behavior of the system is the weighted sum of squares of the output error magnitude:

$$J_k(\theta) = \sum_{l=1}^{k} \beta(k,l)\, e^*(l) e(l) \tag{3.3}$$

where $\beta(k,l)$ is a weighting sequence and $e^*(l)$ is the complex conjugate of $e(l)$. The updating gain is picked to minimize this criterion. The weighting sequence is chosen such that it gives more weight to the most recent measurements, while discarding old data that might not contain information about the present value of the parameters. By picking $\beta(k,l)$ in this way we will keep the updating gain from going to zero [37].

In this context, the estimation problem can be reformulated as a constrained optimization problem. That is, the value of the parameter estimate at time $k\Delta$ is given by

$$\hat{\theta}(k) = \arg \min_{\theta \epsilon C^4} J_k(\theta)$$

subject to

$$y(l) = \mathbf{C}(l)\theta(l), \qquad l = 1, 2, ..., k$$

In its present formulation, the solution of this problem will require the knowledge of all measurements up to time $k\Delta$. This is undesirable from the standpoint of real time implementation. However, it turns out that a recursive solution to this problem exists, and can be easily computed.

First, let us pick the weighting sequence $\beta(k,l)$ such that

$$\beta(k,l) = \alpha(k)\beta(k-1,l), \quad 1 \leq l \leq k-1 \tag{3.4}$$

$$\beta(k,k) = 1 \tag{3.5}$$

where $\alpha(k)$ is a positive number with magnitude less than one. This means that we may write

$$\beta(k,l) = \prod_{m=l+1}^{k} \alpha(m)$$

The recursive solution for the estimation problem posed previously is then given by:

$$\hat{\theta}(k) = \hat{\theta}(k-1) + \mathbf{K}(k)\left(y(k) - \mathbf{C}(k)\hat{\theta}(k-1)\right) \tag{3.6}$$

$$\mathbf{K}(k) = \mathbf{P}(k-1)\,\mathbf{C}^H(k)\left(\alpha(k) + \mathbf{C}(k)\,\mathbf{P}(k-1)\,\mathbf{C}^H(k)\right)^{-1} \tag{3.7}$$

$$\mathbf{P}(k) = \mathbf{P}(k-1) - \frac{\mathbf{P}(k-1)\,\mathbf{C}(k-1)\,\mathbf{C}^H(k-1)\,\mathbf{P}(k-1)}{(\alpha(k) + \mathbf{C}(k-1)\,\mathbf{P}(k-1)\,\mathbf{C}^H(k-1))} \tag{3.8}$$

$$\mathbf{P}(0) = \rho\mathbf{I} \tag{3.9}$$

where ρ is a positive number that reflects our confidence in the initial estimate $\hat{\theta}(0)$ of the parameter values. Note that this algorithm has the form specified in (3.2). The new parameter estimate is based only on the previous estimate $\hat{\theta}(k-1)$ and the measurements at time $k\Delta$. Therefore, we only need to store the current estimate and the covariance[1] matrix $\mathbf{P}(k-1)$.

The current formulation of the RLS algorithm allows the minimum of $J_k(\theta)$ to fall anywhere in the parameter space $\mathcal{C}^4$. Due to physical constraints, this condition is undesirable. For example, negative resistances and inductances are meaningless. Also, the machine parameters can only assume certain ranges of values. Therefore, in order to obtain estimates with physical meaning, those constraints have to be incorporated into the algorithm (3.6)-(3.8). To satisfy these constraints, the algorithm (3.6)-(3.8) should incorporate a projection into the region of allowed parameters values $\mathcal{D}_m$. That implies that instead of using the "true" RLS estimate as described by (3.6) as the parameter update at time $k\Delta$, its projection into $\mathcal{D}_m$ is used.

[1]The term covariance is used in this context to point out the similarity between the structure of the estimator given by (3.6) to (3.8) and the Kalman filter. In general this matrix does not represent the covariance of the estimation error.

3.3.1 Forgetting Factors to Account for Time Variations

An intuitive way to take into account time variations of the system parameters is by giving more weight to the most recent measurements in (3.3). This can be done by letting the weighting sequence $\beta(k,l)$ be of the form,

$$\begin{aligned} \beta(k,l) &= \alpha_0^{k-l} \\ 0 < \alpha_0 &< 1 \end{aligned}$$

or equivalent by

$$\alpha(k) = \alpha_0 \tag{3.10}$$

This kind of weighting will give an exponentially fading memory to the estimator.

To understand the effect of the forgetting factor upon algorithm performance, let us take a look at the equation describing the propagation of the inverse covariance matrix $\mathbf{R}(k)$:

$$\mathbf{R}(k) = \mathbf{P}^{-1}(k) \tag{3.11}$$

$$\mathbf{R}(k) = \alpha_0 \mathbf{R}(k-1) + \mathbf{C}^H(k)\mathbf{C}(k) \tag{3.12}$$

From this equation it is clear that $\mathbf{R}(k)$ is at least a positive semidefinite matrix. This is a first order matrix difference equation, so for $\alpha_0 < 1$ this is a stable system. The solution for this can be easily computed and is given by,

$$\mathbf{R}(k) = \alpha_0^k \mathbf{R}(0) + \sum_{l=1}^{k} \alpha_0^{k-l} \mathbf{C}^H(l)\mathbf{C}(l) \tag{3.13}$$

Proper operation of the algorithm requires the covariance matrix to be kept positive definite [37]. It is clear from (3.11) that this is equivalent to keep $\mathbf{R}(k)$ positive definite. Two things will be of great importance for this: the forgetting factor and the richness of the input signals. The latter is an important condition required for the convergence of least squares algorithm [23].

If the forgetting factor is small the new value of $\mathbf{R}(k)$ given by (3.12) will be dependent mostly on the term $\mathbf{C}^H(k)\mathbf{C}(k)$, which in general is only positive semidefinite. This will have the effect of making $\mathbf{R}(k)$ semidefinite with the effect of $\mathbf{P}(k)$ to blow up. As α_0 approaches 1 the matrices become better behaved. The richness condition on the input signals forces $\mathbf{C}(l)$ to vary sufficiently as l varies, so that the sumation in (3.13) results in a sufficiently positive definite matrix.

In all cases, due to the fact that (3.12) represents the model of a stable system and assuming $\mathbf{C}(k)$ to be bounded, the solution $\mathbf{R}(k)$ is bounded. Furthermore, if $\mathbf{R}(k)$ is positive definite, the inverse in (3.11) is defined. Using these facts it is clear then that the effect of the forgetting factor is to keep the covariance matrix $\mathbf{P}(k)$ from going to zero, and therefore, keeping the updating gain from vanishing.

There are many possibilities for picking α_0. The selection depends on how fast the parameters change as a function of time. A good choice of α_0 must take into account the time constants of the parameter variations as well as the sampling rate. It is interesting to think of the forgetting factor α_0 as

$$\alpha_0 = \exp\left(-\frac{\Delta}{\tau_e}\right)$$

where Δ is the sampling period and τ_e is the exponential age-weighting time constant: the smaller τ_e, the faster the prior data will be aged, and thus forgotten by the estimator. Solving for τ_e we get

$$\tau_e = -\frac{\Delta}{\ln(\alpha_0)} \tag{3.14}$$

A good choice of α_0 would be to pick it so that the time constant of the exponential weighting is smaller than the time constant associated with the parameter time variation, so that in a time interval of length τ_e the variation of the parameters is relatively small.

The faster the time variation is, the smaller the time constant of the exponential weighting should be. A small time constant can be obtained by using a small forgetting

factor or a small sampling interval Δ. Due to the covariance blow up phenomena described previously, numerical problems may arise when a small forgetting factor is used. Also, associated with small forgetting factors are higher steady state gains which make the algorithm more susceptible to noise[2]. On the other hand, by increasing the sampling rate, more computational power is needed. Therefore, the selection of the forgetting factor will be a compromise between noise immunity, computational power, and tracking capabilities. In practice a common choice for α_0 is

$$\begin{aligned} 0.99 \leq \quad & \alpha_0 \quad \leq 0.998 \\ 0.002 \leq \quad & \frac{\Delta}{\tau_e} \quad \leq 0.01 \end{aligned}$$

We can see that the number of significant samples in the estimator memory N can be approximated by [58],

$$N = \frac{\tau_e}{\Delta} = \frac{1}{1-\lambda}$$

In practice [37], it has been found useful to use a time varying forgetting factor $\alpha(k)$ which initially is smaller than α_0 but approaches it asymptotically. In this manner, we will have an algorithm with initially small memory but growing towards the specified length as time increases. This helps initial convergence by removing the effects of initial conditions quickly. When $\alpha(k) = \alpha_0$, these effects decay with a fixed time constant.

3.4 Design of the Estimator

In the previous section, we presented the RLSE algorithm using forgetting factors for the estimation of time-varying parameters in a linear regression model. In this section we will show how the RLSE algorithm is used in combination with the regression models (2.4) and (2.5) to develop an algorithm to estimate the speed and parameters of the induction machine.

[2]This is not surprising since smaller forgetting factors lead to less averaging of the noise

3.4.1 Time-Scale Separation Between Parameters and Speed

Physically, we might expect that the rate of change of the machine parameters is slower than the rate of change associated with the rotor speed. In its present formulation the RLSE algorithm using forgetting factors does not take into account differences in the parameters' rates of change. This will result in a problem when the differences between the rates of change of the different parameters are significant. That is, for the fast parameters we will need to use either a small forgetting factor or high sampling rates in the hardware implementation of the algorithm.

To illustrate this point, simulation results for the RLSE speed estimator, based on (2.5), are shown in Figure 3.2. The parameters of the machine model are given in Table 3.1. The sampling rate is set to 1 kHz. Note how the tracking capabilities of the algorithm are affected by the forgetting factor. The larger the forgetting factor, the larger the tracking error. It seems that a forgetting factor of 0.7 will do a reasonable job. On the other hand using a forgetting factor of 0.7 for the full RLSE speed and parameters estimator, based on (2.4), will cause the covariance matrix $\mathbf{P}(k)$ to blow up.

Since the machine parameters change during operation, it will be necessary to periodically update the values of the parameters used by the speed-only estimator (i.e. the RLSE based on (2.5)) in order to have an accurate speed estimate. A simulation result for the speed-only estimator with the rotor resistance changed by 50 % is shown in Figure 3.4. Note that having the wrong parameter values will introduce bias into the steady state value of the estimate.

There is evidently a conflict between the desired speed tracking capabilities and issues related to the implementation of the algorithm. If the RLSE based on (2.4) is used to do both speed and parameter estimation, we will require (expensive) hardware with fast computational power in order to do good speed tracking. A solution to this is

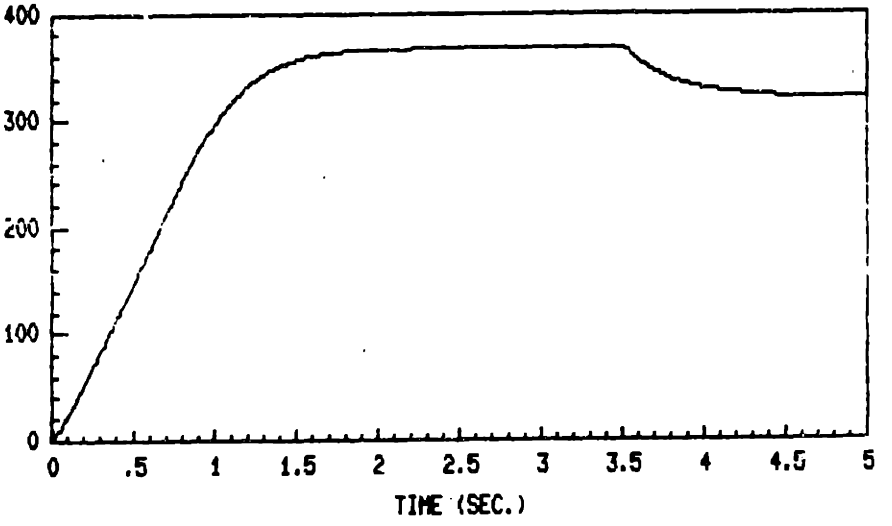

(a)

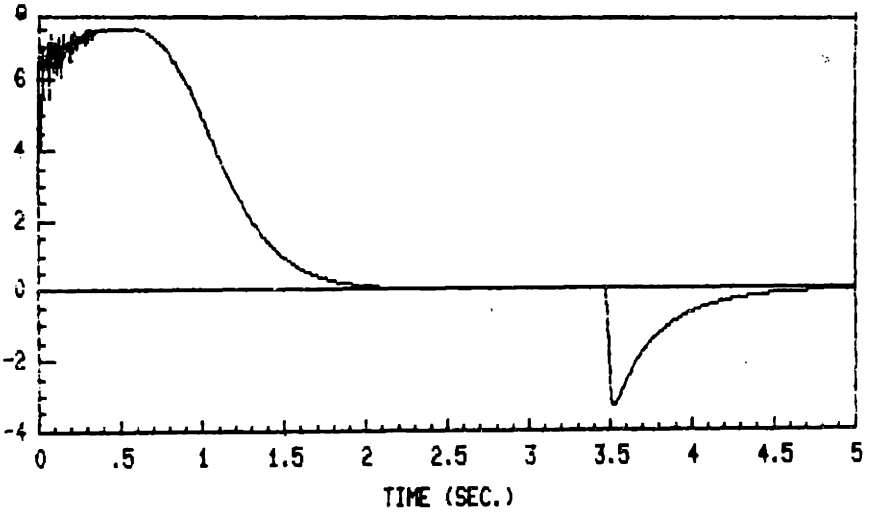

(b)

Figure 3.2: Simulation Results for the Speed-Only Estimator for $\alpha_0 = 0.7$: (a) Speed Estimate, (b) Error in Speed Estimate.

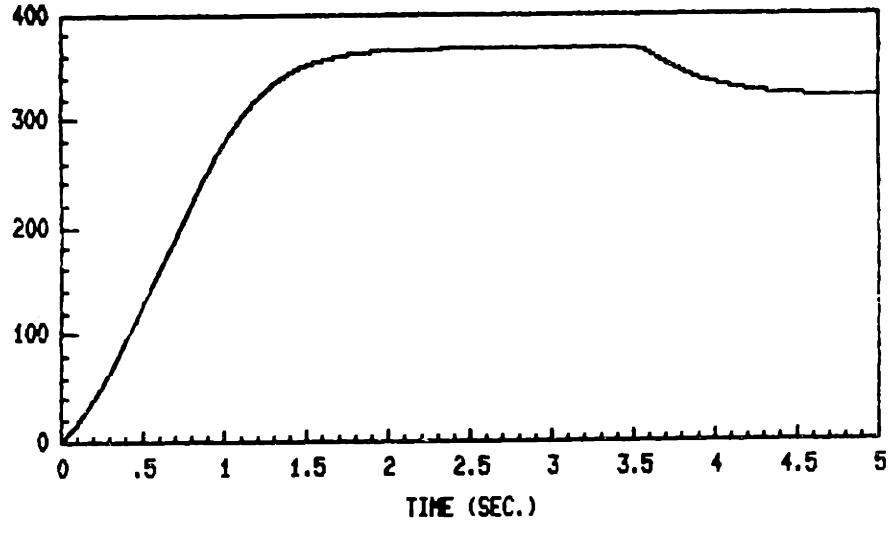

(a)

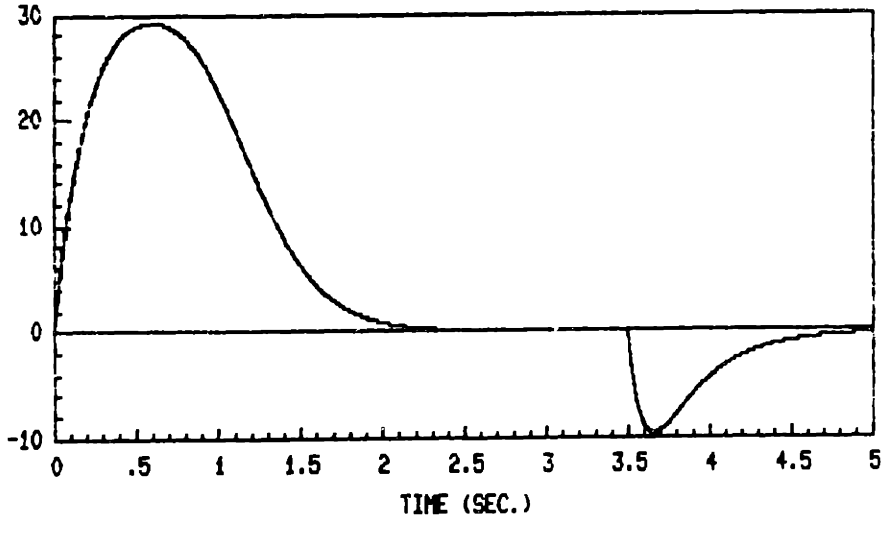

(b)

Figure 3.3: Simulation Results for the Speed-Only Estimator for $\alpha_0 = 0.99$:(a) Speed Estimate, (b) Error in Speed Estimate.

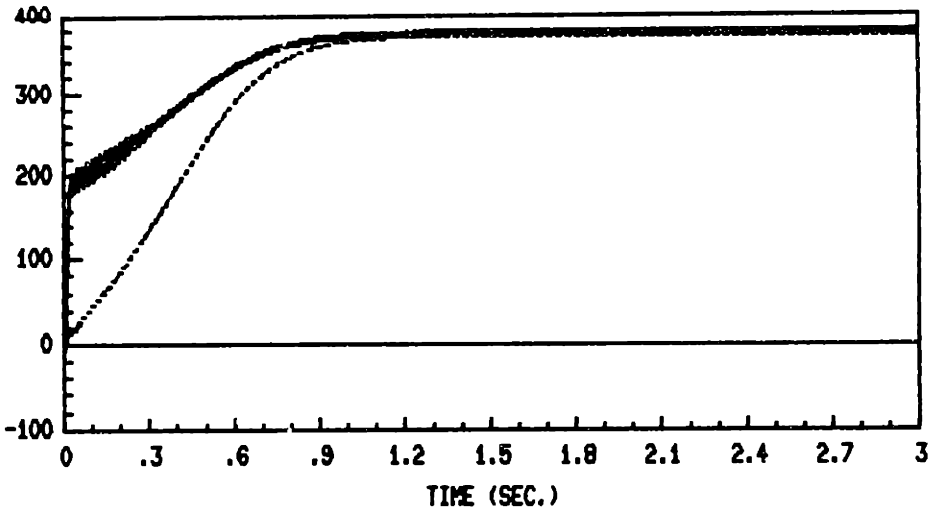

(a)

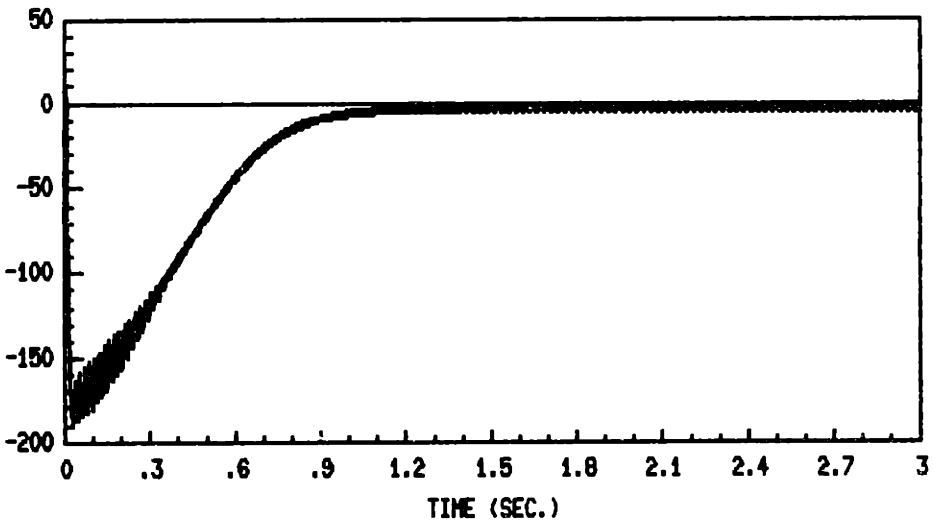

(b)

Figure 3.4: Speed-Only Estimator with 50 % Error in the Value of the Rotor Resistance ($\alpha_0 = 0.7$): (a) True and Estimated Rotor Speed, (b) Error in Speed Estimate.

Parameter Name	Value
R_s	0.4350 Ω
R_r	0.8160 Ω
L_s	0.0713 H
L_r	0.0713 H
M	0.0693 H

Table 3.1: Parameters of the 3 hp Machine

proposed next, using a two-stage estimator. This estimator takes advantage of the time scale separation between the variations in the rotor speed and the machine parameters.

3.4.2 Two-Stage Estimator

Due to the time scale separation between variations in the machine parameters and the rotor speed, the estimation procedure will be decomposed into two parallel procedures: a fast estimator that will be in charge of estimating only the rotor speed and an estimator that will estimate the machine parameters. This is illustrated in Figure 3.5. The fast or speed-only estimator is the RLSE for the regression model (2.5). Similarly, the slow or full estimator is the RLSE for the regressionmodel (2.4).

The algorithm will work as follows. The main procedure is the speed-only estimator, while the full estimator will work as an auxiliary procedure that will interrupt the speed-only estimator to update the parameter values used by the speed-only estimator.

Due to this two-stage estimation procedure, we are able to design each estimator independently, so the designer can choose the design parameters so that each estimator has the tracking capabilities necessary for each estimation problem. The speed-only estimator is designed with a small forgetting factor so that it can track the faster variations associated with the rotor speed. For the speed-only estimator a small forgetting factor will not represent a problem, since the associated inverse covariance matrix is a

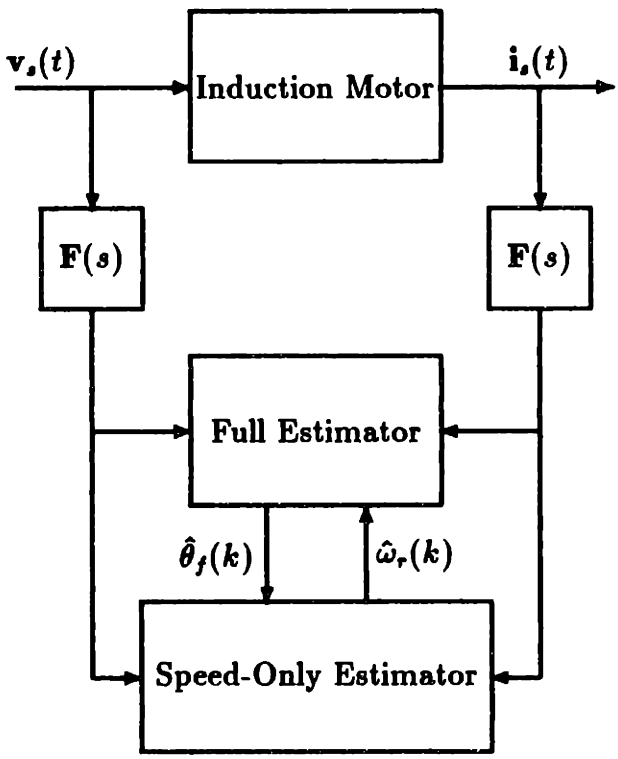

Figure 3.5: Block Diagram of the Two-Stage Estimator.

scalar quantity. The full estimator can use a larger forgetting factor since the parameter variations are slower. This will improve the estimator's numerical robustness. A flowchart describing the two-stage estimator is shown in Figure 3.6.

The recursion is started with the speed only estimator using the initial parameter values obtained from the blocked-rotor and no-load tests. After certain amount of time the full estimator interrupts the speed-only estimator and takes control over the estimation. Before computing the new parameter estimate the imaginary part of $\hat{\theta}_f$ of the full estimator is updated by incorporating the most recent estimate of the rotor speed $\hat{\omega}_r$ obtained from the speed-only estimator. This is needed because during the time when the full estimator is off the rotor speed may have changed significantly from the value at the time when the last parameter update was made. After updating the machine parameters the control of the estimation is transfer back to the speed-only estimator. Note that even thought the speed is estimated as part of the parameters in the full estimator the obtained value is not used by the speed-only estimator when the control is transfer back. This is because in the simulations we observed that the estimates behave better when this is done.

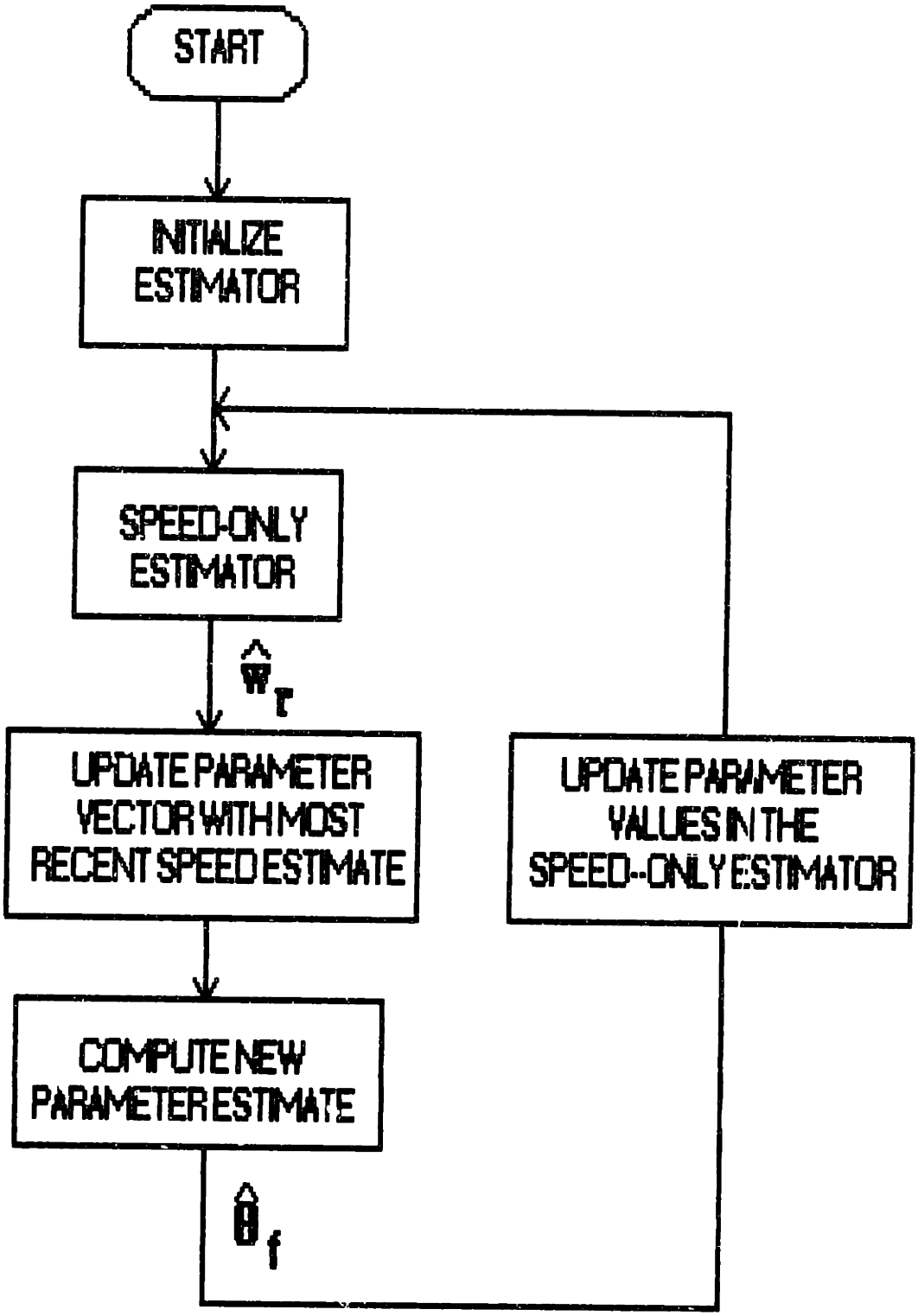

Figure 3.6: Flowchart of the Estimation Algorithm.

Chapter 4

Simulation Studies for the Estimation Algorithm

4.1 Introduction

The study of the estimator from the analytical point of view is very difficult due to the nonlinear time-varying nature of the algorithm. In this section we will study the performance of the estimator through simulations. We will focus our attention on trying to understand its tracking capabilities and study the performance of the estimator under uncertainties in the measured quantities.

4.2 Study of Tracking Capabilities

In this section the estimator tracking capabilities for speed and parameter variations using noise free measurements are studied. The parameters of the machine used are the same as in Table 3.1. The estimator parameters for the simulation are as follows:

$$\begin{aligned} \hat{\omega}_r(0) &= 0 \\ \hat{\theta}_f(0) &= [\ 285.48\ \ 1136.07\ \ 228.20\ \ 2611.65\ ]^T \\ \alpha_{\omega,0} &= 0.7 \end{aligned}$$

$$\mathbf{P}(0) = \mathbf{I}$$

A time varying forgetting factor of the form

$$\alpha_f(k) = g_0\, \alpha_f(k-1) + (1 - g_0)\, \alpha_{f_s}$$

where

$$\alpha_f(0) = 0.9, \quad \alpha_{f_s} = 0.99, \quad g_0 = 0.99$$

was used by the full estimator. The subscripts ω and f refer to the speed-only and full estimator respectively. The values for the time varying forgetting factor of the parameter estimator are obtained from empirical information presented in [37].

The simulation results are shown in Figures 4.1. Only real parts of the complex coefficients a_1, a_0, b_1 b_0 are plotted. The results show that the algorithm exhibits a good tracking performance for speed variations as well as for parameter variations.

Note the interesting behavior of the parameters estimates. The parameters associated with the coefficients of the derivative quantities, a_{1R}, b_1, converge faster than those associated with the non derivative terms a_{0R}, b_{0R}. This behavior can be explained by looking at the sensitivity of $y(k)$ with respect to these parameters. That is,

$$\begin{aligned}
\frac{dy(k)}{da_1} &= -\frac{di_s}{dt} \\
\frac{dy(k)}{da_0} &= -i_s \\
\frac{dy(k)}{db_1} &= \frac{dv_s}{dt} \\
\frac{dy(k)}{db_0} &= v_s
\end{aligned}$$

Since the richness of the derivative terms is larger than the richness of the non derivative terms, $y(k)$ is more sensitive to the parameters associated with the derivative terms. Therefore, is reasonable to think that a_1 and b_1 are more identifiable from the

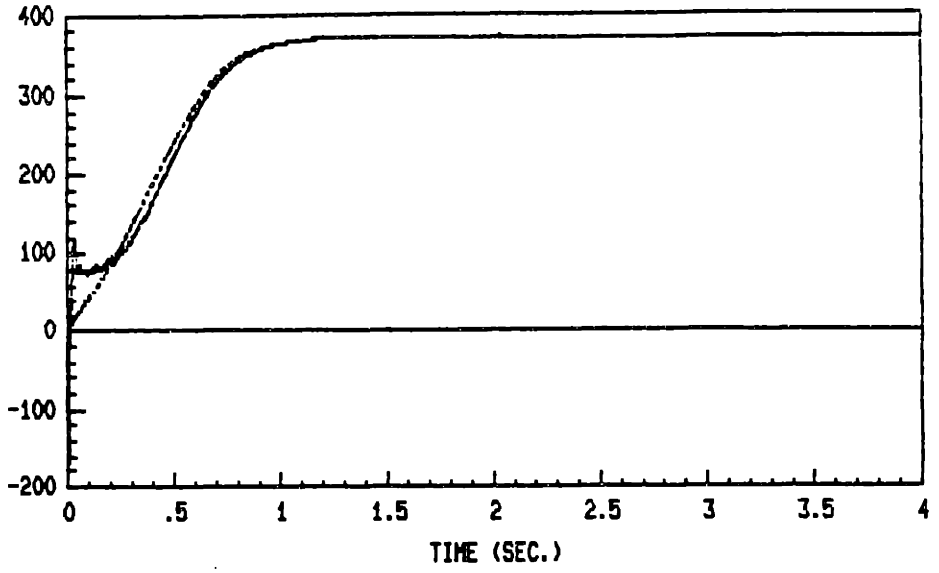

(a)

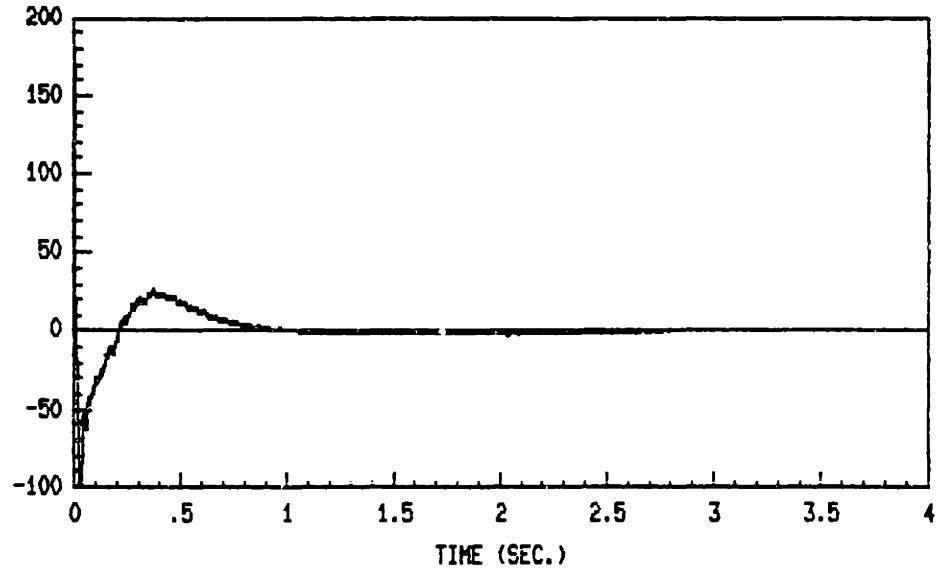

(b)

Figure 4.1: Performance of the Two-Stage Estimator: (a) True Speed and Speed Estimate, (b) Error in the Speed Estimate.

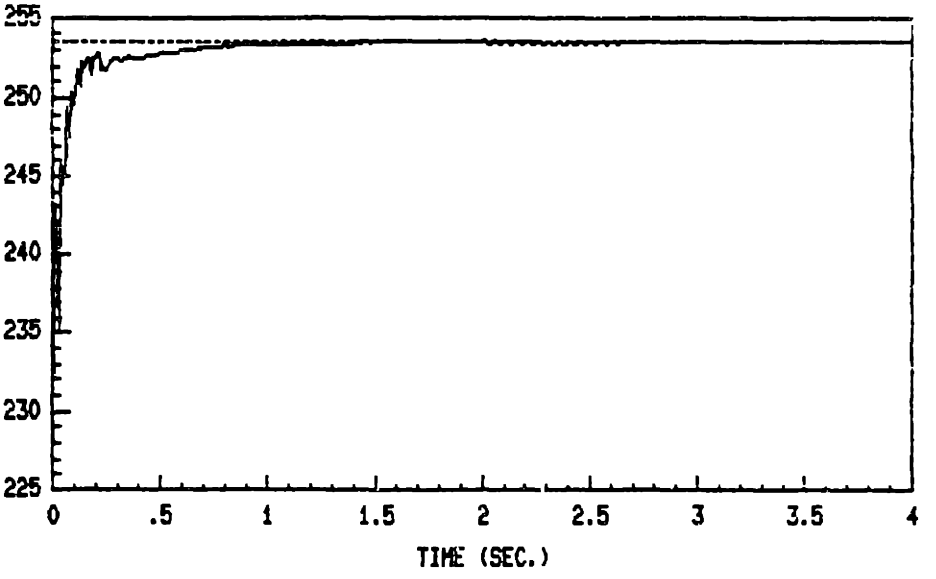

(a)

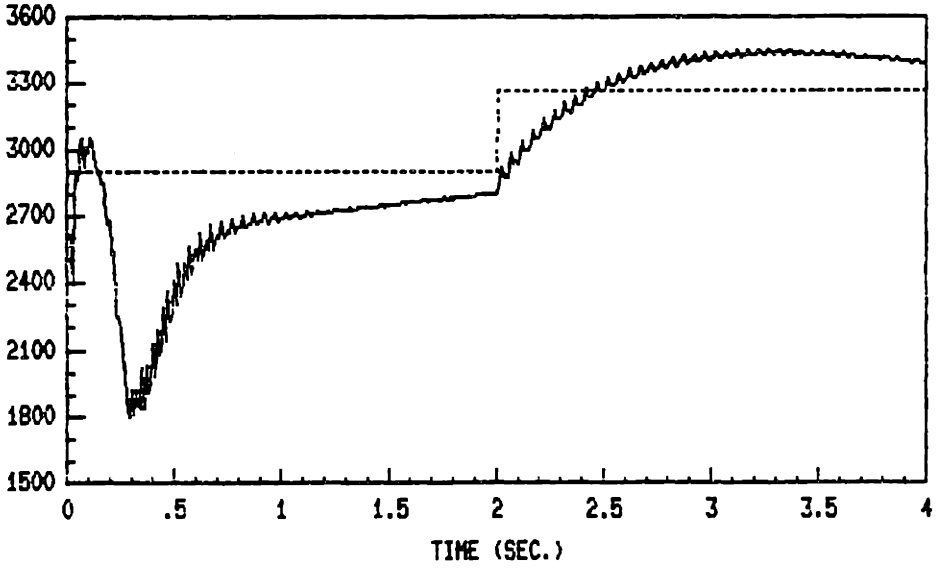

(b)

Figure 4.2: Performance of the Estimator: (a) Estimate of a_{1R}, (b) Estimate of a_{0R}.

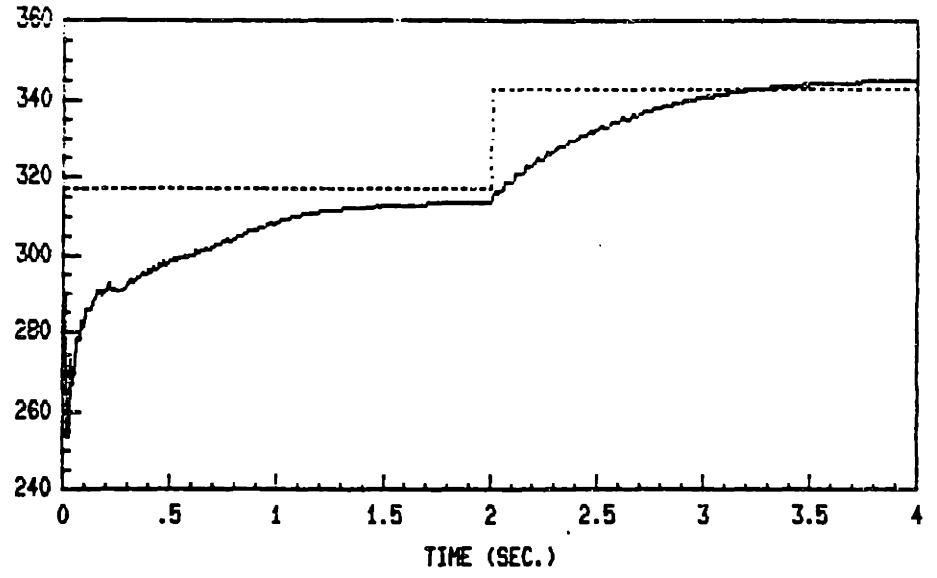

(a)

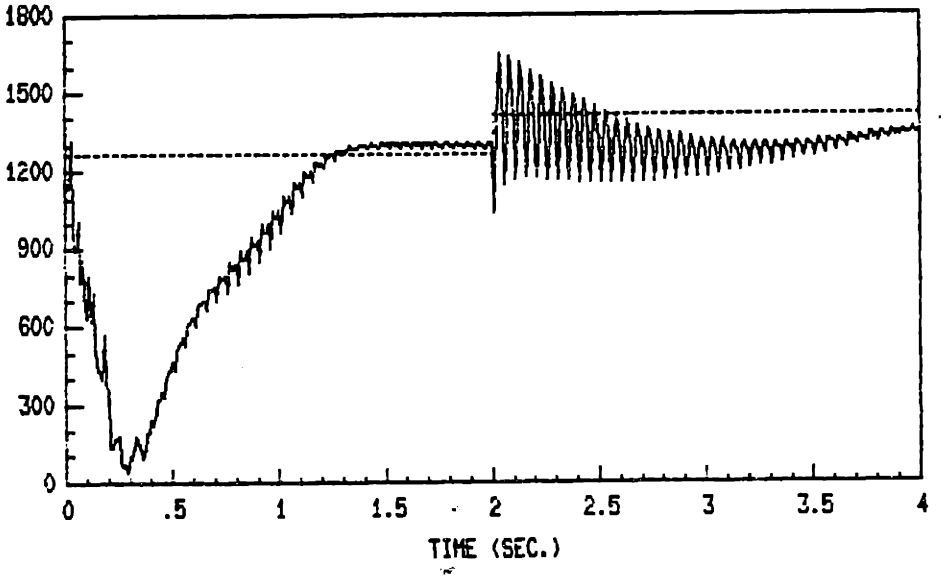

(b)

Figure 4.3: Performance of the Estimator: (a) Estimate of b_1, (b) Estimate of b_{0R}.

measured quantities than a_0 and b_0. Note that the sensitivity parameters described previously are highly dependent on scaling of the measurements.

4.3 Effect of Disturbances

The estimation algorithm presented in Chapter 3 was based on a deterministic problem formulation. We have shown, by means of simulations, the ability of this algorithm to estimate and track variations of the rotor speed and the induction machine parameters. In the case where measurements of stator voltages and currents are corrupted by noise, it is of interest to study the behavior of the proposed estimator as well.

In its present formulation, the estimator based on least squares assumes that the uncertainty is constrained to be in the measurement $y(k)$ while the $\mathbf{C}(k)$ matrix of the linear regression model is assumed to be known perfectly. However, since $\mathbf{C}(k)$ and $y(k)$ are both dependent on the measurements obtained from the output of the state variable filter, we will have uncertainties present in both quantities. If the uncertainty in $\mathbf{C}(k)$ is small, we should expect that the estimator based on the least squares criterion should produce good estimates of the parameter vector θ. However, as the uncertainty in $\mathbf{C}(k)$ increases, the estimates based on the least squares should be poor.

We focus our attention on trying to understand the effect of these uncertainties in an intuitive manner, rather than complicating our discussion with examination of random processes. Furthermore, to keep the discussion simple, our attention is limited to the constant speed and parameters case. The reason for this is that by keeping the speed and parameters constant the resulting machine model is time invariant, so it is easier to visualize the effects of the disturbances on the performance of the estimator.

4.3.1 Batch Estimation

Since we are dealing with constant speed and parameters, it is possible to estimate the values of the rotor and machine parameters in batch mode. In this section we will look at the noise effects on the batch estimates of the speed and machine parameters for the full regressor model (2.4).

Let us define the following vector quantities:

$$\begin{aligned} \mathbf{Y}_k &= [y(1)\ \ y(2) \ldots y(k)]^T \\ \mathbf{C}_k &= \left[\mathbf{C}^H(1)\ \ \mathbf{C}^H(2) \ldots \mathbf{C}^H(k)\right]^H \end{aligned}$$

In terms of these vector quantities the measurement equation is given by,

$$\mathbf{Y}_k = \mathbf{C}_k\, \theta$$

The least squares estimate is the value of θ that minimizes:

$$J(\theta) = (\mathbf{Y}_k - \mathbf{C}_k\theta)^H (\mathbf{Y}_k - \mathbf{C}_k\theta)$$

and is given by

$$\hat{\theta} = \left(\mathbf{C}_k^H \mathbf{C}_k\right)^{-1} \mathbf{C}_k^H\ \mathbf{Y}_k \tag{4.1}$$

In Table 4.1 the batch LS estimates of the transfer function coefficients for different signal to noise ratios (SNRs)[1] are shown. From these results we can see that by increasing the uncertainty in $\mathbf{C}_k$ the LS estimate degrades. The effect of the uncertainty in $\mathbf{C}_k$ on the parameter estimates using least squares is to introduce bias in the estimates. Furthermore, those parameters associated with the filtered stator voltages and currents have the largest estimation errors. The estimates of the coefficients associated with the filtered derivatives seem to be more robust to the uncertainty in $\mathbf{C}_k$. This agrees with the sensitivity analysis done previously.

4.3.2 Two-Stage Estimator with Noisy Measurements

In the previous section we studied how noise in the measurements can affect the estimates of the rotor speed and machine parameters by looking at the batch estimates. In this section we will study, by means of simulations the effect of noisy measurements

[1]The SNR in this example is defined as the minimum SNR of the signals output by the state variable filters. The SNR is computed as the ratio of the mean square value of the signal over the mean squared value of the noise.

Parameter	SNR				
	True	166.36	6.6542	1.6636	.01663
ω_r	360.00	360.26	355.60	343.94	-123.34
a_{1R}	317.20	317.23	319.52	324.09	475.19
a_{0R}	126.23	957.07	-6,469.1	-16,907	-26,304
b_1	253.56	253.59	253.94	254.09	228.18
b_{0R}	2901.8	2919.5	2766.0	2572.4	8924.8

Table 4.1: Batch LS Estimates of the Speed and Real Part of the Transfer Function Coefficients for the Constant Speed and Parameters Case.

upon the performance of the actual two-stage estimator. We will limit our attention to the constant speed and parameter case, and examine the convergence and the steady state behavior of the estimator.

Before looking at the simulation results, let us discuss how the noise affects the estimator behavior. If the estimates at some time lock in with the true values of the parameters, the output error will be due mainly to the measurement noise. However, since the updating gain will never go to zero, the noise will drive the estimator, changing the values of the parameter estimate accordingly. As a result the estimates will never converge to the true value of the parameters. Rather, they will be randomly varying quantities with mean around the steady-state values shown in Table 4.1.

The simulation results for the noise free and noisy LTI case are shown in Figures 4.4 to 4.9. The estimates for the noise free case converge fast to their true values. For the noisy case (SNR = 1.66), the speed and parameter estimates have a different behavior. First, the estimates do not converge to their true values; they are randomly varying quantities with means close to the values predicted by the batch estimates given previously. Due to the smaller forgetting factor the speed estimate is much noisier than the parameter estimates. This is not surprising because, by using a smaller forgetting factor, the averaging over the noise is smaller. In general the selection of forgetting

factor will represent a tradeoff between tracking capabilities and noise immunity.

4.4 Final Comments on Simulations

We ran many simulations of the estimator. In this section we sumarize some observations regarding the two-stage estimator that are not brought out by the simulation results shown here:

- The convergence rate is highly affected by initial conditions. Specifically, picking the initial covariance matrix $\mathbf{P}(0)$, to be large (small) makes the algorithm to converge fast (slow). However, with large initial covariance we have the worst transient behavior because of the large overshoots.

- The speed-only estimator will converge (during constant speed), or stay close to the true value (during speed transients) whenever the estimated value of the parameters is close to their true value. If the error in the estimated parameters is large the speed estimator will not get close to the true value of the speed until the parameters get close to their true values.

- After extended operation the estimator may become unstable due to roundoff errors. This is because the covariance matrix $\mathbf{P}(k)$ becomes negative definite. To avoid that, better methods for computing the covariance matrix $\mathbf{P}(k)$ are needed. Also the covariance matrix can get very small so periodic covariance resetting is needed in order to mantain the tracking capabilities of the algorithm.

- During steady state operation of the machine, the richness of the signals may decrease making the covariance matrixx of the full estimator blow up. So it is desirable to use time varying forgetting factors so that in steady state they are close to 1. Another method is to incorporate a richness test that turn on or off the estimator depending on the richness of the signals input to the algorithm.

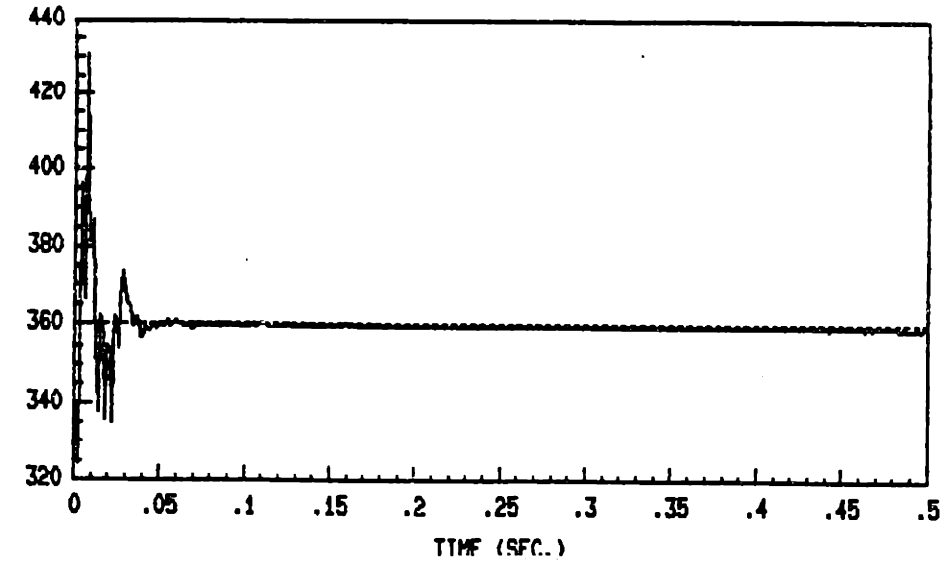

(a)

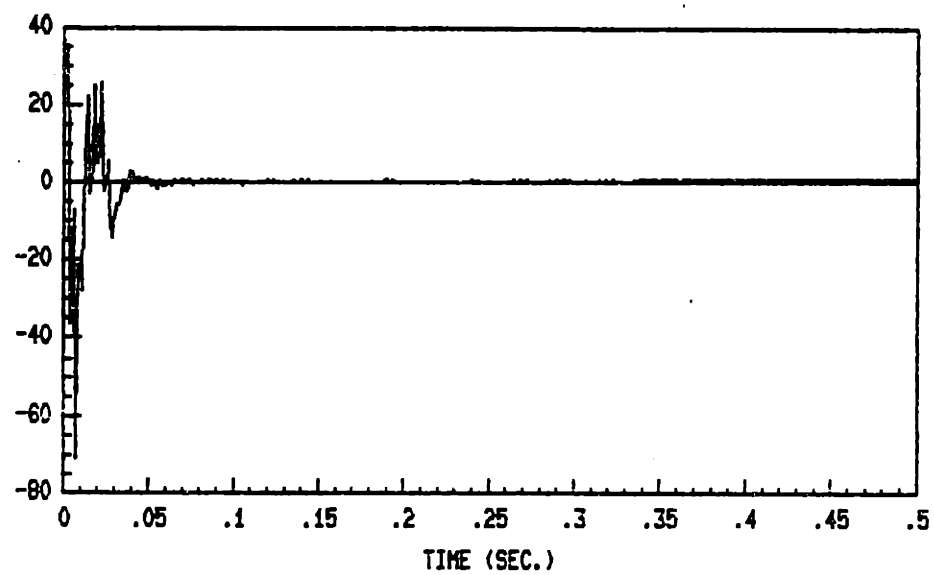

(b)

Figure 4.4: Performance of the Two-Stage Estimator (LTI with Noise Free Measurements): (a) True Speed and Speed Estimate, (b) Error in the Speed Estimate.

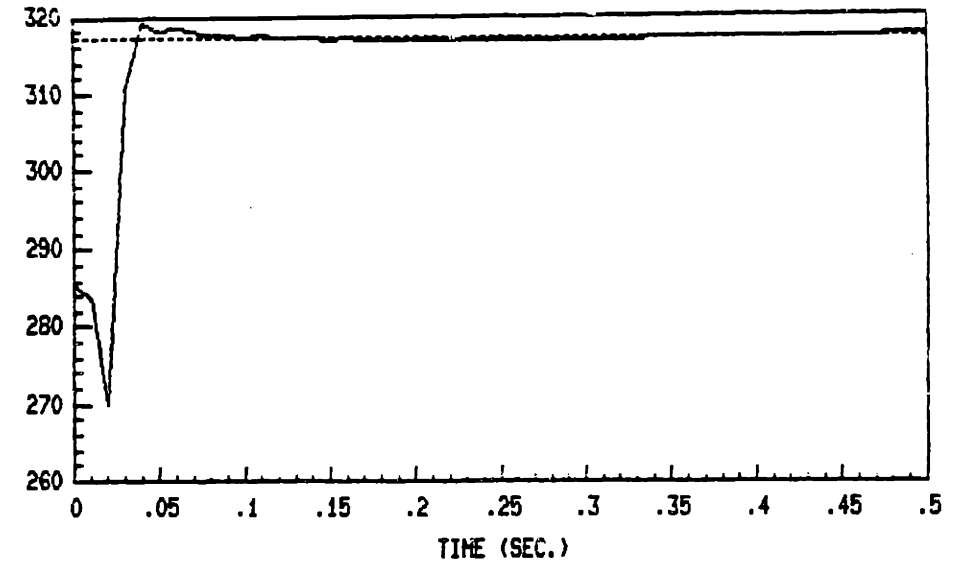

(a)

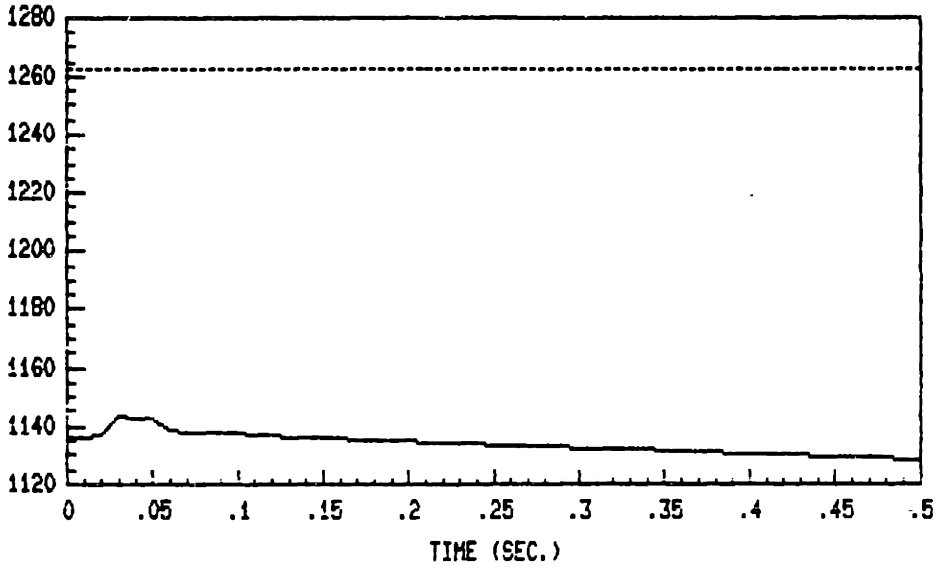

(b)

Figure 4.5: Performance of the Two-Stage Estimator (LTI with Noise Free Measurements): (a) Estimate of a_{1R}, (b) Estimate of a_{0R}.

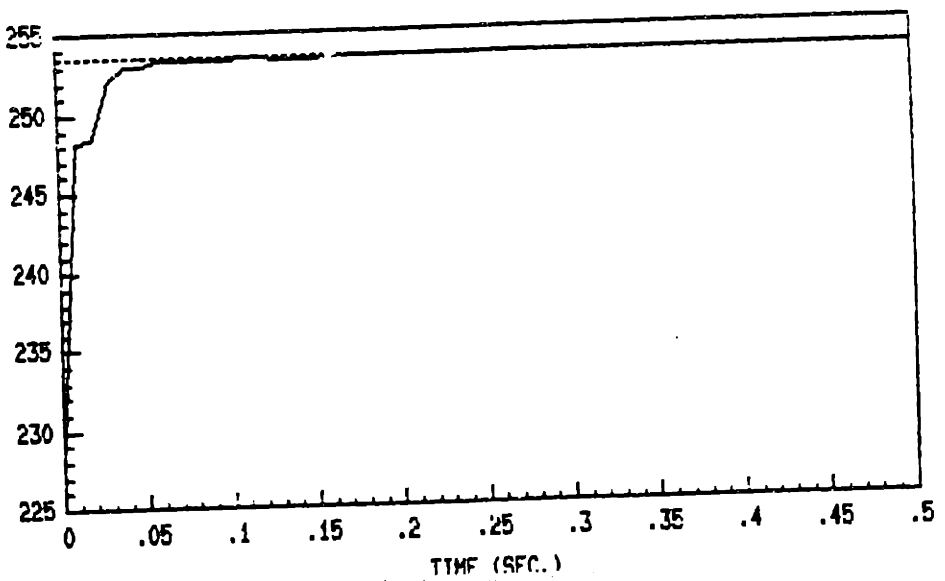

(a)

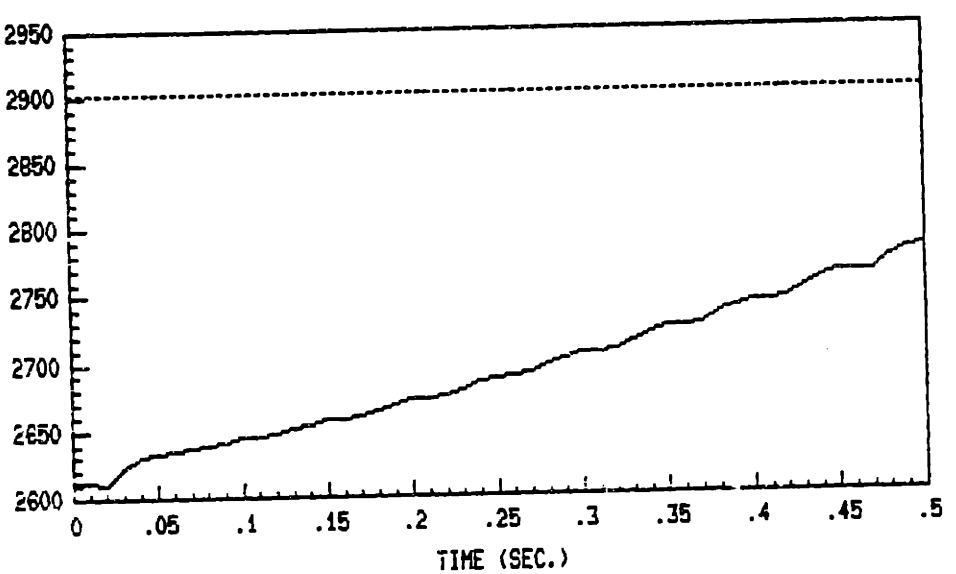

(b)

Figure 4.6: Performance of the Two-Stage Estimator (LTI with Noise Free Measurements): (a) Estimate of b_1, (b) Estimate of b_{0R}.

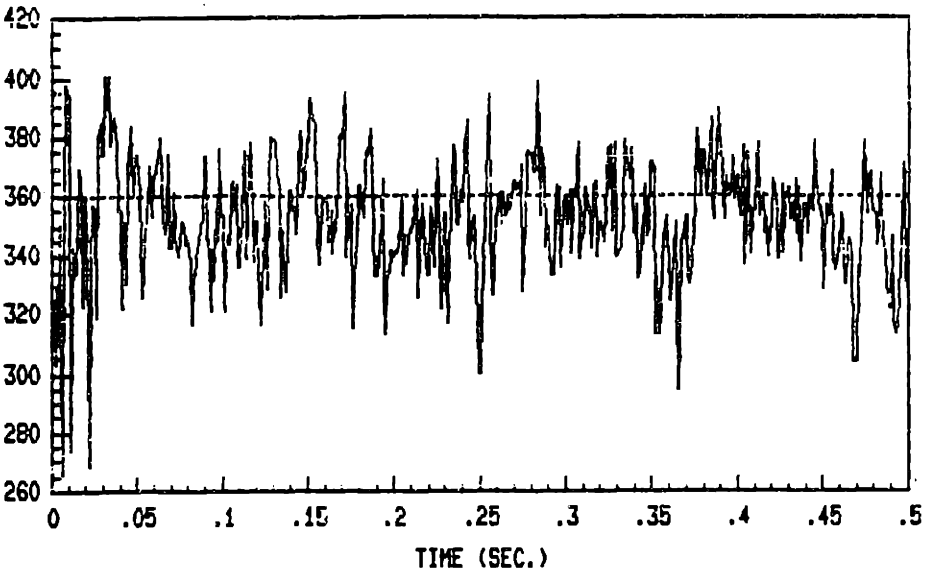

(a)

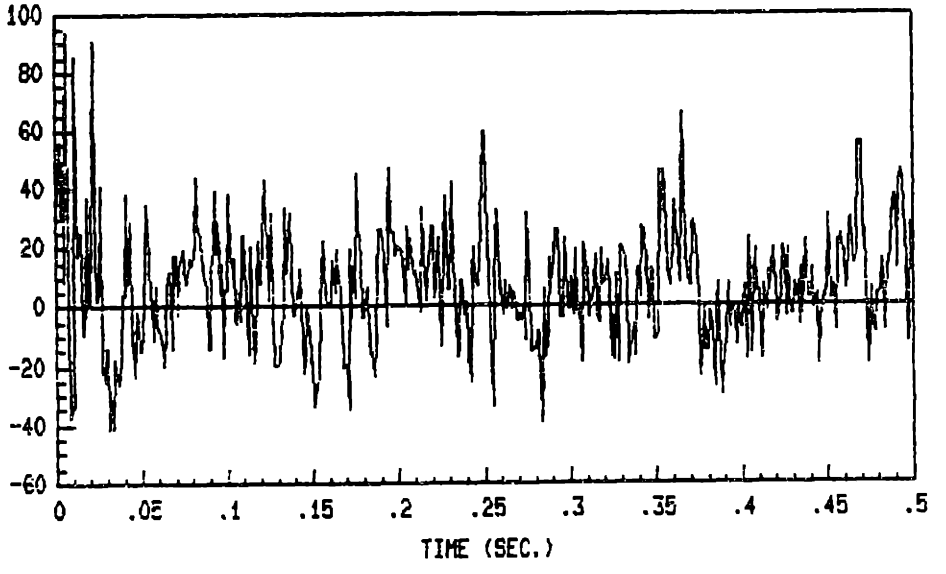

(b)

Figure 4.7: Performance of the Two-Stage Estimator (LTI with Noisy Measurements): (a) True Speed and Speed Estimate, (b) Error in the Speed Estimate.

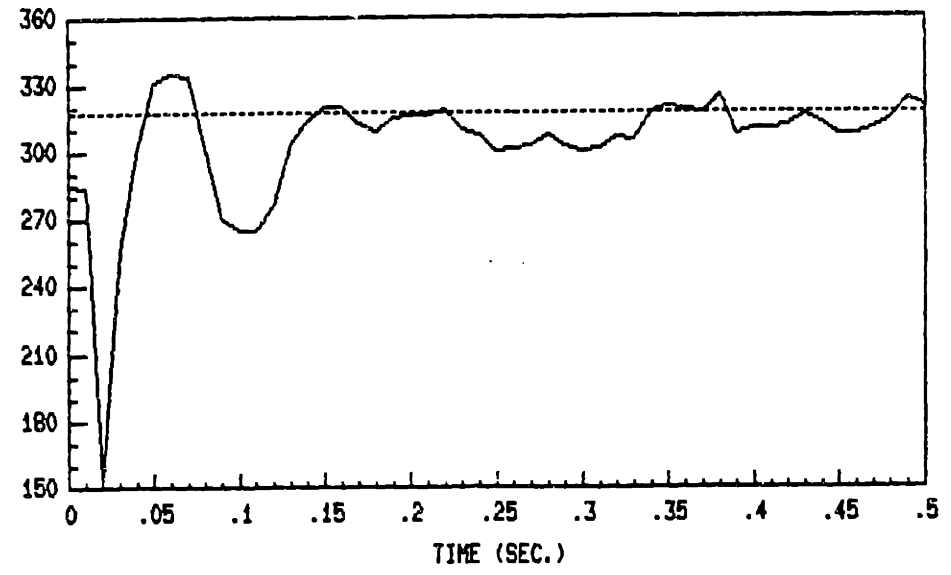

(a)

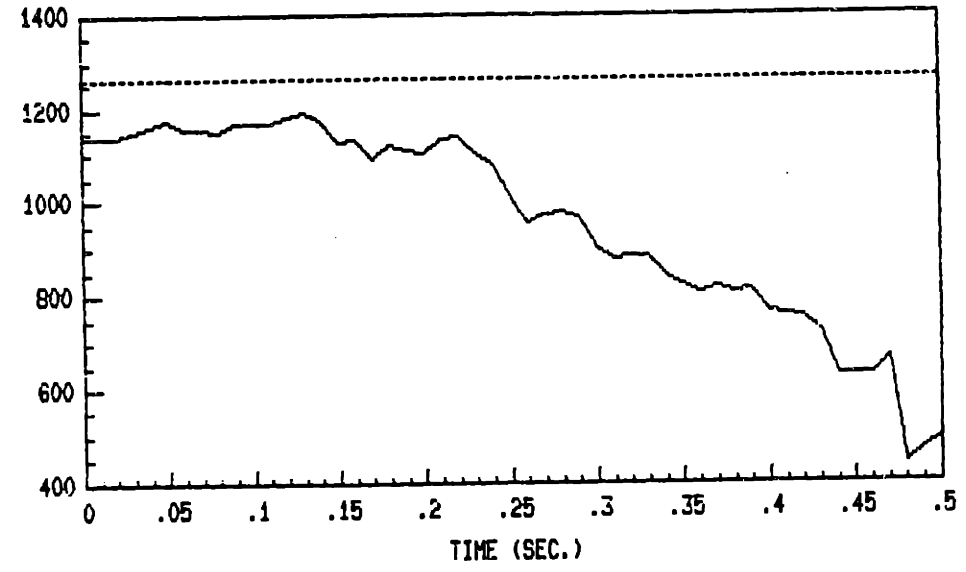

(b)

Figure 4.8: Performance of the Two-Stage Estimator (LTI with Noisy Measurements): (a) Estimate of a_{1R}, (b) Estimate of a_{0R}.

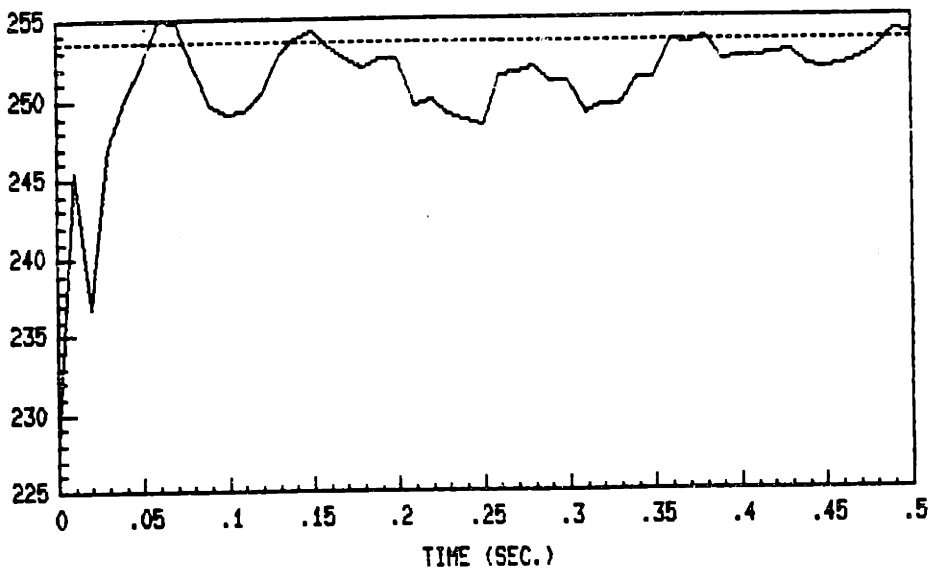

(a)

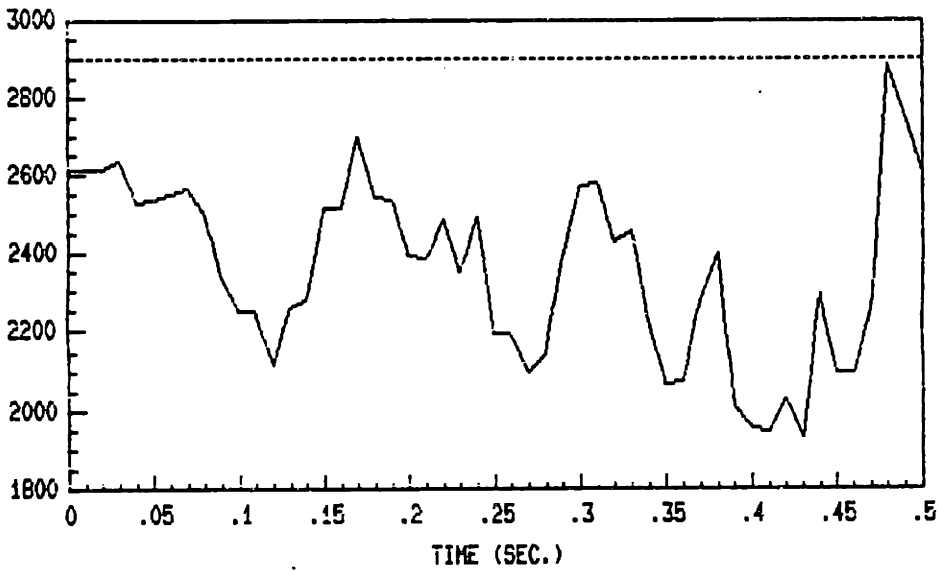

(b)

Figure 4.9: Performance of the Two-Stage Estimator (LTI with Noisy Measurements): (a) Estimate of b_1, (b) Estimate of b_{0R}.

Chapter 5

Off-Line Experiments and Results

5.1 Introduction

The estimator simulations presented previously were useful to understand and predict the behavior of the estimator. The next logical step in evaluating this algorithm is to test it off-line on data taken from an actual induction machine drive. In order to test the estimator with real-world data, we designed a test bench using Industrial Drives' ASC-3 induction machine drive system. The test bench was designed to provide the outputs of the state variable filters as inputs to the estimation algorithm. The idea is to have a system suitable for eventual on-line experimentation as well. The rotor speed is also measured by a tachometer, to compare with its estimated value.

The data for off-line experimentation is acquired using the data acquisistion system DAS-20 from MetraByte Co. The acquired data is then downloaded to a VAX 11/175 computer where it is processed using the MATRIXX software package on which our algorithms and simulations were carried out. Figure 5.1 shows a block diagram of the experimental system.

Tests on real data have only recently begun, and have not yet produced results of the quality that we would like to (and expect to) eventually see. This chapter describes the hardware available for experimentation and gives some suggestions to improve its

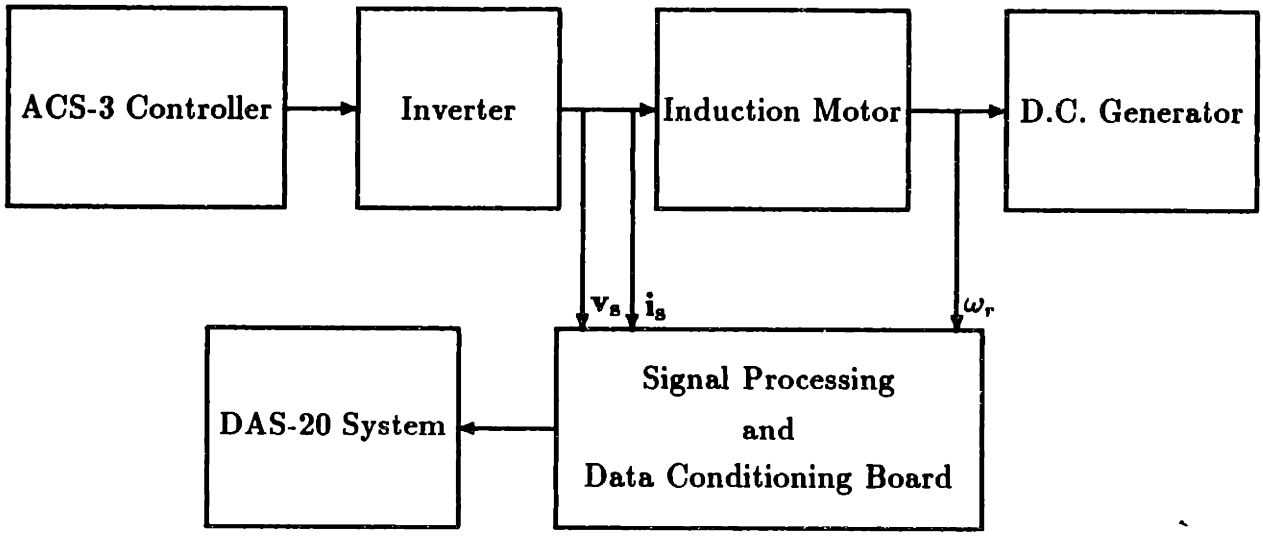

Figure 5.1: Experimental Set-Up for Off-Line Experimentation.

performance. In particular, difficulties with the signal processing board are mentioned. The chapter then describes the experiments carried so far and discussed their results.

5.2 Experimental Set-Up

5.2.1 Hardware for Experiment

5.2.1.1 Drive System

All the experiments of this thesis were conducted using an induction machine drive system (model ASC3) donated by Industrial Drives, Inc. The system includes a three phase rectifier, an inverter, a controller board, and a 3.1 hp induction motor. As supplied, the drive system was equipped with a tachometer to provide speed measurements, and Hall effect sensors with the required buffering circuitry to provide current

measurements. A resistively loaded dc generator was used to provide a mechanical load to the motor.

5.2.1.2 Data Acquisition and Signal Conditioning Hardware

For data acquisition MetraByte's DAS-20 data acquisition system was used. MetraByte's model DAS-20 is a multifunction high speed analog/digital I/O expansion board for the IBM PC that can be used for data acquisition and signal analysis. For our purposes it provides 16 analog input channels, the necessary A/D conversion as well as the capability to store the data into the computer memory from where it can be accessed for further analysis. The DAS-20 system is installed in a Compac-386 personal computer.

Since voltage signals are not provided by the ASC3 system, a three phase Y-Y step-down transformer was connected in parallel to the induction motor. The transformer provides the isolation from the high voltage output of the inverter and normalizes the 300 V signals to voltage levels that can be handled by the signal processing hardware. The machine phase voltages can be obtained from the phase voltages of the transformer secondary winding. If the transformer has high input impedance in the high voltage winding, it will not disturb the drive system. A scope picture of the line and phase voltages output by the transformer is shown in Figure 5.2. The upper trace is the line voltage and the lower trace is the phase voltage. Another posibility is to get the voltage signals from the inverter gating signals. The last idea seems more reasonable from the point of view of industrial implementation.

A signal processing and data conditioning board was designed to provide the necessary anti-aliasing and state variable filtering for the current and voltage signals. The board consists of four anti-aliasing and state variable filtering stages connected in parallel to process the two measured voltage signals (v_{an}, v_{cn}) and the two current signals (i_a, i_c). The outputs of the board are ± 10 V signals for the filtered stator line currents

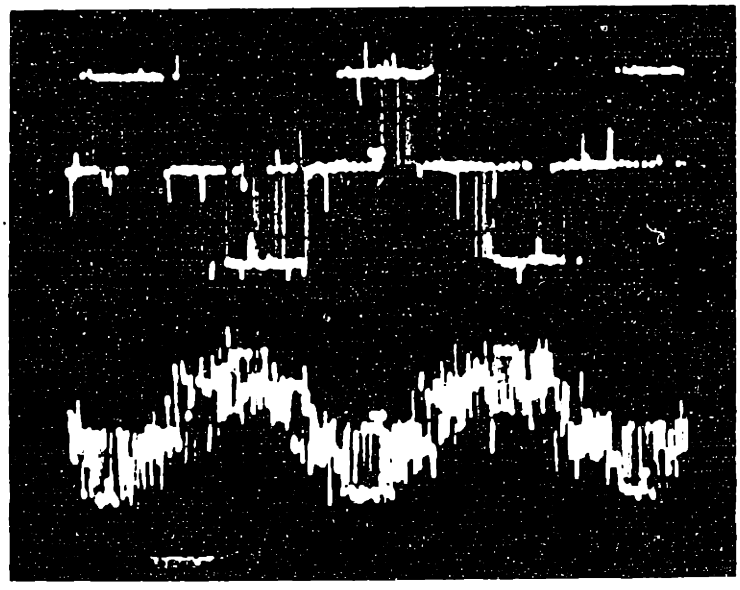

Figure 5.2: Scope Picture of the Line and Phase Voltages Output by the Transformer

i_{af} and i_{cf} and the filtered line to neutral voltages v_{anf} and v_{cnf} with the desired corresponding derivative terms. The speed signal is acquired to compare with its estimate. This sums up to 11 output analog channels that are fed to the DAS-20.

The anti-aliasing and state variable filtering circuits are shown in Figure 5.3. For the hardware implementation of the filters, a standard 741 was used to implement the anti-aliasing filter and National Semiconductor's AF100 state variable active filter was used for the state variable filter. Since the maximum frequency of the fundamental component of the current and voltage signals is 150 Hz (at 4000 rpm), the bandwidth of the anti-aliasing and state variable filter was chosen at 500 Hz. Each filter stage was designed using second order Bessel filters with cutoff frequencies of 500 Hz. For strict anti-aliasing, the sampling rate should be larger than 1000 Hz. This is needed to preserve the richness of the signals input to the estimation algorithm.

The DAS-20 has the capability of addressing sequentially the 11 output analog channels of the signal processing board. However, these channels are accessed through an analog multiplexer (in the DAS-20). Therefore sample-and-hold circuitry is provided

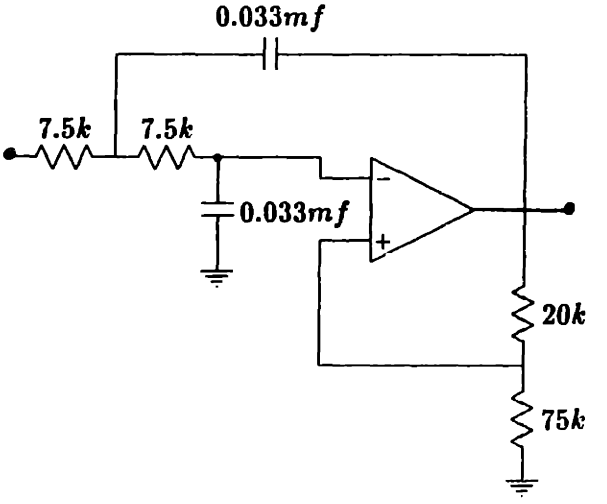

(a)

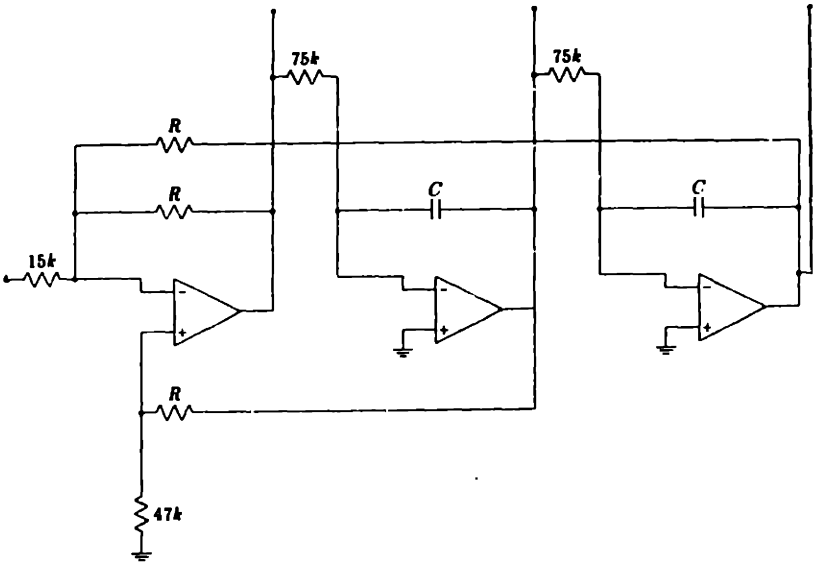

(b)

Figure 5.3: Filtering Circuitry: (a) Anti-aliasing Filter, (b) State Variable Filter.

as a means for holding all eleven signals to wait until conversion.

5.2.2 Software for Off-Line Experimentation

The data acquisition algorithm works in the following way. The outputs of the signal processing board are sampled sequentially, and the corresponding binary values are stored in the Compac-386 RAM buffer using the DMA feature of the DAS-20. Once the memory buffer is full, the sampling is stopped. The data is output via a DAS-20 system routine that formats the binary numbers as integers. Later the data is changed from this integer format into a format that represents the analog voltage processed by the A/D converter. The resulting data is stored in the hard disk. The overall control and interface with the DAS-20 system subroutines for off-line data acquisition is done using a BASIC code program on the Compac-386, see [44]. Using this program we could have sampling frequencies up to 2 kHz and store up to 2000 samples. For further reference on the different features of the DAS-20 system the reader is referred to [1].

To see the performance of the data acquisition system, the acquired signals are compared to the true signals. A plot of the current signals acquired by the DAS-20 system is shown in Figure 5.4. A photo of the actual current signal output by the state variable filter is shown in Figure 5.5.

5.3 Off-Line Testing

After the data has been collected it can be processed using the MATLAB or MATRIXX software available at LEES. These two software packages are among the best for control design and signal processing. During the course of this research work we have been using both. For this part we used MATRIXX. The estimation algorithms have been written as MATRIXX macros, and used to process the simulated data. To process the real data obtained from the system, we feed the real data to the same MATRIXX

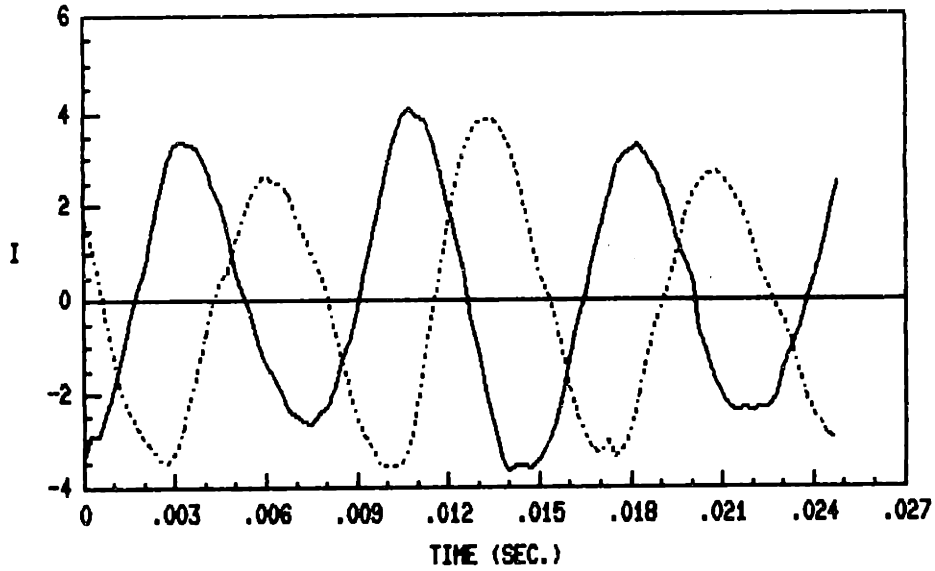

Figure 5.4: Plot of the Current Signal Acquired Signals Using the DAS-20.

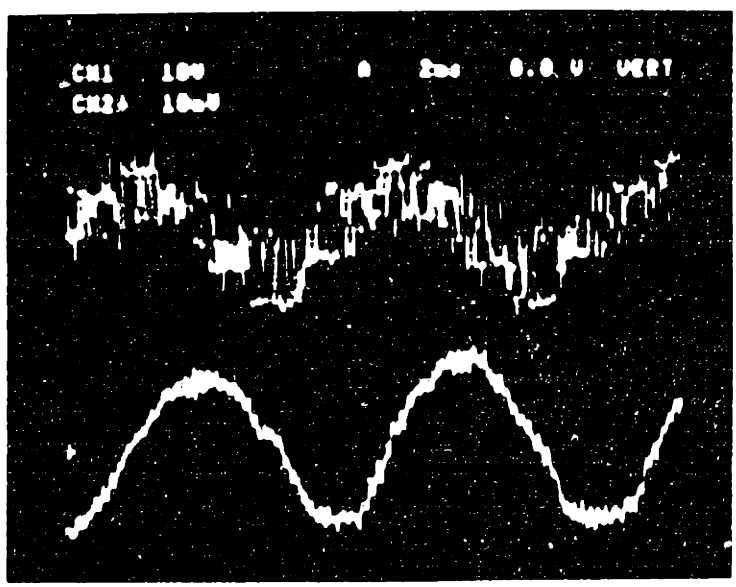

Figure 5.5: True Current Signal from the Induction Motor.

Channel Number	Scaling Factor
1	0.9467
2	133.63
3	0.3326
5	45.41
6	6333
7	0.3435
8	48.32
9	6620

Table 5.1: Scaling Factor for Each Output Channel of the Signal Conditioning Board.

macro used to process the data generated by the simulations.

Some pre-processing has to be done on the acquired signals before they are fed to the estimator. First, they have to be scaled so that the relative magnitudes of the signals are within the same range as the true signals. The scaling factors for the signals obtained from the signal processing board are shown in Table 5.1. Second, recall that the machine and regression models presented in this thesis assume the electrical variables to be in the dq frame. The measured quantities are in the so called abc frame [30] so, before feeding the data to the estimator, it has to be transformed to the dq frame. The transformation matrix to change from the stator currents i_a and i_c to the dq quantities i_d and i_q is,

$$\begin{bmatrix} i_d \\ i_q \end{bmatrix} = \begin{bmatrix} 1 & 0 \\ \frac{1}{\sqrt{3}} & \frac{2}{\sqrt{3}} \end{bmatrix} \begin{bmatrix} i_a \\ i_c \end{bmatrix} \tag{5.1}$$

In the derivation of this matrix it is assumed that

$$i_b = -(i_a + i_c)$$

The same relationship holds between the voltage signals v_{an} and v_{bn} and the corresponding dq quantities v_d and v_q.

Parameter	Value
L_s	0.0315 H
L_r	0.0315 H
M	0.0293 H
R_r	0.3700 Ω
R_s	0.1260 Ω

Table 5.2: Machine Parameters from Blocked-Rotor and No-Load Test.

Parameter	Value
a_{1R}	118.35
a_{0R}	353.71
b_1	238.74
b_{0R}	956.0

Table 5.3: Estimate of the Real Part of the Parameters of the Full Regressor Based on No-Load and Blocked-Rotor Tests.

5.3.1 Initial Parameter Estimates

An initial estimate of the parameters of the experimental induction motor can be obtained from the locked rotor and no-load test [18]. The resulting values are shown in Table 5.2. Estimates of the real parts of the coefficients of the transfer function can be deduced from this and are shown in Table 5.3.

It is important to point out that the parameter estimates based on these two tests might not be very good. This is because the rotor has deep bars so that the effective resistance changes a lot between the two operating points used for the test. The data obtained from the test agrees very well with that provided by the manufacturer.

5.4 Results from Off-Line Experimentation

In the beginning of the chapter we said that a test bench was designed to provide all the signals needed by the estimator. Due to certain problems with the hardware we were unable to use the signals output by the state variable filters for offline experimentation. Instead we only collected the voltage and current signals processed by the anti-aliasing filters. The state variable filtering was implemented using the System Build facility of MATRIXX. We expect that the digital implementation of the state variable filters will work in the same way as the analog one as long as high sampling rates are used. The state variable filter implemented in the computer was the same as the one shown in Figure 2.3 of Chapter 2. A sampling rate of 4 kHz was used.

5.4..1 Constant Speed Operation (Batch)

Data was collected during constant and time varying speed operation. This is done to study the performance of the estimator during different transient condiditons.

Since we are operating at constant speed the batch estimates of the parameters can be obtained following the same procedure as the one described in Chapter 4. Two different sets of data were collected at $\omega_m = 337.2$ rad/sec. From now on we use ω_m to refer to the rotor speed in mechanical degrees and ω_r as the rotor speed in electrical degrees. They are related by

$$\omega_r = N\,\omega_m$$

where N refers to the number of pole pairs of the machine; for the experimental machine $N = 2$. For this example $\omega_r = 674.4$ rad/sec. The resulting batch estimates are shown in Table 5.4.

The resulting batch estimates show a similar behavior to the simulated data. First the estimates of the coefficients of the derivative terms are closer to the values obtained from the blocked-rotor and no-load tests (see Table 5.4) than those associated with the

Parameter	Estimate	
	Example 1	Example 2
ω_r	569.82	496.92
a_{1R}	1,084.6	1,203.0
a_{0R}	-1,052,200	-998,210
b_1	206.37	209.51
b_{0R}	-35,527	-31,215

Table 5.4: Experimental Batch Estimates.

nonderivative terms. Furthermore, note that the speed estimate is quite good for the first case and that the estimate of b_1 is very good in both cases.

5.4..2 Time Varying Speed (Speed-Only Estimator)

Time variation of the rotor speed was forced by introducing comanding a speed of

$$\omega_m^c = 418 + 104\ sin(2\pi t)$$

A plot of the measured speed is shown in Figure 5.6.

To continue the data analysis, estimation runs using the speed-only estimator were done, and the results are plotted in Figures 5.7 and 5.8. Since we were sampling at 4 kHz a forgetting factor of 0.9 were used. Note that the estimates are very noisy. The effect of the noise is better viewed by looking at the error in the estimate. The error is very noisy, but after an initial transient it reaches a steady-state condition. In steady state the error looks like a random process with zero mean.

5.5 Discussion of Results

Let us discuss the performance of the estimator based on the observations from the experimental data. There are several error sources, including modeling errors and noise

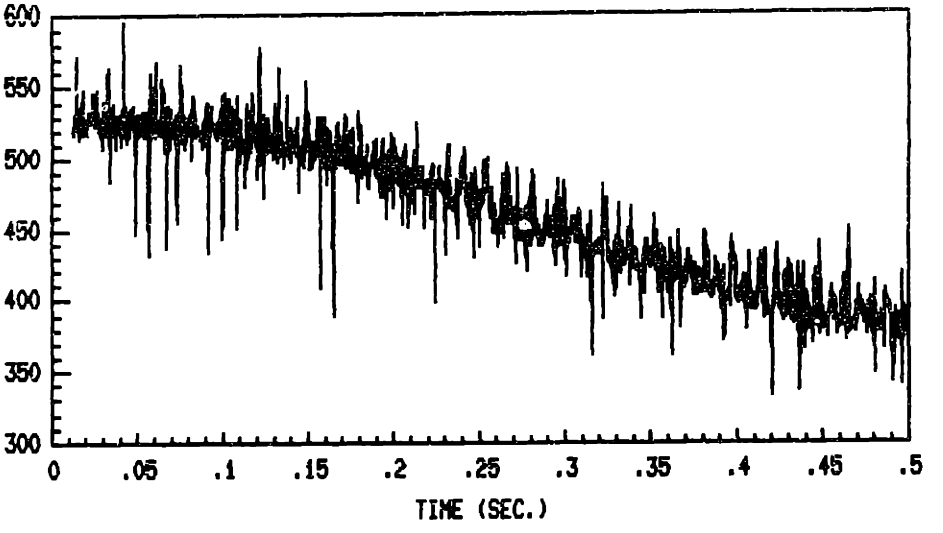

Figure 5.6: Acquired Rotor Speed Using DAS-20.

disturbances. The errors seen in the figures are due mainly to the noise disturbance.

The obtained results show that by improving the quality of the data acquired it might be posible to successfully run the estimator. From the batch estimates in the constant speed case it is clear that we can estimate the rotor speed from the real stator voltages and currents. Again it is observed that the coefficients associated with the derivatives are better estimated.

For the off-line experiments it seems rather convenient to only acquire the voltage and current signals of the machine and do the state variable filtering in MATRIXX. This allows us to have more flexibility. The only constraint is that we need fast sampling rates; in these examples we used 4 kHz.

5.6 Suggestions to Improve Test Bench

The state variable filter is currently implemented using the AF100 state variable active filter. It seems that the filter introduces a lot of distortion into its bandpass and

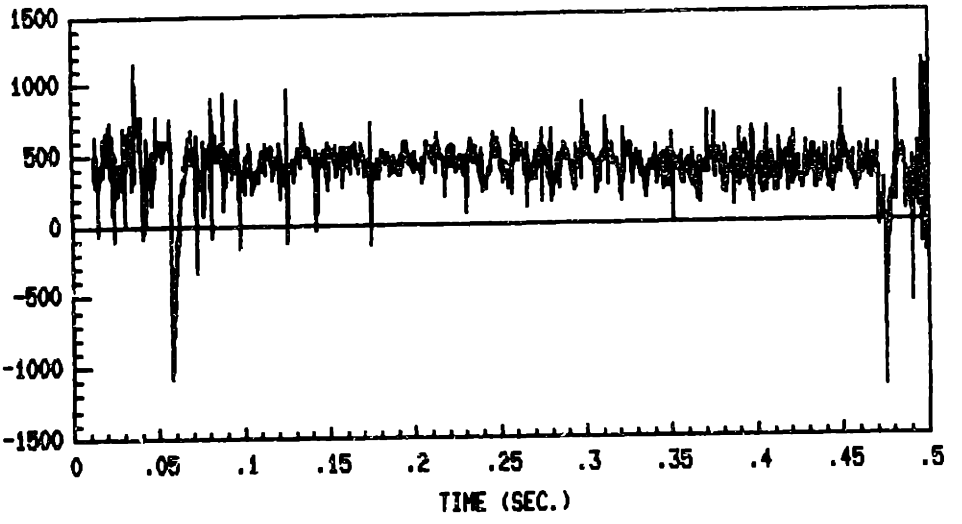

(a)

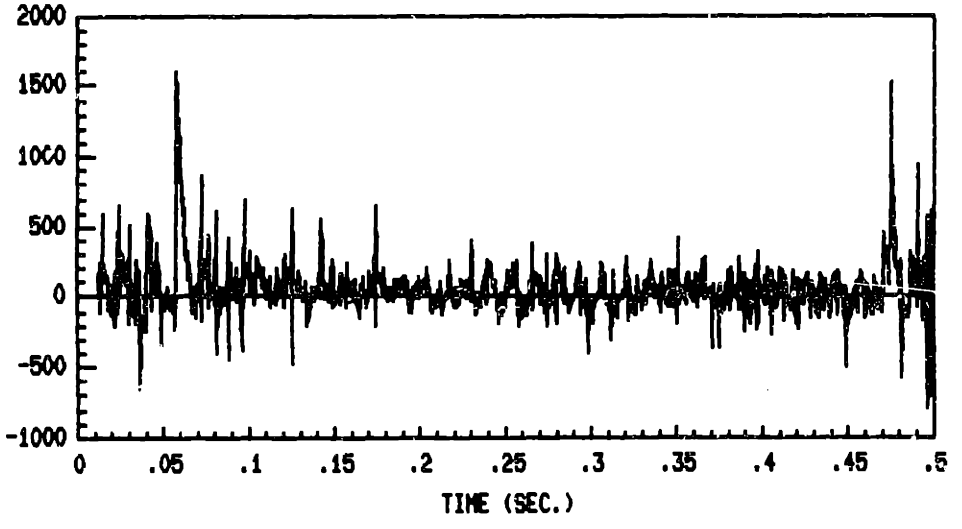

(b)

Figure 5.7: Estimate of the Rotor Speed Using the Speed-Only Estimator (Example 1): (a) Speed Estimate, (b) Error in Speed Estimate

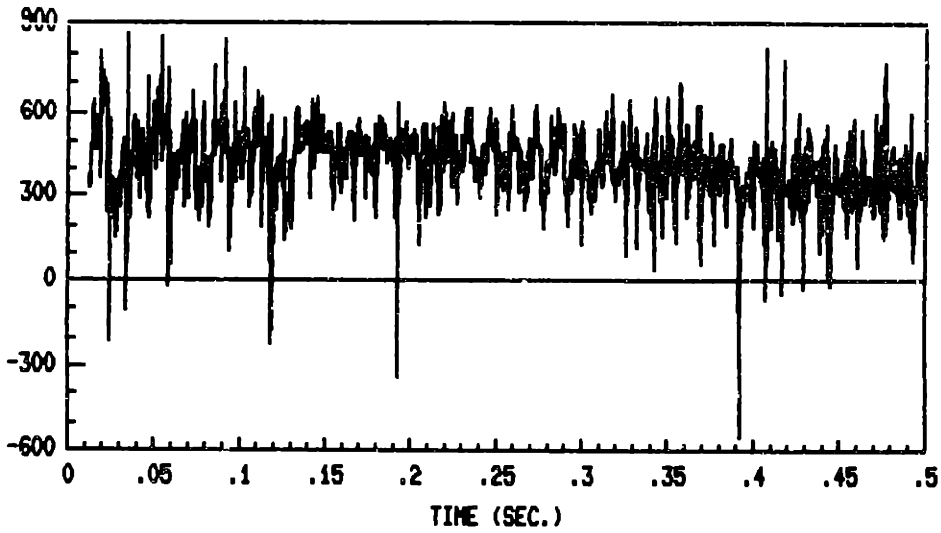

(a)

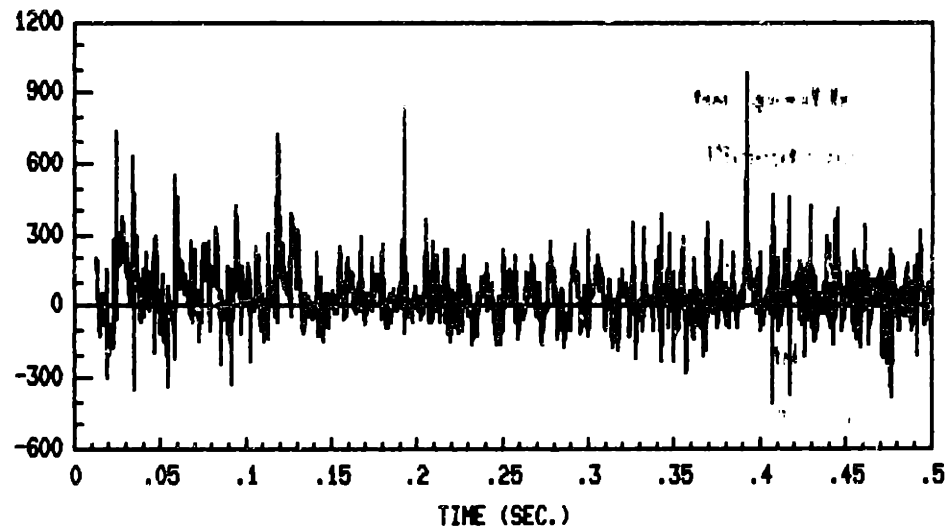

(b)

Figure 5.8: Estimate of the Rotor Speed Using the Speed-Only Estimator (Example 2): (a) Speed Estimate, (b) Error in Speed Estimate.

highpass output at low frequencies, so higher quality filters should be used. Also we need to check for possible noise sources that are affecting the quality of the acquired signals. As seen in the time varying experiments, the estimates are very noisy.

Chapter 6

Summary and Suggestions for Further Work

6.1 Summary

In this thesis we have addressed the problem of estimating the rotor speed and machine parameters based on measurements of the stator voltages and currents. We have combined the ideas and tools of parameter estimation theory with the properties of the induction machine system to come up with an estimation algorithm for the desired quantities. The contribution of this research work is the methodology used to derive the estimator, and the foundation laid for practical implementation.

In Chapter 2, we derive, based on the two-time-scale property of the induction machine, two linear regression models that relate the machine parameters and speed to the stator voltages and currents, and their derivatives. It is shown how, by using so-called state variable filters, the problems associated with the determination of the derivative terms of the stator voltages and currents are avoided.

In Chapter 3 the problem of estimating the machine parameters and rotor speed was reformulated as the problem of estimating the parameters of the two linear regressor models developed in Chapter 2. We saw how output error methods from estimation

theory are well suited to approach the estimation of the parameters of the regressor models (2.4) and (2.5). The algorithm selected was based on the least squares approach. To take into account time variations of parameters we included into the cost functional the forgetting factors. The equations for the recursive least squares algorithm were presented. Exploiting the time scale separation between the rates of change associated with the speed and machine parameters, we devised an estimator with two stages, one in charge of the speed estimation, the other in charge of the parameter estimation. The speed estimation stage estimates the rotor speed at a very fast rate, based on the most recent parameter estimates. The estimates of the machine parameters are updated at a slower rate. This time separation allow the design of the two estimators to be carried out almost independently.

The performance of the proposed estimator is studied in Chapter 4 with numerical simulations. In general, the estimator shows good tracking performance during speed transients, as desired. The performance in the presence of noisy measurements was studied. It is pointed out that because of the way that noise enters into the regression models, the performance of the estimator based on the LS approach might be seriously affected at higher noise levels, leading to biases (and eventually breakdown of the algorithm).

In Chapter 5, we described the experimental set-up designed during the course of this research to do off-line experimentation. The results of initial experiments were presented. Even though they were not nearly as good as desired, they give us confidence in the possibilities for the algorithm to work and pointed out necessary improvements on the hardware system. The difficulties encountered, and possible solutions for successful off-line experimentation have been described. Further results involving more on the experimental work will appear in [52].

Appendix A discusses how the participation factors can be used to analyze the dynamic structure of the induction machine model. We analyzed the structure of

the linearized machine model at different operating points. From this analysis and by looking at the eigenvalue structure of the system, we identified certain dynamic patterns. The nonlinear reduced order models then are derived by neglecting the fast dynamics of the system. Simulation results of the reduced order nonlinear models are shown and the results presented agree very well with the results from the linearized model analysis.

6.2 Suggestions for Further Work

Certainly there are many issues related to the estimator design that need to be refined, specially for real time implementation of this algorithm. In general the RLSE suffers from the fact that it requires a lot of computational power to be implemented in real time. The two-stage estimator tries to approach this problem by reducing the frequency of the parameter updates. Another computational simplification that can be done is to use the common assumption that machine inductances do not change frequently so the parameter estimator of the two-stage estimator will need only to estimate the rotor and stator resistances. The separation approach presented in this thesis might be of interest for further research in the area of system identification.

After formulating the speed and parameter estimation problem as the estimation of the parameters of a linear regression model using output error methods, we can allow ourselves as designers to use methods other than the RLSE presented in this thesis. These methods might be simpler from the computational point of view, but will represent tradeoffs between the estimator tracking capabilities, noise immunity and other performance indicators.

Hardware implementation of the estimator is the next step after the off-line experimentation is finished. There are many things to be considered in this part of the research. First, we have to decide whether the least squares estimator or a simplified algorithm is going to be used. If the RLSE is used, then we have to consider ways

to implement the algorithm equations in a way that is suited for real time operation. The reader is referred to Chapter 6 of [37] for further discussion. Another issue is the hardware to be used: special purpose DSP processors like the TMS32020 family from Texas Instruments seem to be ideal for use in the experimental work. They have very fast computational power and the programming tools are well developed and available at LEES. The first step in real-time implementation will appear in a Bachelor's Thesis byC Louis Roehrs [44], where an implementation of the speed-only estimator using the TMS32020 is presented.

After all the work of tuning up the estimator, there are still issues related to the implementation of an adaptive controller using the proposed estimator. These are not discussed here but have to be considered in further research. Specifically, robustness and stability of such controllers are key issues.

We expect the basis laid in this thesis to lead in the next one or two years to a successful, robust, real time speed and parameter estimation scheme.

Appendix A

Reduced Order Modeling of Induction Machines

A.1 Introduction

Reduced order modeling of electrical machinery is usually based on experience and empirical knowledge, rather than on systematically deduced features of the unreduced model. In the power systems literature, different linear and nonlinear reduced order models for large machines have been presented. A good discussion of these models for synchronous and induction machines is presented in [30]. The analysis and validation of these models is done by comparison of simulations of the full order model and the reduced order model for the nonlinear case, and of eigenvalues in the linear case. More analytical work is needed however, to understand the validity of these models. For example, we shall see later that reduced order models for small machines might be quite different from those that are appropiate for large machines. In [30], the same reduced order model is used for large and small induction machines. It is noted there that the accuracy of the model increases with the rating, but no further work is done to understand this difference. A different approach to reduced order modeling of electrical machinery can be found in [15,47,46,54]

In this Appendix, we illustrate the use of participation factors to study the dynamic

structure of the machine model, by application to the induction machine model. Issues related to how this dynamic structure changes with machine rating and operating conditions are addressed. The implications for reduced order modeling are pointed out.

A.2 Linearized Model of the Induction Machine

The nonlinearities involved in the induction machine model make it difficult to understand how the electrical and mechanical subsystems interact. To study the machine dynamic structure a linearized model of the machine is used. It turns out that the linearized model for operation at constant nominal speed is linear and time invariant, which makes possible the use of the participation factors introduced in [43] to study the dynamic structure of the linearized model.

Let us assume that the machine is in steady state, running at constant speed $\bar{\omega}_r$. The linearized model around steady state operation in the synchronous rotating reference frame with fixed input voltage waveforms and constant load torque is given by the following set of equations:

$$\begin{bmatrix} \frac{d\mathbf{x}_E}{dt} \\ \\ \frac{d\mathbf{x}_M}{dt} \end{bmatrix} = \begin{bmatrix} \mathbf{A}_{EE} & \mathbf{A}_{EM} \\ \\ \mathbf{A}_{ME} & \mathbf{A}_{MM} \end{bmatrix} \begin{bmatrix} \mathbf{x}_E \\ \\ \mathbf{x}_M \end{bmatrix} \tag{A.1}$$

where

$$\mathbf{A}_{EE} = -\left(\mathbf{R} + \begin{bmatrix} \omega_e \mathbf{J} & \mathbf{0} \\ \mathbf{0} & (\omega_e - \bar{\omega}_r)\mathbf{J} \end{bmatrix}\right)$$

$$\mathbf{A}_{EM} = \begin{bmatrix} \mathbf{0} & \mathbf{0} \\ \mathbf{0} & \mathbf{J} \end{bmatrix} \bar{\lambda}$$

$$\mathbf{A}_{ME} = \frac{1}{H} \frac{M^2}{L_S L_R - M^2} \bar{\lambda}^T \begin{bmatrix} \mathbf{0} & \mathbf{J} \\ -\mathbf{J} & \mathbf{0} \end{bmatrix}$$

$$\mathbf{A}_{MM} = -\frac{B}{H}$$

$$\mathbf{x}_E = \hat{\lambda} \qquad \mathbf{x}_M = \hat{\omega}_r$$

where the subscripts E and M stand for "electrical" and "mechanical", and $\hat{\lambda}$ and $\hat{\omega}_r$ refer to small perturbations around steady state values $\bar{\lambda}$ and $\bar{\omega}_r$ respectively.

A.3 Reduced-Order Modeling

A.3.1 A Natural Decomposition

A natural way to decompose the machine model is into its two physical subsystems [54], the mechanical and the electrical subsystem. This is already suggested by the partitioning in (A.1). To get some qualitative insight into the interactions between the electrical and mechanical subsystems, let us take a closer look at equation (A.1). The matrix

$$\mathbf{A} = \begin{bmatrix} \mathbf{A}_{EE} & \mathbf{A}_{EM} \\ \mathbf{A}_{ME} & \mathbf{A}_{MM} \end{bmatrix}$$

reduces to the matrix

$$\hat{\mathbf{A}} = \begin{bmatrix} \mathbf{A}_{EE} & \mathbf{0} \\ \mathbf{0} & \mathbf{A}_{MM} \end{bmatrix} \tag{A.2}$$

when the steady state value of the machine flux $\bar{\lambda}$ is zero. Increasing the machine flux makes the off-diagonal blocks of $\hat{\mathbf{A}}$ increase from zero to $\mathbf{A}_{EM}$ and $\mathbf{A}_{ME}$, which causes the eigenvalues to move from those of $\mathbf{A}_{EE}$ and $\mathbf{A}_{MM}$ to those of $\mathbf{A}$. This suggests that, if the coupling between the eigenstructures of $\mathbf{A}_{EE}$ and $\mathbf{A}_{MM}$ that is induced by $\mathbf{A}_{EM}$ and $\mathbf{A}_{ME}$ is small relative to the separation between these eigenstructures, then the eigenstructure of $\mathbf{A}$ will consist of two relatively separated parts, one centered around the eigenstructure of $\mathbf{A}_{EE}$, the other around that of $\mathbf{A}_{MM}$. This suggests a possible method to study the coupling between the electrical and mechanical subsystems, by computing the eigenvalues of the linearized model and comparing them with the eigenvalues of $\mathbf{A}_{EE}$ and $\mathbf{A}_{MM}$.

To illustrate this, let us take a look at the eigenvalue structures of the linearized model at no-load steady state operation for a 3 hp and a 500 hp induction machine. The parameters of these machines (taken from [30]) are given in Table A.1. The eigenvalues

Machine rating		Parameters				
hp	V_m	$\bar{\omega}_r$	R_s	L_s, L_r	R_r	M
3	220	367.42	0.435	0.0713	0.816	0.0693
500	2300	376.79	0.262	0.1465	0.187	0.1433

Table A.1: Parameters and operating voltage, speed and frequency for the induction machine examples.

Machine	$\mu_{1,2}$	$\mu_{3,4}$	μ_5
3	-86.62±315.71j	-228.44±71.04j	-4.38
500	-14.83±17.26j	-41.56±373.88j	-29.09

Table A.2: Eigenvalues of the 3 hp and 500 hp machines.

of the linearized model and those of $\mathbf{A}_{EE}$ and $\mathbf{A}_{MM}$ are given in Tables A.2 and A.3 respectively. For the 3 hp machine the eigenvalues of the linearized model fall into two groups: one close to the eigenvalues of $\mathbf{A}_{EE}$ and another close to those of $\mathbf{A}_{MM}$. This is what is expected from the natural decomposition discussed above. However, for the 500 hp machine this is not the case. We shall see later that this "natural" decomposition is not justified for large machines.

Machine	$\mathbf{A}_{EE}$	$\mathbf{A}_{MM}$
3	-86.34±316.09j -230.86±70.49j	-0.1124
500	-41.49±373.87j -29.44±3.43j	-0.0136

Table A.3: Eigenvalues of $\mathbf{A}_{EE}$ and $\mathbf{A}_{MM}$ for the 3 hp and the 500 hp machines.

State Variable	Participation Factors		
	$\mu_{1,2}$	$\mu_{3,4}$	μ_5
λ_{S1}	**0.5722**	-0.0722	0
λ_{S2}	**0.5732**	-0.0732	0.0001
λ_{R1}	-0.0730	**0.5834**	-0.0207
λ_{R2}	-0.0715	**0.5712**	0.0005
ω_r	-0.0009	-0.0092	**1.0200**

Table A.4: Participation Factors for the 3 hp Machine.

A.3.2 Participation Factors

To get quantitative insight into the coupling between the electrical and mechanical subsystems, the participation factors are used. The participation factors [43] give a measure of the relative contribution of each state variable to each eigenvalue.

To introduce the participation factors, let us consider the i-th mode of the system

$$\frac{d\mathbf{x}}{dt} = \mathbf{A}\mathbf{x} \tag{A.3}$$

with eigenvalue μ_i of multiplicity one, and associated left and right eigenvectors $\mathbf{w}_i$ and $\mathbf{v}_i$ respectively. Let us choose $\mathbf{w}_i$ and $\mathbf{v}_i$ such that $\mathbf{w}_i^T\mathbf{v}_i = 1$. Recall that $\mathbf{w}_i^T\mathbf{v}_j = 0$ for $i \neq j$. The participation factor (p_{ki}) of the kth state variable in the ith mode is given by

$$p_{ki} = w_{ki}v_{ki} \tag{A.4}$$

where w_{ki} and v_{ki} are the kth entries of the left and right eigenvectors. The term v_{ki} will reflect the activity of the kth state variable when the ith mode is excited, while w_{ki} will weight the contribution of this activity to the mode. Note that p_{ki} is invariant under changes of units on the state variables. Also, the p_{ki} sum to 1 over k and over i.

The participation factors for the 3 hp machine are shown in Table A.4. Note the interesting pattern in this example. Based on the participation factors, we are able to discern clear dynamic patterns , i.e. associations of state variables with eigenvalues.

Submatrix	Eigenvalues
$\mathbf{A}_S$	-110.3±377.0j
$\mathbf{A}_R$	-209.9±9.58j

Table A.5: Eigenvalues of the finer partition in the 3 hp machine

There are three groups: the "stator eigenvalues" $\mu_{1,2}$, the "rotor eigenvalues" $\mu_{3,4}$, and a "rotor speed" eigenvalue μ_5. This suggests why the overall eigenvalues are well approximated by those of $\mathbf{A}_{EE}$ and $\mathbf{A}_{MM}$. In fact, the eigenvalues of $\mathbf{A}_{EE}$ themselves be can well approximated by those of its "stator subsystem" and "rotor subsystem", in accordance with the results in Table A.4. This is shown in Table A.5

A.3.3 Small Versus Large Machines

At this point we have seen the utility of the participation factors in studying the dynamic structure of the linearized machine model using an example of a 3 hp induction machine. In this section we will use them to study the differences in dynamic patterns between the 3 hp and the 500 hp induction machines.

Looking at the eigenvalues for the 500 hp machine in Table A.2 we can see an eigenvalue pattern different from the 3 hp machine. The fast eigenvalues of the system (i.e. with the larger real part) are the complex conjugate pair $\mu_{3,4}$ and the real eigenvalue μ_5. The (slowly decaying or) slow eigenvalues correspond to the other complex conjugate pair $\mu_{1,2}$. However, the eigenvalues are not well approximated by eigenvalues of $\mathbf{A}_{EE}$ and the eigenvalue of $\mathbf{A}_{MM}$.

To visualize the interactions between the different subsystems and how they differ from the 3 hp machine, the participation factors were computed and are shown in Table A.6. Based on the values of the participation factors, a different eigenvalue/state variable association pattern can be made. The (fast) complex conjugate pair $\mu_{3,4}$ are

State Variable	Participation Factors		
	$\mu_{1,2}$	$\mu_{3,4}$	μ_5
λ_{S1}	0.0001	**0.5042**	-0.0082
λ_{S2}	0.0043	**0.5042**	0.0001
λ_{R1}	**0.5142**	-0.0042	-0.0199
λ_{R2}	0.0020	-0.0042	**1.0044**
ω_r	**0.4881**	0.0000	0.0236

Table A.6: Participation factors for the 500 hp machine

Submatrix	$\mathbf{A}_S$	$\mathbf{A}_R$
Eigenvalues	-41.39±377j	-14.78±17.01j
		-29.53

Table A.7: Eigenvalues of the $\mathbf{A}_S$ and $\mathbf{A}_R$ submatrices.

the "stator eigenvalues". The real eigenvalue μ_5 is associated with λ_{R2}. The (slow) complex conjugate pair of eigenvalues $\mu_{1,2}$ are associated with λ_{R1} and ω_r.

This difference between the eigenvalue/state variable association for the 3 hp machine and for the 500 hp machine leads us to a different subsystem decomposition of the model of the 500 hp induction machine. The two subsystems are defined in the following way: the first (fast) subsystem groups the stator flux λ_s, and the second (slow) subsystem groups the rotor flux λ_r and the rotor speed ω_r. The system matrix in term of this partition is given by

$$\mathbf{A} = \begin{bmatrix} \mathbf{A}_S & \mathbf{A}_{SR} \\ \mathbf{A}_{RS} & \mathbf{A}_R \end{bmatrix} \tag{A.5}$$

where the subscripts S and R refer to the stator flux, and to the rotor speed and flux respectively. The eigenvalues of the diagonal blocks are given in Table A.7. Comparing this with the eigenvalues of the full order linearized model (Table A.2) we can see how accurately this decomposition can predict the eigenvalues of the full order model. Once again, a three-fold decomposition can also be made, based on the results in Table A.6,

Submatrix	Eigenvalue
$\mathbf{A}_{R1M}$	-14.78±17.02
$\mathbf{A}_{R2}$	-29.54

Table A.8: Eigenvalues of the finer partition for the 500 hp machine

with the eigenvalues of $\mathbf{A}_R$ well approximated by those of its "λ_{R1}, ω_r subsystem " and its "λ_{R2} subsystem". The eigenvalues for the finer decomposition are shown in Table A.8.

A.3.4 Analysis at Different Operating Points

In the previous section we studied the coupling between and within the electrical and mechanical subsystems in the induction machine by studying the local dynamics of the machine model at no-load steady state operation. This analysis was useful to get some insight about the system interactions and the way that participation factors can be used to study the dynamic structure of the linearized machine model. With the linearized model we studied the local dynamics of the machine model around a specific operating point, but the obtained results should not be used to describe the global structure of the nonlinear model. In this section we will show an approach to study the global dynamic structure of the machine model using the participation factors.

Suppose the load torque is set to specific value, keeping nominal voltage and frequency (60 Hz) constant, and the machine model is linearized around the resulting steady state operation. By changing the load torque we vary the rotor speed from zero to its no-load value. At each operating point the local dynamic structure is studied using the participation factors. By studying how the participation factors change at each operating point we might expect to deduce some important characteristics of the global structure of the machine model.

The eigenvalue locus of the linearized machine model and of $\mathbf{A}_{EE}$ as the speed changes from zero to no-load speed for the 3 hp machine are shown in Figure A.1. Note that for this example the eigenvalue of $\mathbf{A}_{MM}$ is independent of the speed. The participation factors for the linearized model eigenvalues at different operating points were computed and are presented as functions of speed in Figure A.2. From these plots we can see that the structure of this machine remain unchanged, i.e. the fast modes of the system are always associated with the electrical variables while the slow ones are associated with the rotor speed.

For the 500 hp machine the eigenvalues loci as well as the participation factors are plot in Figures A.3 to A.4. Note that at speeds below 300 rad/sec the linearized model has a structure similar to the small machine. However, at higher speeds the structure changes to the one described previously. These results show us a more complicated dynamic structure for large machines. The interactions shown here cannot be seen from the previous analysis at no-load steady state operation.

A.4 Reduced Order Models

In this section reduced order models of the fifth order nonlinear model of the induction machine are derived based on the information provided by the analysis using the participation factors. The order reduction will follow an approach similar to singular perturbation methods [7,28], i.e. the transients associated with the fast subsystem are assumed to be infinitely *fast* so the fast state variables reaches a quasi-steady-state condition instantaneously. The reduced order model is obtained by computing the quasi-steady-state solution of the fast subsystem and substituting it back into the slow variables. Note that the machine model presented in this note does not have an explicit perturbation parameter. Therefore, the singular perturbation method is followed formally, without the mathematical rigor.

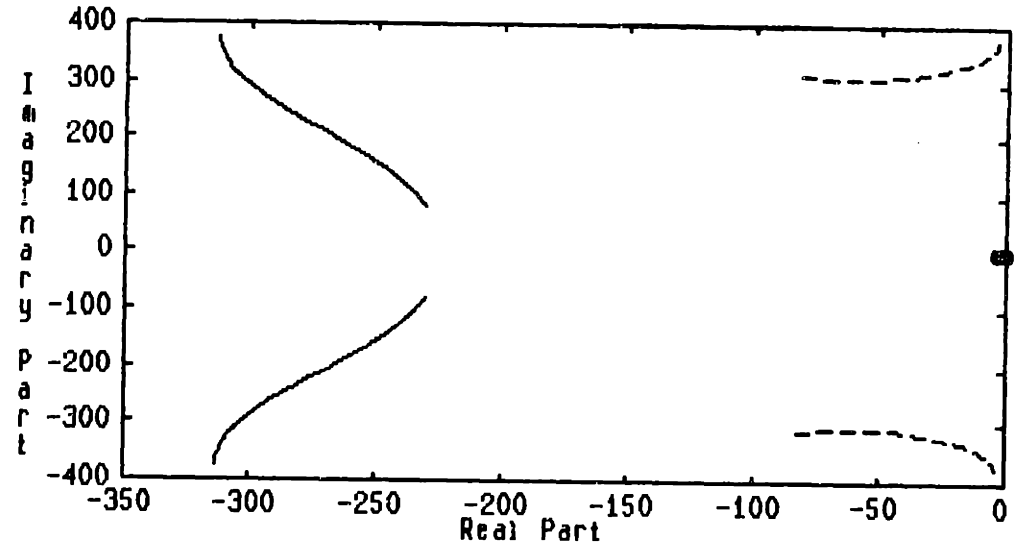

(a)

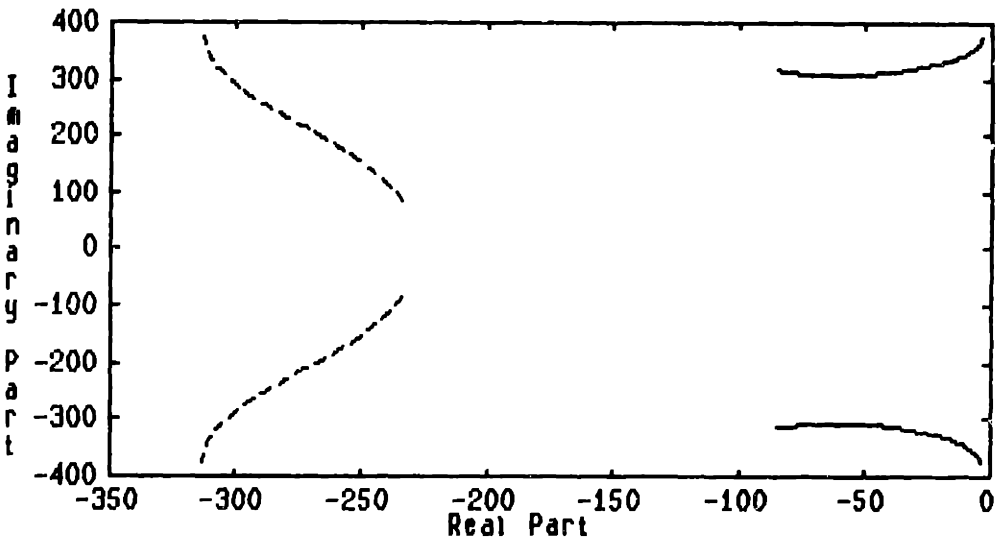

(b)

Figure A.1: Eigenvalues locus for the 3 hp machine: (a) linearized model, (b) $\mathbf{A}_{EE}$

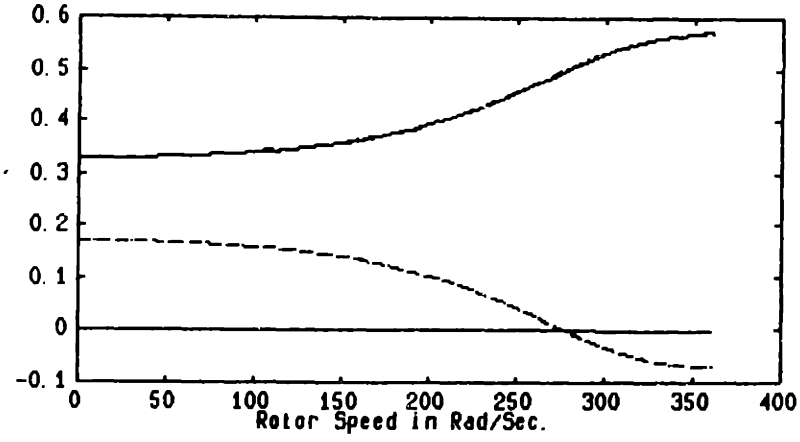

(a)

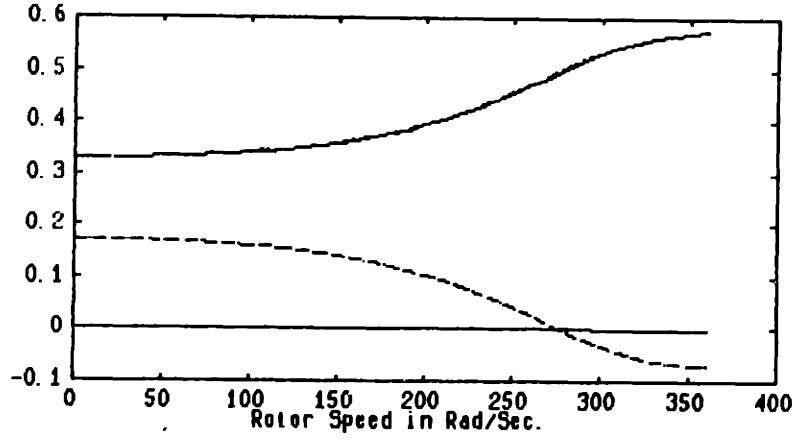

(b)

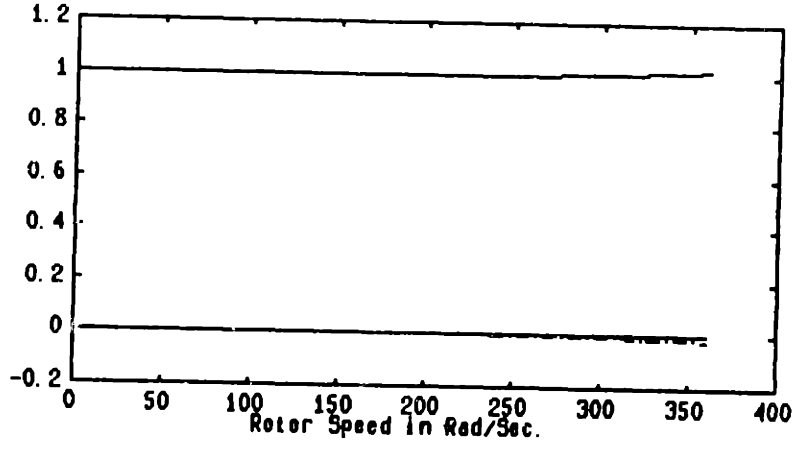

(c)

Figure A.2: Participation factors for the 3 hp machine: (a) $\mu_{1,2}$, (b) $\mu_{3,4}$, (c) μ_5.

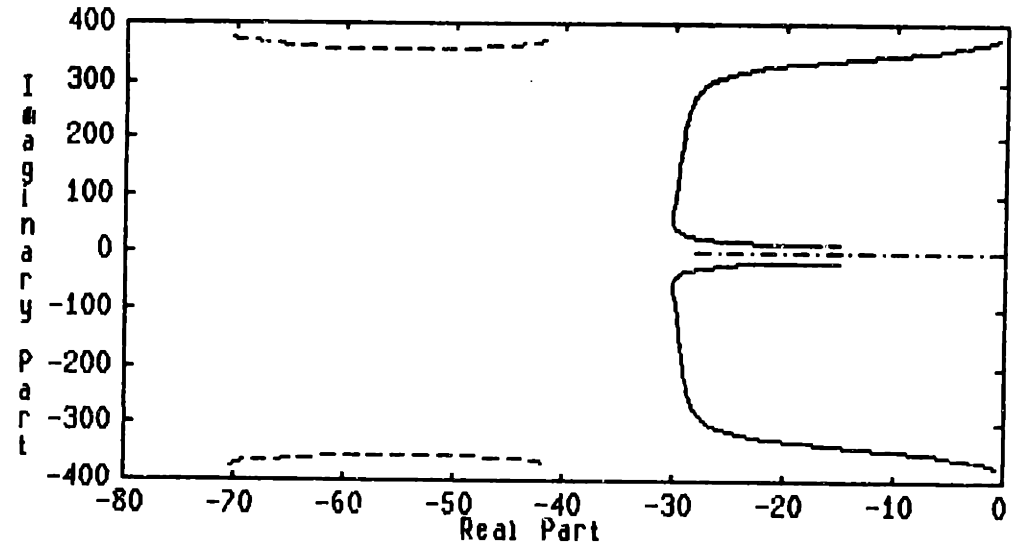

(a)

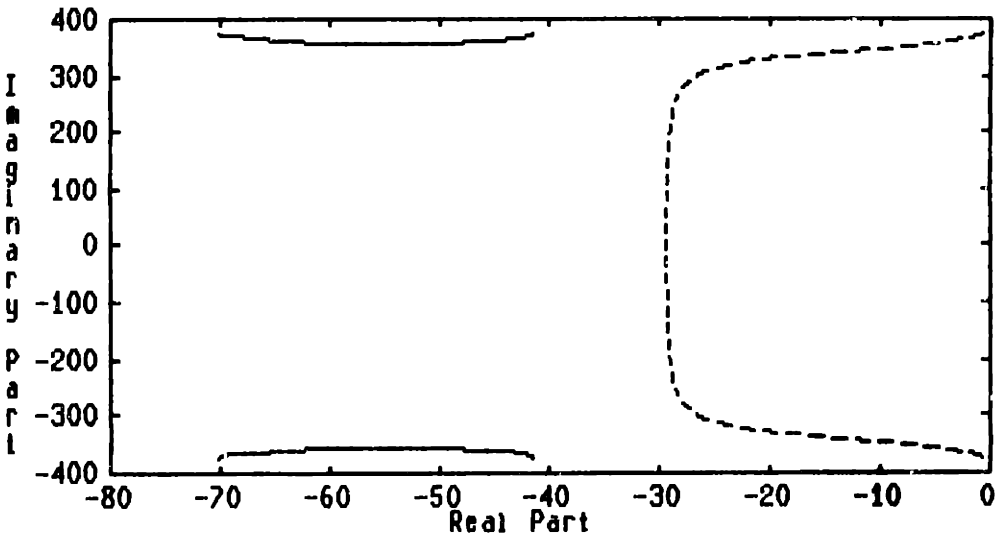

(b)

Figure A.3: Eigenvalues locus for the 500 hp machine: (a) linearized model, (b) $\mathbf{A}_{EE}$

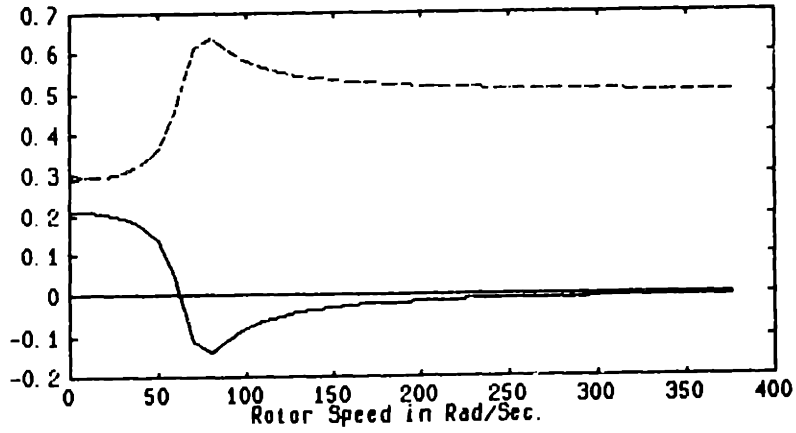

(a)

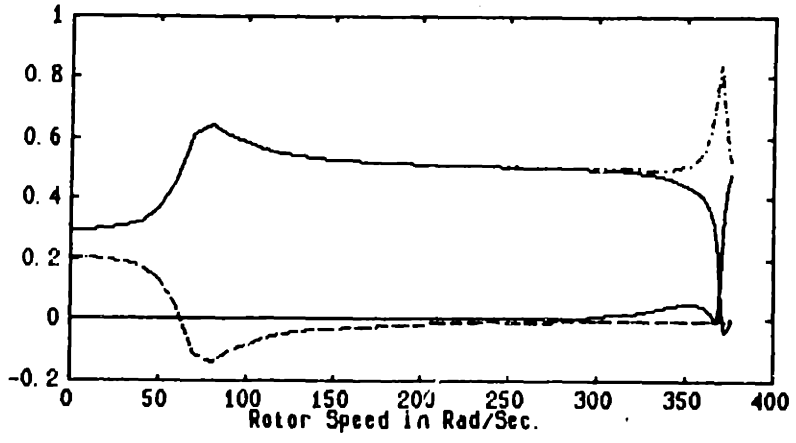

(b)

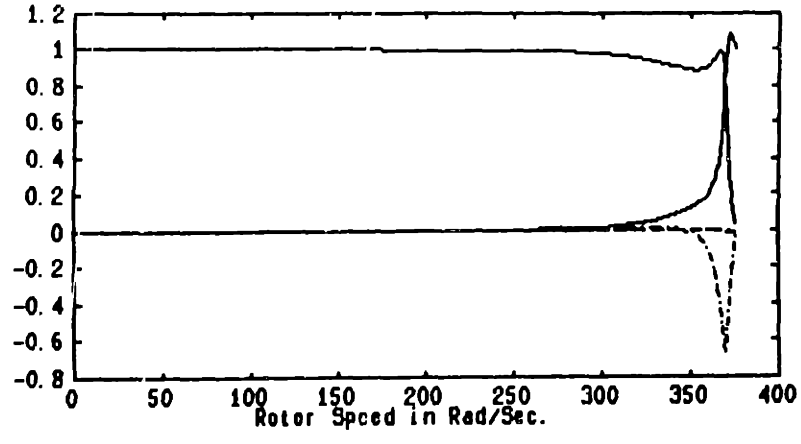

(c)

Figure A.4: Participation factors for the 500 hp machine: (a) $\mu_{1,2}$, (b) $\mu_{3,4}$, (c) μ_5.

The nonlinear fifth order model of the induction machine in the synchronous reference frame is described by the following set of equations:

$$\frac{d\lambda}{dt} = -\left(\mathbf{R}\,\mathbf{L}^{-1} + \omega_e \begin{bmatrix} \mathbf{J} & \mathbf{0} \\ \mathbf{0} & \mathbf{J} \end{bmatrix}\right)\lambda + \omega_r \begin{bmatrix} \mathbf{0} & \mathbf{0} \\ \mathbf{0} & \mathbf{J} \end{bmatrix}\lambda + \begin{bmatrix} \mathbf{I} \\ \mathbf{0} \end{bmatrix} \tag{A.6}$$

$$\frac{d\omega_r}{dt} = -\frac{B}{H}\,\omega_r + \frac{(\tau_{em} - \tau_L)}{H} \tag{A.7}$$

$$\tau_{em} = \frac{1}{2}\,\frac{M}{L_s L_r - M^2}\,\lambda^T \begin{bmatrix} \mathbf{0} & \mathbf{J} \\ -\mathbf{J} & \mathbf{0} \end{bmatrix}\lambda \tag{A.8}$$

$$\mathbf{i} = \mathbf{L}^{-1}\lambda \tag{A.9}$$

It is important to point out that all the variables in the synchronous reference frame are dc quantities when a sinusoidal waveform with frequency ω_e is applied to the stator.

The analysis of the 3 hp machine using the participation factors shows that this machine exhibits a well defined two-time-scale structure, where the fast subsystem is related to the electrical variables (i.e. the machine fluxes) and the slow subsystem is associated with the mechanical variable (i.e. the rotor speed). A first order model of the 3 hp machine is obtained by substituting the quasi-steady-state solution for the electrical variables into the mechanical equation (A.8). The first order model is described by the following set of equations:

$$\frac{d\omega_{rs}}{dt} = -\frac{B}{H}\,\omega_{rs} + \frac{(T_{ems} - T_L)}{H} \tag{A.10}$$

$$T_{ems} = \frac{(\omega_e - \omega_{rs})M^2 R_r V_m^2}{[R_s R_r + \omega_e(\omega_e - \omega_{rs})\sigma]^2 + [\omega_e L_s R_r + (\omega_e - \omega_{rs})L_r R_s]^2} \tag{A.11}$$

where the s in the subscript means that this model is derived by substituting the quasy-steady-state solution of (A.6) into (A.7) and (A.8). Note that equation (A.11) is the expression for the steady state electromagnetic torque as a function of rotor speed.

Simulation of the start-up transient of the induction machine for the first order and the full order models has been done using SIMNON. The results are shown in

Figure A.5 and Figure A.6. Note that the first order reduced order model predicts accurately the speed characteristic of the full order model.

Similary, a third order model for the 500 hp machine can be derived. This model is described by the following set of equations:

$$\lambda_{ss} = \left[\frac{R_s L_r}{\sigma}\mathbf{I} + \omega_e \mathbf{J}\right]^{-1}\left[\mathbf{V}_s + \frac{R_s M}{\sigma}\lambda_{rs}\right] \tag{A.12}$$

$$\frac{d\lambda_{rs}}{dt} = -\left[\frac{R_r L_s}{\sigma}\mathbf{I} + (\omega_e - \omega_{rs})\mathbf{J}\right]\lambda_{rs} + \frac{R_r M^2}{\sigma}\lambda_{ss} \tag{A.13}$$

$$\frac{d\omega_{rs}}{dt} = -\frac{B}{H}\omega_{rs} + \frac{(T_{ems} - T_L)}{H} \tag{A.14}$$

$$T_{ems} = \frac{M}{L_s L_r - M^2}\lambda_{ss}^T \mathbf{J}\lambda_{rs} \tag{A.15}$$

Note that this model corresponds to the common third order model used in transient stability studies of power systems where the stator transients of the machine model in the synchronous rotating frame are neglected [30].

Simulations using SIMNON were done for the starting transient of the 500 hp machine using the full order and third order models of the machine. The results are shown in Figures A.7 to A.8.

In the response of the full order model, two transients of different speeds can be identified. This is a good example of the two-time-scale phenomena present in induction machines. The fast transients only occur during the first two seconds until the electrical variables reach the quasi-steady-state condition. After that point the transient of the system is dominated by the slow transient of the rotor speed.

In Figure A.8 the responses of the rotor flux and the rotor speed of the third order model are shown. In this response the fast oscillations corresponding to the fast transients are not present. This is what we could expect since we made the transients of the fast variables infinitely fast when we derived the model.

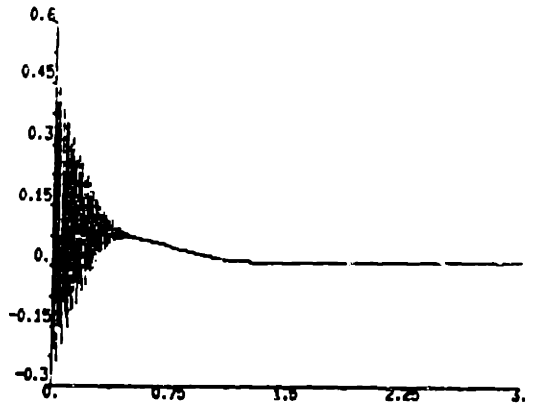

(a)

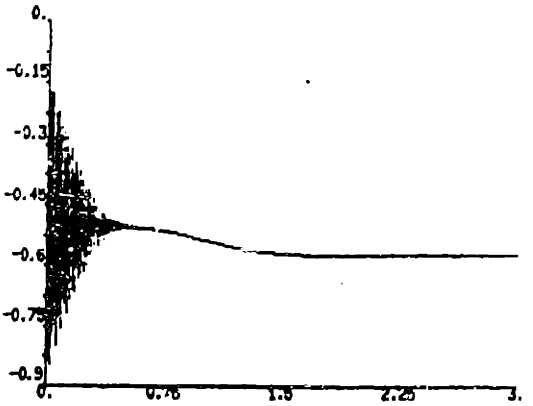

(b)

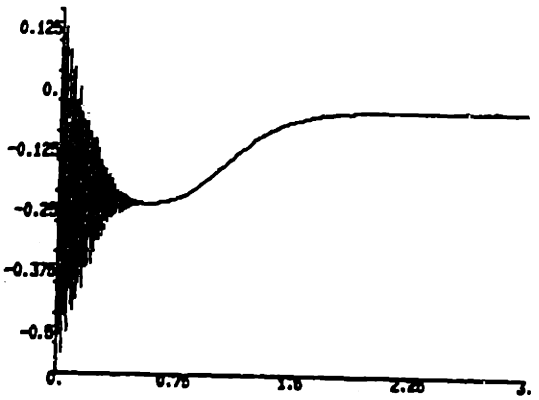

(c)

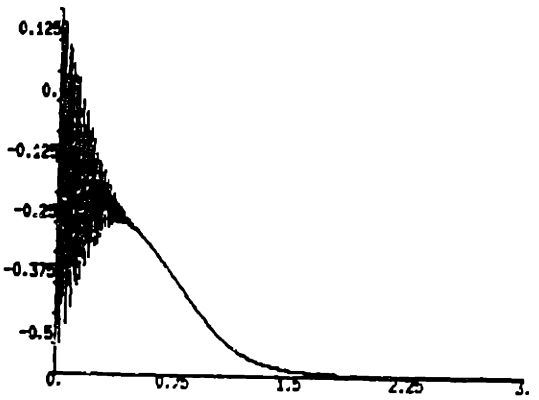

(d)

(e)

Figure A.5: Starting-up Transient of the 3 hp Machine: (a) λ_{S1} response, (b) λ_{S2} response, (c) λ_{R1} response, (d) λ_{R2} response (e) rotor speed response.

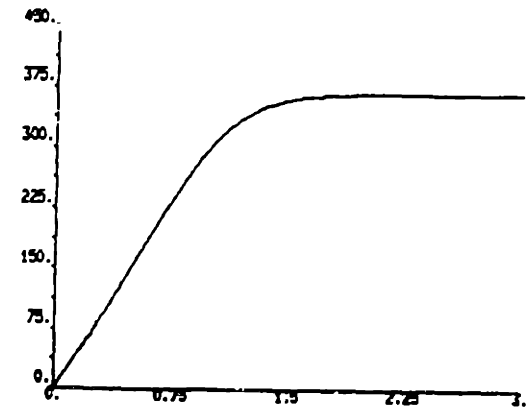

(a)

(b)

Figure A.6: Speed Response of the First Order Model for the 3 hp machine: (a) full order model speed response, (b) first order model response.

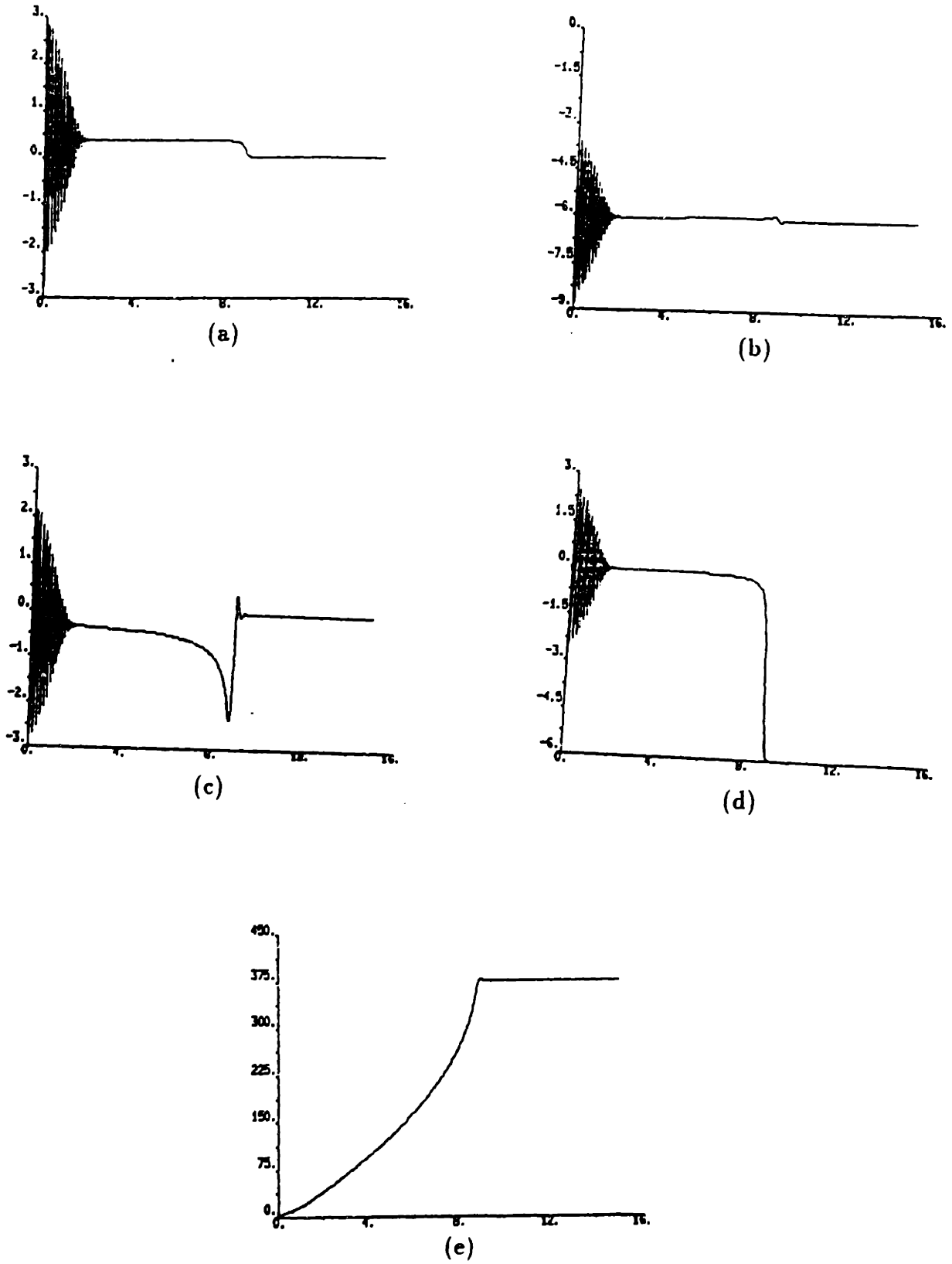

Figure A.7: Starting-up Transient Response of the Full Order Model for a 500 hp machine: (a) λ_{S1} response, (b) λ_{S2} response, (c) λ_{R1} response, (d) λ_{R2} response, (e) rotor speed response.

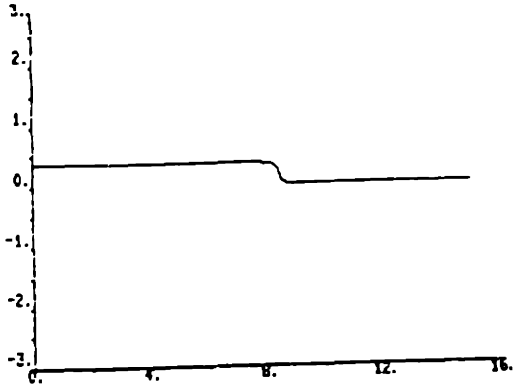

(a)

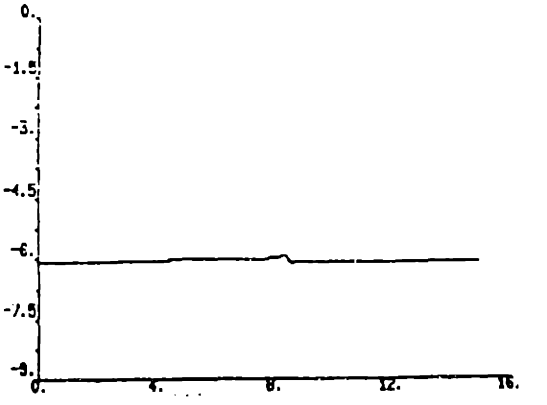

(b)

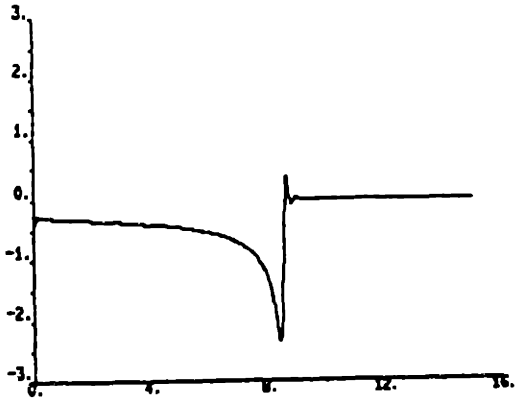

(c)

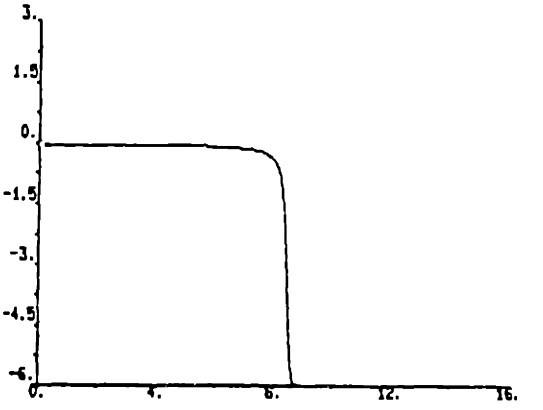

(d)

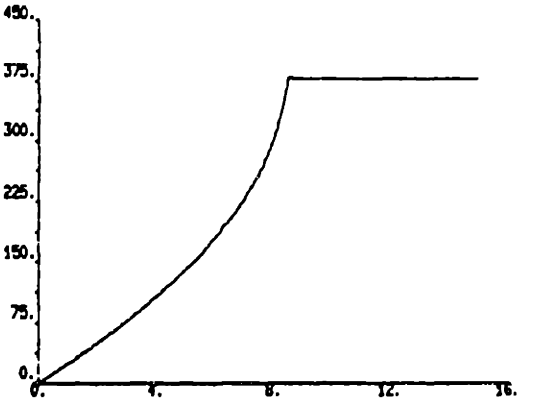

(e)

Figure A.8: Response of the Third Order Model of the 500 hp machine: (a) λ_{S1} response, (b) λ_{S2} response, (c) λ_{R1} response, (d) λ_{R2} response, (e) rotor speed response.

A.5 Conclusion

In summary, we have seen how participation factors can help us to group the machine state variables into sets of coupled variables. Due to the nonlinearities of the machine model the dynamic structure of the system will change due to machine size and operating conditions. However, the information provided by the participation factors at different operating points can help us to deduce reduced order models of the machine.

Participation factors are powerful in the analysis of linear time invariant systems. In this appendix we have seen that it is possible to use these tools to gain some insight into nonlinear models as well.

Bibliography

[1] *DAS-20 Manual.* MetraByte Corporation, 1987.

[2] A. Abondanti and M. Brennen. Variable speed induction motor drives use electronic slip calculator based on motor voltages and currents. *IEEE Transactions on Industry Applications*, IA-11(5), 1975.

[3] A. Bellini, A. de Carli, and M. La Cava. Parameter identification for induction motor simulation. In *Proceedings of the IFAC Symposium on Identification and System Parameter Estimation*, 1977.

[4] A. Blondel. *Synchronous Motor and Converters, Part III.* Mc.Graw Hill, 1913.

[5] B.K. Bose. *Power Electronics and AC Drives.* Prentice Hall, 1986.

[6] R.G. Brown. *Introduction to Random Signal Analysis and Kalman Filtering.* John Wiley and Sons, 1983.

[7] J.H. Chow. *Time-Scale Modeling of Dynamic Networks with Applications to Power Systems.* Springer-Verlag, 1982.

[8] A. Consoli, L. Fortuna, and A. Gallo. Identification of an induction motor by a microcomputer based structure. *IEEE Transactions on Industrial Electronics*, IE-34(4), 1987.

[9] V.C. Cotter. *Implementation of Sampled-Data Secondary Flux Observer for an Induction Machine and Minimization of its Sensitivity to Parameter Variation.* Master's thesis, University of Tokio, 1987.

[10] V.C. Cotter. A novel induction machine flux observer and its application to a high performance ac drive. In *IFAC 10th World Congress on Automatic Control*, 1987.

[11] B. de Fornel, J.M. Farines, and J.C. Hapiot. Numerical estimation of the speed of an asynchronous machine supplied by a static converter. In *IEEE-IAS Annual Meeting*, 1979.

[12] B. de Fornel, J. Faucher, and A. Sague. A method for estimating the flux and slip of a voltage supplied asynchronous machine. In *Industrial Electronics Conference-IECON*, 1986.

[13] B. de Fornel, Cl. Reboulet, and M. Boidin. Speed control by microprocessor for an induction machine fed by a static converter. In *Proceedings of IFAC Symposium on Control in Power Electronics and Electrical Drives*, 1983.

[14] Y. Dote and K. Anbo. Combined parameter and state estimation of controlled current induction motor drive system via stochastic nonlinear filtering technique. In *IEEE-IAS Annual Meeting*, 1979.

[15] H.A. Nour Eldin and L.F. Lopez. Modeling and model reduction of the synchronous machine through singular perturbations. In *Proceedings of the IMACS International Symposium*, 1984.

[16] P. Eykhoff. *System Identification.* John Wiley & Sons, 1974.

[17] D. Filbert. Fault diagnosis in nonlinear electromechanical systems by continuous time parameter estimation. In *Proceedings: ISA International Conference and Exhibition*, 1984.

[18] A.E. Fizgerald, C. Kingsley, and S.D. Umans. *Electric Machinery.* Mc.Graw Hill, 1983.

[19] R. Gabriel and W. Leonhard. Microprocessor control of induction motor. In *Proceedings International Semiconductor Power Conference*, 1982.

[20] L.J. Garces. Parameter adaptation for the speed controlled static ac drive with a squirrel cage induction motor. *IEEE Transactions on Industry Applications*, IA-16(2), 1980.

[21] G Geiger. Monitoring of an electrical driven pump using continuous-time parameter estimation methods. In *Proceedings of the IFAC Symposium on Identification and System Parameter Estimation*, 1982.

[22] G. Geiger. On-line fault detection and localization in electrical dc-drives based on process parameter estimation and statistical decision methods. In *Proceedings of IFAC Symposium on Control in Power Electronics and Electrical Drives*, 1983.

[23] G.C. Goodwin and K.S. Sin. *Adaptive Filtering Prediction and Control.* Prentice-Hall, Inc., 1984.

[24] F. Hillenbrand. A method for determining the speed and rotor flux of the asynchronous machine by meassuring the terminal quantities only. In *Proceedings of IFAC Symposium on Control in Power Electronics and Electrical Drives*, 1984.

[25] T. Irisa, S. Takata, R. Ueda, T. Sonoda, and T. Mochizuki. A novel approach on parameter self-tunning method in ac servo system. In *Proceedings of IFAC Symposium on Control in Power Electronics and Electrical Drives*, 1983.

[26] R. Iserman. Process fault detection based on modeling and estimation methods. In *Proceedings of IFAC Symposium on Control in Power Electronics and Electrical Drives*, 1982.

[27] R. Joetten and G. Maeder. Control methods for good dynamic performance induction motor drives based on current and voltages as measured quantities. *IEEE Transactions on Industry Applications*, IA-19(3), 1983.

[28] P.V. Kokotovic and H.K. Khalil, editors. *Singular Perturbations in Systems and Control.* IEEE Press, 1986.

[29] M. Koyama, M. Yano, I. Kamiyama, and S. Yano. Microprocessor-based vector control system for induction motor drives with rotor time constant identification function. *IEEE Transactions on Industry Applications*, IA-22(3), 1986.

[30] P.C. Krause. *Analysis of Electric Machinery.* Mc.Graw Hill, 1986.

[31] R. Krishnan and F.C. Doran. Study on parameter sensitivity in high performance inverter-fed induction motor drive systems. In *IEEE-IAS Annual Meeting*, 1984.

[32] H. Kubota, K. Matsuse, and T. Fukao. New control method of inverter-fed induction motor drive by using state observer with rotor resistance identification. In *IEEE-IAS Annual Meeting*, 1985.

[33] Y.D. Landau. *Adaptive Control: The Model Reference Approach.* Marcel Dekker, Inc., 1979.

[34] W. Leonhard. *Control of Electrical Drives.* Springer-Verlag, 1985.

[35] W. Leonhard. Microcomputer control of high dynamic performance ac-drives. *Automatica*, 22(1), 1986.

[36] X.Z. Liu, G.C. Verghese, J.H. Lang, and Melih K. Onder. Extending the Blondel-Park transformation to generalized electrical machines: necessary and sufficient conditions. In *Proceeding of The 12th IMACS World Congress*, 1988.

[37] L. Ljung and T. Soderstrom. *Theory and Practice of Recursive Identification.* The MIT Press, 1983.

[38] T. Matsuo and T.A. Lipo. A rotor identification scheme for vector-controlled induction motor drives. *IEEE Transactions on Industry Applications*, IA-21(4), 1985.

[39] A. Nabae, I. Takashi, H. Akagi, and H. Nakano. Inverter fed induction motor drive systems with an instantaneous slip-frequency estimation circuit. In *IEEE Power Electronics Specialist Conference*, 1982.

[40] D. Naunin. Digital speed control of an induction motor with and without a speed sensor. In *Proceeding of the International Power Electronics Conference*, 1983.

[41] D.W. Novotny and J.H. Wouterse. Induction machine transfer fuctions and dynamic response by means of complex time variables. *IEEE Transactions on Power Apparatus and Systems*, PAS-95(4), 1976.

[42] R.H. Park. Two-reaction theory of synchronous machines-part I. *Transactions AIEE*, 48(2), 1929.

[43] I.J. Perez-Arriaga, G.C. Verghese, and F.C. Schweppe. Selective modal analysis with applications to electric power systems, parts 1 and 2. *IEEE Transactions on Power Apparatus and Systems*, PAS-101, 1982.

[44] Louis Roehrs. *Microprocessor Real-Time Induction Machine Speed Estimation.* Bachelor's Thesis, Massachusetts Institute of Technology, May 1988.

[45] S.R. Sanders. *State Estimation in Induction Machines.* Master's thesis, Massachusetts Institute of Technology, 1985.

[46] P.W. Sauer, S. Ahmed-Zaid, and P.W. Kokotovic. An integral manifold approach to reduced order dynamic modeling of synchronous machine. In *IEEE Power Engineering Society Winter Meeting*, 1986.

[47] P.W. Sauer, S. Ahmed-Zaid, and M.A. Pai. Systematic inclusion of stator transients in reduced order synchronous machine models. *IEEE Transactions on Power Apparatus and Systems*, PAS-103(6), 1986.

[48] H. Sugimoto and S. Tamai. Secondary resistance identification of an induction motor applied model reference adaptive system and its characteristics. In *IEEE-IAS Annual Meeting*, 1985.

[49] S.K. Sul and M.H. Park. A novel technique for optimal efficiency control of current source inverter fed induction motor. In *IEEE-IAS Annual Meeting*, 1986.

[50] S. Tamai, H. Sugimoto, and M. Yano. Speed sensor-less vector control of induction motor with model reference adaptive system. In *IEEE-IAS Annual Meeting*, 1987.

[51] M. Velez-Reyes and G.C. Verghese. Reduced order modeling of electrical machines using participation factors. In *Proceedings of the 12th IMACS World Congress*, July, 1988.

[52] Miguel Vélez-Reyes and George C. Verghese. *Speed and parameter estimation for induction machines.* Report To the Laboratory of Electromagnetic and Electronic Systems, MIT. To be Published after the experimental work is finished.

[53] R. Venkataraman, B. Ramaswami, and J. Holtz. Electronic analog slip calculator for induction motor drives. *IEEE Transactions on Industry Applications*, IA-27(2), 1980.

[54] G.C. Verghese, J.H. Lang, and L.F. Casey. Analysis of instability in electrical machines. *IEEE Transactions on Industry Applications*, IA-22(5), 1986.

[55] G.C. Verghese and S.R. Sanders. Observers for faster flux estimation in induction machines. In *IEEE Power Electronics Specialist Conference*, 1985.

[56] G.C. Verghese and S.R. Sanders. Observers for flux estimation in induction machines. *IEEE Transactions on Industrial Electronics*, 35(1), 1985.

[57] Y. Yoshida, R. Ueda, and T. Sonoda. A new inverter-fed induction motor drive with a function for correcting rotor citcuit time constant. In *Proceeding of the International Power Electronics Conference*, 1983.

[58] P. Young. *Recursive Estimation and Time-Series Analysis.* Springer-Verlag, 1984.

[59] L.C. Zai and T.A. Lipo. An extended Kalman filter approach to rotor time constant measurements in pwm induction motor drives. In *IEEE-IAS Annual Meeting*, 1987.